Subset selection in signal processing using sparsity-inducing norms

Ph.D. Dissertation

Author: Luis Blanco Botana

Advisor: Dra. Montse Nájar Martón

Department of Signal Theory and Communications
Universitat Politècnica de Catalunya (UPC)

Barcelona, Spain, May 2017

Abstract

This dissertation deals with different subset selection problems in wireless communications systems. These type of problems have a combinatorial nature, which makes them computationally intractable for medium and large-scale sizes. In particular, two different types of problems are addressed in this thesis: cardinality minimization and cardinality-constrained problems. Different mathematical relaxations are proposed with the aim of obtaining algorithms that approximately solve the proposed problems with a tractable computational cost. Namely, to address the NP-hardness of the problems addressed in the thesis, different mathematical frameworks are considered, such as, for instance, semidefinite programming relaxations, Difference-of-Convex-functions (DC) programming, reweighted norms and the LARS/homotopy algorithm.

The first part of the dissertation deals with the angle of arrival estimation in an antenna array and falls within the so-called sparse signal representation framework. A simple, fast and accurate algorithm is proposed for finding the angles of arrival of multiple sources that impinge on an array of antennas. In contrast to other methods in the literature, the considered technique is not based on *ad-hoc* hyperparameters and does not require the previous knowledge of the number of incoming sources or a previous initialization.

The second part of the thesis addresses the selection of the appropriate subset of cooperative nodes in dense relay-assisted wireless networks and constitutes the main focus of the research activities carried out in this thesis. In order to cope with the huge data traffic in the next generation of wireless networks, the number of access nodes and communication links will be densified, having as a result, an increase of the network complexity. Within this framework, subset selection problems naturally arise to reduce the overall system management. The activation of many relay links, in dense relay-assisted wireless networks, is impractical due to the communications and processing overhead required to maintain the synchronization amongst all the spatially distributed nodes in the wireless network, which makes the network complexity unaffordable. The selection of the most suitable subset of spatially distributed relays, in this context, is a key issue, since it has a dramatic effect in the overall system performance. In particular, the thesis addresses the joint distributed beamforming optimization and relay subset assignment in a multi-user scenario with non-orthogonal transmission and in a scenario with a single source-destination pair. Different design criteria are analyzed, all of them lead to challenging combinatorial nonlinear problems, which are non-convex and non-smooth.

Dealing with the multiple relay selection problem in an ad-hoc wireless relay network with a single source-destination pair, a new algorithm is proposed for finding the best subset

of cooperative relays, and their beamforming weights, so that the SNR is maximized at the destination terminal. This problem is addressed taking into account per-relay power constraints and second-order channel state information. In this context, a sub-optimal method, based on a semidefinite programming relaxation, is proposed. It achieves a near-optimal performance with a reduced computational complexity.

The joint relay assignment and distributed beamforming optimization in multi-user wireless relay networks deserves a special attention. Two major problems are addressed: i) the selection of the minimum number of cooperative nodes that guarantees some predefined Quality of Service (QoS) requirements at the destination nodes and; ii) the selection of the best subset of K relays that minimizes the total relay transmit power, satisfying QoS constraints at the destinations. The mathematical formulations of these problems involve non-convex objective functions coupled with non-convex constraints. They are fit into the DC optimization framework and solved using novel path-following methods based on the penalty convex-concave procedure. The proposed techniques exhibit a low complexity and are able to achieve high-quality solutions close to the global optimum.

Resumen

Esta tesis aborda diversos problemas de selección de subconjuntos en comunicaciones inalámbricas. Este tipo de problemas tiene una naturaleza combinatoria que los hace computacionalmente intratables. En concreto, se consideran dos tipos de problemas: i) la minimización de la cardinalidad y ii) la optimización de problemas con restricciones de cardinalidad. Se proponen diversas relajaciones matemáticas, con el fin de desarrollar algoritmos capaces de obtener un rendimiento casi óptimo y una baja complejidad computacional.

La primera parte de la tesis se centra en el problema de estimación de los ángulos de llegada en una agrupación de antenas y se enmarca dentro de los llamados problemas de representación sparse. En este contexto, se propone un algoritmo rápido, preciso y simple para la estimación de las direcciones de llegada en una agrupación de antenas. Al contrario que otras técnicas en la literatura, el método propuesto, no se basa en hiperparámetros y no requiere el conocimiento a priori del número de fuentes o una inicialización previa.

La segunda parte de la tesis aborda el problema de selección del mejor subconjunto de nodos cooperativos en una red densa de relays inalámbricos. Con el fin de lidiar con el inmenso tráfico de datos en las próximas generaciones de redes inalámbricas, la densidad del número de puntos de acceso y de conexiones aumentará, teniendo como resultado un incremento de la complejidad de la red y de su optimización. Dentro de este marco, los problemas de selección de subconjuntos aparecen de modo natural con el fin de reducir la complejidad de la gestión de la red. La activación de un gran número de terminales, en redes densas de nodos cooperativos, no es factible debido al gran intercambio de información adicional que se requiere entre los terminales, que se encuentran espacialmente distribuidos en diferentes localizaciones. En este contexto, la selección del mejor subconjunto de estos nodos es de gran importancia dado el elevado impacto que tiene en el rendimiento del sistema. Esta tesis aborda la optimización conjunta del conformador de haz (beamformer) y la selección del mejor subconjunto nodos en diversos escenarios cooperativos. Se analizan diversos criterios de diseño, todos ellos conducen a complejos problemas combinatorios no lineales y no convexos.

Dentro del contexto de la selección de múltiples nodos en redes inalámbricas cooperativas con un par origen-destino, se propone un algoritmo para encontrar el mejor subconjunto de terminales cooperativos y sus respectivos pesos, de manera que la SNR se maximice en el nodo de destino. Este problema se trata teniendo en cuenta restricciones individuales de potencia en los nodos cooperativos e información estadística de segundo orden de los canales inalámbricos de la red. En este contexto, se presenta un algoritmo con una baja complejidad y un rendimiento cercano al óptimo.

La optimización conjunta de los pesos del conformador distribuido y la selección del subconjunto de nodos cooperativos en redes inalámbricas multiusuario merece una atención especial. En esta tesis se abordan dos problemas relevantes: 1) la selección del mínimo número de nodos cooperativos capaces de garantizar una cierta calidad de servicio en los nodos destino y; 2) la selección del mejor subconjunto de K terminales repetidores que minimiza la potencia total transmitida, cumpliendo con ciertas restricciones de calidad de servicio en los nodos destino. La formulación matemática de estos problemas involucra funciones objetivo no convexas acopladas con restricciones que tampoco son convexas. Para aliviar la elevada complejidad de estos problemas se proponen nuevos algoritmos con una baja carga computacional y un rendimiento casi óptimo.

A mi familia.

Table of Contents

Notation

In general, uppercase boldface letters, e.g. $\mathbf{A}$, denote matrices, lowercase boldface letters, e.g. $\mathbf{a}$, denote column vectors.

$\mathbf{A}^T, \mathbf{A}^H$	Transpose and conjugate transpose of a matrix $\mathbf{A}$, respectively.
$\mathbf{A}^{-1}$	Inverse of $\mathbf{A}$.
$\mathbf{A}^{1/2}$	Positive definite Hermitian square-root of $\mathbf{A}$, i.e. $\mathbf{A}^{1/2}\mathbf{A}^{1/2} = \mathbf{A}$.
$\mathrm{Tr}\{\mathbf{A}\}$	Trace of a matrix $\mathbf{A}$.
$\|\mathbf{A}\|_2^2$	Square of the Frobenius norm of a matrix $\mathbf{A}$, $\|\mathbf{A}\|_2 = \left(\mathrm{Tr}\left[\mathbf{A}^H\mathbf{A}\right]\right)^{1/2}$.
A_{ij}, $[\mathbf{A}]_{ij}$	(i,j)th entry of a matrix $\mathbf{A}$, corresponding to the ith row and the jth column.
$\mathrm{rank}(\mathbf{A})$	Rank of a matrix $\mathbf{A}$.
$\|\mathbf{A}\|$	Element-wise absolute value of a matrix $\mathbf{A}$.
$\mathbf{A} \succeq 0$	Positive semidefinite matrix $\mathbf{A}$.
$\mathrm{vec}(\mathbf{A})$	Vectorization of a matrix $\mathbf{A}$.
$\|\mathbf{a}\|_1$, $\|\mathbf{a}\|_2$	l_1-norm and the Euclidean norm of a vector $\mathbf{a}$, $\|\mathbf{a}\| \triangleq \|\mathbf{a}\|_2 = \left(\mathbf{a}^H\mathbf{a}\right)^{1/2}$.
$\|\mathbf{a}\|_0$, $\mathrm{card}(\mathbf{a})$	l_0-norm, cardinality of the vector $\mathbf{a}$, i.e. the number of non-zero entries of $\mathbf{a}$.
a_i, $[\mathbf{a}]_i$, $(\mathbf{a})_i$	ith entry of a vector $\mathbf{a}$.
$\mathbf{a} \otimes \mathbf{b}$	Kronecker product of two vectors $\mathbf{a}$ and $\mathbf{b}$.
$\mathbf{a} \odot \mathbf{b}$	Schur-Hadamard of two vectors $\mathbf{a}$ and $\mathbf{b}$.

$\mathbf{a} \in \{0,1\}^N$	Vector $\mathbf{a}$ of length N with binary entries.
$\mathbf{a} \in [0,1]^N$	Vector $\mathbf{a}$ of length N with entries $a_i \in [0,1]$ $\forall i = 1,...,N$.
$\mathbf{1}_N$	All-one column vector of length N.
$\mathbf{0}_N$	All-zero column vector of length N.
$\mathbf{I}_M$	The $M \times M$ identity matrix.
$\mathbb{R}, \mathbb{C}$	The set of real and complex numbers, respectively.
$\mathbb{R}^N, \mathbb{C}^N$	The set of N-dimensional vectors with entries in $\mathbb{R}$ and $\mathbb{C}$, respectively.
$\mathbb{R}_+^N$	The set of N-dimensional vectors with non-negative entries.
$\mathbb{R}^{M\times N}, \mathbb{C}^{M\times N}$	The set of $M \times N$ matrices with entries in $\mathbb{R}$ and $\mathbb{C}$, respectively.
H_N^+	Set of $N \times N$ Hermitian positive semidefinite matrices.
$E\{\cdot\}$	Expectation operator.
$\Re\{\cdot\}$, $\Im\{\cdot\}$	Real and imaginary part operators, respectively.
j	Imaginary unit, $j = \sqrt{-1}$.
$\lvert S\rvert, S(i)$	For a given set S, $\lvert S\rvert$ denotes its cardinality and $S(i)$ stands for the ith element of the set
iid	A set of random variables are independent and identically distributed.
$\mathcal{N}(\boldsymbol{\mu}, \boldsymbol{\Sigma})$	Multivariate Gaussian distribution with mean $\boldsymbol{\mu}$ and covariance $\boldsymbol{\Sigma}$.
$\mathcal{CN}(\boldsymbol{\mu}, \boldsymbol{\Sigma})$	Multivariate complex Gaussian distribution with mean $\boldsymbol{\mu}$ and covariance $\boldsymbol{\Sigma}$.

$\mathcal{X}^2(2)$	Chi-square distribution of two degrees of freedom.
$\sim$	Distributed according to.
$\|a\|$	Modulus of a complex number a.
$\nabla_{\mathbf{x}} f(\mathbf{x})$	Gradient of a function $f(\mathbf{x})$ w.r.t. $\mathbf{x}$.
$\text{var}\{\cdot\}$	Variance.
arg	Argument.
$\subseteq$	Subset.
$\min_{\mathbf{x}} f(\mathbf{x})$	Minimization of an objective function $f(\mathbf{x})$ w.r.t. the variable $\mathbf{x}$.
$\max_{\mathbf{x}} f(\mathbf{x})$	Maximization of an objective function $f(\mathbf{x})$ w.r.t. the variable $\mathbf{x}$.
$\mathbf{x}^*$	Optimal value of a given optimization problem.

Acronyms

ADMM Alternating Direction Method of Multipliers

AF Amplify-and-Forward

AIC Akaike Information Criterion

AoA Angles of Arrival

AWGN Additive White Gaussian Noise

BBU Baseband Unit

BPDN Basis Pursuit Denoising

CCP Convex-Concave Procedure

CDF Cumulative Distribution Function

CoMP Coordinated Multipoint

C-RAN Cloud Radio Access Network

CSI Cannel state information

DC Difference of Convex functions

DoA Directions of Arrival

DPR1 Diagonal Plus Rank-one matrix

KKT Karush-Kuhn-Tucker

K-S Kolmogorov-Smirnov

LARS Least Angle Regression

LASSO Least Absolute Shrinkage and Selection Operator

LP Linear Programming

MIMO Multiple-Input Multiple-Output

MINLP Mixed-Integer NonLinear Program

MMV Multiple Measurement Vectors

MUSIC MUltiple SIgnal Classification

NCS Normalized Cumulative Spectrum

NOMA Non-Orthogonal Multiple Access

NP-hard Non-deterministic Polynomial-time hard

OMP Orthogonal Matching Pursuit

PCA Principal Component Analysis

QCQP Quadratically Constrained Quadratic Program

QoS Quality of Service

QP Quadratic Programming

RMSE Root Mean Square Error

RRH Remote Radio Head

SCA Successive Convex Approximation

SDP Semidefinite Programming

SDR Semidefinite Relaxation

SIC Successive Interference Cancelation

SINR Signal-to-Interference-plus-Noise-Ratio

SNR Signal-to-Noise Ratio

SOCP Second-Order Cone Programming

SPICE SParse Iterative Covariance-based Estimation approach

SVD Singular Value Decomposition

ULA Uniform Linear Array

VMIMO Virtual MIMO

WSN Wireless Sensor Network

Chapter 1

Introduction

1.1 Scope and research motivation

This dissertation deals with the following types of mathematical optimization problems:

$$\begin{aligned} \min_{\mathbf{x}} \quad & \|\mathbf{x}\|_0 \\ \text{s.t.} \quad & \mathbf{x} \in \mathcal{Q}, \end{aligned} \tag{1.1}$$

and

$$\begin{aligned} \min_{\mathbf{x}} \quad & f(\mathbf{x}) \\ \text{s.t.} \quad & \mathbf{x} \in \mathcal{Q} \\ & \|\mathbf{x}\|_0 = K, \end{aligned} \tag{1.2}$$

where $\mathbf{x}$ is the unknown vector of variables, $f(\mathbf{x})$ denotes the objective function, K is a given constant and $\mathcal{Q}$ denotes the feasible set of the problem. This set can be a linear or nonlinear convex set or even a nonlinear and non-convex set. The operator $\|\mathbf{x}\|_0$ denotes the l_0-norm [1], i.e., the cardinality operator, the counting function that returns the number of non-zero elements of its argument. As normally used in the literature, throughout this dissertation, the l_0-norm will be denoted as $\|\mathbf{x}\|_0$ or $\text{card}(\mathbf{x})$. Both notations will be used indistinctly to designate the cardinality of a vector $\mathbf{x}$. Furthermore, as a matter of fact, finite dimensional spaces, are considered here. Thus, it is assumed that $\mathbf{x} \in \mathbb{C}^N$or $\mathbb{R}^N$.

Yet another problem that will be considered in this thesis is the maximization of a non-convex objective function subject to cardinality constraints

$$\begin{aligned} \max_{\mathbf{x}} \quad & f(\mathbf{x}) \\ \text{s.t.} \quad & \mathbf{x} \in \mathcal{Q} \\ & \|\mathbf{x}\|_0 = K. \end{aligned} \tag{1.3}$$

This type of problems can be reformulated as a cardinality-constrained problem of type (1.2). Hence, we will focus our attention on problems of type (1.1) and (1.2). Throughout the present chapter, we will refer to (1.1) as cardinality minimization problem and to (1.2) as cardinality-constrained optimization problem.

The l_0-norm is a non a non-convex, non-smooth and integer-valued function, and optimization problems that involve the cardinality in its objective or constraints are NP-hard [2] in general and, consequently, computationally intractable. The common approach to deal with the discontinuity of the l_0-norm is to approximate $\|\mathbf{x}\|_0$ by a continuous surrogate function [3, 4, 5, 6].

The next sections provide a brief overview of some relevant subset selection problems in the literature and describe the general framework of the dissertation.

1.1.1 The minimum cardinality problem

The optimization problem presented in (1.1) aims to find the sparsest solution, i.e., the vector with lowest number of active entries that satisfies the set of constraints defined by $\mathcal{Q}$. This type of problems appears frequently in the context of sparse signal representation [7,8], which has been considered in a plethora of fields, e.g. spectral estimation, array processing, image reconstruction, channel coding, to name a few. Each of these fields has developed its own mathematical tools but there are important resemblances between the different disciplines; all of them are based on the fact that discrete signals can be well-represented by a small number of non-vanishing coefficients in a suitable domain, e.g, space, time or frequency. The difficulty in reconstructing a sparse signal arises from the fact that the number of non-zero coefficients and the location of these non-vanishing entries is not known *a priori*. In order to overcome these difficulties a lot of effort has been devoted by researchers to develop feasible recovery algorithms and to provide rigorous proofs of the ability of these techniques to achieve a perfect reconstruction.

Sparse signal representation seeks to approximate a target signal by a linear combination of few elementary signals extracted from a known collection. We will start describing

the general setup. The most basic problem is the reconstruction of a vector $\mathbf{x}$ from an observation vector $\mathbf{y} = \mathbf{A}\mathbf{x}$, where $\mathbf{A}$ is the so-called dictionary, a known matrix of size $M \times N$. This matrix is usually overcomplete, i.e., it has more columns than rows. Under the assumption that the unknown is sparse, i.e., it has few non-zero entries relative to its dimension, the natural approach is to seek the maximally sparse representation of the observed vector $\mathbf{y}$. Formally, this can expressed as

$$\min_{\mathbf{x}} \|\mathbf{x}\|_0 \qquad \text{s.t. } \mathbf{y} = \mathbf{A}\mathbf{x}. \tag{1.4}$$

It is worth noting that without imposing a sparsity prior on $\mathbf{x}$, the system of equations $\mathbf{y} = \mathbf{A}\mathbf{x}$ is underdetermined and admits an infinite number of solutions. This type of problems have applications across various fields, including compressive sensing [9,10], image recovery [11, 12] and array processing [13].

The problem exposed in (1.4) is an intractable NP-hard combinatorial problem in general [14]. Fortunately, over the past decade, researchers have developed tools for solving sparse approximation problems with computationally tractable algorithms (for further information about these methods see [4, 6, 8, 15] and Chapter 2). Among all the proposed techniques in the literature, the use convex norms that promote sparsity [5, 16] and greedy methods [17], such as Orthogonal Matching Pursuit (OMP), have deserved special attention. OMP is an iterative method that selects at each step the column that is most correlated with the residual signal and can be viewed as Successive Interference Cancellation (SIC) method, due to its sequential nature [18].

To circumvent the computational bottleneck of the combinatorial problem presented in (1.4) the most common approach is to replace the non-convex l_0-norm by the l_1-norm, which is defined as $\|\mathbf{x}\|_1 = \sum_i |x_i|$. This approach leads to problems with a lower computational complexity

$$\min_{\mathbf{x}} \|\mathbf{x}\|_1 \qquad \text{s.t. } \mathbf{y} = \mathbf{A}\mathbf{x}. \tag{1.5}$$

The conditions that guarantee the equivalence of the solutions of (1.4) and (1.5) were studied in [19], [20], [21]. In general, the l_1-minimization problem in (1.5) is more successful than OMP algorithms in provinding the sparsest solution of (1.4) [22].

The l_1-minimization is considered as one of the most successful methods to find sparse solutions to a linear system of equations. Nevertheless, the l_1-norm penalizes large coefficientes to the detriment of smaller entries [23, 24]. While the l_0-norm only counts the

non-zero entries of a vector, the main disadvantage of using $\|\mathbf{x}\|_1$ to approximate the l_0-norm is that the amplitudes of the non-zero entries of the vector $\mathbf{x}$ come into play. Thus, seeking for more effective methods, the iteratively reweighted l_1-norm minimization has been proposed by Candes, Wakin and Boyd in [23]. It is based on the approximation of the l_0-norm by the concave and continuous log-sum surrogate function [23, 3] and yields the following reweighted algorithm:

$$\begin{aligned} \mathbf{x}^{(k+1)} = \arg\min_{\mathbf{x}} \quad & \sum_{i=1}^{N} \frac{|x_i|}{|x_i^k| + \varepsilon} \\ \text{s.t.} \quad & \mathbf{y} = \mathbf{A}\mathbf{x}, \end{aligned} \tag{1.6}$$

where k denotes the iteration number, and x_i^k is the ith component of the solution at the kth iteration of the algorithm. Note that to compensate the amplitudes of the non-zero entries of $\mathbf{x}$, the argument of the l_1-norm is iteratively normalized to make this norm a better proxy of the cardinality operator. The weighting updates in the objective function $1/(|x_i^k|+\varepsilon)$ encourage small entries of the vector $\mathbf{x}$ to tend to zero and avoid the inadequate supression of large entries.

The aforementioned problems are noiseless. However, this is, in general, an oversimplification of practical problems. In real problems a non-negligible level of noise is normally present in the measurement vector $\mathbf{y}$ or modelling errors may be relevant. If some noise is present in the observation, or $\mathbf{x}$ can only be assumed to be approximated by a sparse vector, a natural variation is to relax the exact match between $\mathbf{y}$ and $\mathbf{A}\mathbf{x}$ to allow some error tolerance. This leads to the following minimization problem

$$\min_{\mathbf{x}} \|\mathbf{y} - \mathbf{A}\mathbf{x}\|_2^2 \quad \text{subject to} \quad \|\mathbf{x}\|_1 \leq \beta, \tag{1.7}$$

which is the so-called LASSO (Least Absolute Shrinkage and Selection Operator) problem. It has been proposed by Tibshirani in reference [25]. The unconstrained version of the LASSO problem is given by

$$\min_{\mathbf{x}} \|\mathbf{y} - \mathbf{A}\mathbf{x}\|_2^2 + \tau \|\mathbf{x}\|_1, \tag{1.8}$$

where τ is a Lagrange multiplier. This type of problems arises frequently in the context of sparse regression in statistics [26] and feature selection in statistical learning and data science [27, 28].

So far, some relevant problems in the context of sparse signal representation have been presented. Nevertheless, the family of cardinality minimization problems is large and

many possible variations can be considered. Depending on the framework of application and on performance metric used, many different convex or non-convex functions can be considered for the definition of the feasible set $\mathcal{Q}$ of the minimum cardinality problem (1.1), such as, for example, quality of service requirements, user rate constraints or bounds on the available energy or power. In wireless communications, some relevant examples of cardinality minimization problems can be found in the recent literature of sensor selection for wireless sensor networks [29, 30].

1.1.2 Cardinality-constrained optimization

Cardinality-constrained problems appear across many of the technologies that are nowadays under consideration for the next generation of cellular networks. In order to deal with the huge data traffic in 5G networks, the number of access nodes and the number of communication links per unit area will be densified [31]. Within this context, subset selection problems naturally arise in order to reduce the network management and the overall system complexity. Many of the technology enablers that are currently under investigation for the next generation of wireless networks consider cardinality-based problems. As an example, let us enumerate some relevant problems addressed in the literature:

- Cloud-RAN. Cloud Radio Access Network (Cloud-RAN) has been proposed as a promising network architecture [32] to cope with the immense amount of mobile data traffic in 5G cellular systems. In Cloud-RAN, the baseband signal processing is shifted to a single Baseband Unit (BBU) pool, which is in charge of the interference management and the resource allocation. Meanwhile, the traditional powerful base stations are replaced by low-cost and low-power Remote Radio Heads (RRHs) with limited processing capabilities. The RRHs are connected to the BBU pool through optical links. In this context, the joint RRH selection and power minimization problem is of paramount important and has been studied in several recent works [33, 34, 35].

- Coordinated Multipoint (CoMP). CoMP transmission is an effective mechanism for mitigating the intercell inteference and increasing the system throughput in single frequency reuse networks. Reference [36] addresses the joint network optimization and downlink beamforming design with the objective of minimizing the total base station power consumption.

- Device-to-device communications. It constitutes a new paradigm in cellular communications. The direct connection between nearby devices is established with the

minimal intervention of the network. The direct transmission closely located devices improves the efficient use of resources due to the local spectrum reuse. The clustering problem in device-to-device assisted Virtual MIMO (VMIMO) systems with limited feedback that has been presented in [37].

Cardinality-constrained problems have also been considered in many other applications, such as, for instance in:

- Antenna selection [38, 39]. In particular, reference [38] deals with the joint multicast beamforming and antenna subset selection in multi-group multicasting.
- Sparse Principal Component Analysis (PCA) in statistics [40, 3]. PCA is a popular tool in statistics for data analysis, data compression and data visualization. PCA is used to reduce the dimensionality of a model, i.e., to compress data without losing much information. The consideration of cardinality constraints leads to results that can be more easily interpreted.
- Sensor selection [41, 42, 43].

1.1.3 Presentation of the general framework of the thesis

This dissertation addresses various cardinality-based problems in wireless communication systems. In particular, the first part of the thesis deals with the angle of arrival estimation in an antenna array. This problem falls within the framework of the aforementioned sparse signal representation problems. The second part is focused on the selection of the appropriate subset of cooperative nodes in dense relay-assisted wireless networks and constitutes the most recent work considered in this dissertation.

As will presented with further detail below, in modern relay-assisted wireless networks, the number of potential relays could be large. In these scenarios, it is unaffordable in terms of network complexity to activate many cooperative nodes due to: i) the huge signaling overhead needed to transmit control and data signals between the terminals and; ii) the difficulty required to maintain the spatially distributed nodes in the wireless network synchronized. Choosing a smaller number of relay nodes can enjoy of a performance close to that of using all the potential cooperative nodes with a reduced complexity.

In order to deal with the combinatorial nature of the subset selection problems presented in this dissertation, different relaxations are proposed with the goal of obtaining

sub-optimal algorithms that approximately solve the proposed problems with a tractable computational cost. Namely, to address the NP-hardness of the problems addressed in this thesis, we consider different mathematical frameworks, such as, for example, semidefinite programming relaxations [44], Difference-of-Convex-functions (DC) programming [45], reweighted norms [23] and the LARS/homotopy algorithm [46].

1.2 Outline of the dissertation and research contributions

The thesis is structured in six chapters. It addresses different subset selection problems in signal processing for communications. In particular, as exposed above, our attention is focused on two frameworks: dense relay-assisted wireless networks and angle of arrival estimation in array processing. The next paragraphs summarize the content of each chapter and the main research contributions. It should be pointed out that the order of chapters follows the original timeline of the publications. Therefore, the work exposed in the initial chapters corresponds to the journals published earlier in time, and most recent works are presented at the end of the dissertation.

Chapter 2

The second chapter introduces some basics on sparse regularization for solving ill-posed problems and provides a brief overview of methods for solving sparse approximation problems. This chapter is motivated by the fact that in most of applications where sparsity plays a significant role, one is dealing with ill-conditioned problems.

Chapter 3

This chapter proposes a simple, fast and accurate algorithm for finding the angles of arrival of multiple sources that impinge on an array of antennas. In contrast to other methods in the literature, the proposed method is not based on ad-hoc regularization parameters and does not require either the knowledge of the number of sources or a previous initialization. This technique considers an structured covariance matrix model based on overcomplete basis representation and tries to fit the unknown signal power to the sample covariance. The final problem is reduced to an iterative algorithm that solves at each iteration a

reduced-size system of equations until a stopping condition is fulfilled. This stopping criterion is based on the residual spectrum and, to the best of author's knowledge, it has never been considered before in sparse signal representation.

Chapter 4

This chapter addresses the node subset selection problem in dense relay-assisted wireless networks. In this type of scenarios, the activation of all (or many) relays is impractical or even unfeasible (see the references [47, 48, 49, 50, 51, 52]). In many practical situations the number of potential cooperating nodes could be large, e.g., in device-to-device communication networks, and the benefits of the cooperation with all the relays can be outweighed by the costs of the cooperation. These costs include the signaling overhead and the efforts needed to maintain the synchronization between all the nodes [47, 48, 49, 50]. In this context, by considering relay selection, the overall processing in the network can be simplified achieving a significant reduction in the implementation complexity [47, 49, 50, 51, 52]. The proper selection of the relay nodes is a key issue, since it has a dramatic effect in the overall system performance.

Chapter 4 deals with the multiple relay selection problem in an ad-hoc wireless relay network with one source-destination pair. In particular, this thesis proposes a new technique for the selection of the best subset of K cooperative nodes and their corresponding beamforming weights so that the signal-to-noise ratio (SNR) is maximized at the destination. Contrary to other approaches in the literature, the problem is addressed with per-relay power constraints and considering second-order channel state information of the relay channels. This problem is computationally demanding and requires an exhaustive search over all the possible combinations. In order to reduce the complexity, a new suboptimal method is proposed. This technique exhibits a near-optimal performance with a computational burden that is much lower than the one required by the exhaustive search. The proposed method is based on the use of the l_1-norm squared and the Charnes-Cooper transformation and naturally leads to a semidefinite programming relaxation [44] with an affordable computational cost.

Chapter 5

In the fifth chapter, the joint relay assignment and beamforming optimization in a multiuser wireless relay network is analyzed. In particular, it deals with the relay subset selection

problem in an ad-hoc wireless relay network consisting of M source-destination pairs communicating, in a pairwise manner, with the help of N potential cooperative nodes. It should be remarked that the subset assignment problem in multi-user wireless relay networks is challenging [53]. The main reason is that the proper design of a relay subset selection method has to take into account the interference provoked by the simultaneous transmission of multiple users and this requires the development of very sophisticated techniques.

Chapter 5 adresses two different problems:

1. The joint selection of the minimum number of relay nodes and the computation of the corresponding distributed beamforming weights that guarantee a predefined SINR at the destination nodes in a multi-user amplify-and-forward wireless relay network. This problem is addressed considering individual power constraints at the relays. The selection of the minimum number of active links is of practical interest in wireless networks because it reduces the overall network complexity as well as the communications and processing overhead. Furthermore, by considering the selection of relay nodes, the links with the lowest quality are discarded and this fact increases the robustness against link failures. The mathematical formulation of the proposed problem involves a non-convex objective function with non-convex constraints. This problem is reformulated as a Difference-of-Convex-functions (DC) programming problem [45] and a low-complexity sub-optimal method, based on the Convex-Concave Procedure (CCP) [54], is proposed to solve it. The application of this procedure leads to an iterative reweighted l_1-norm [23] over the convexified set of SINR constraints.

2. The second problem considered in this chapter is the joint design of the distributed beamforming and the selection of the best subset of K cooperative nodes that minimize the total relay transmit power. This problem is addressed taking into account the SINR requirements at the destination nodes and individual power constraints at the relays. It involves non-convex constraints due to the SINR requirements and binary constraints and constitutes a very challenging non-convex mixed-integer nonlinear program (MINLP) [55]. It should be remarked that leaving aside the subset selection issue, finding the optimal beamforming weights that minimize the total relay transmit power with SINR requirements and per-relay power constraints is a hard non-convex Quadratically Constrained Quadratic Problem (QCQP) [56, 57] that has been analyzed in [58]. In chapter 5, the joint subset selection and distributed beamforming computation is rewritten as a DC program and solved with a new iterative

algorithm based on the penalty convex-concave procedure which has been recently presented in references [59, 60]. As will be shown in chapter 5, the proposed technique constitutes a novel approach to binary non-convex MINLPs and leads to a path-following algorithm which is able to achieve approximate solutions close to the global optimal solutions.

As a final remark, let us point out that contrary to other approaches in the literature of relay clustering in multi-user wireless relay networks, which are based on perfect channel state information (CSI), the proposed techniques in chapter 5 can be applied in scenarios with imperfect CSI as well.

Chapter 6

The final chapter presents the conclusions of the thesis and exposes some possible future research lines.

1.3 List of publications

The work presented in this dissertation has been published or submitted for future publication in the next journal articles and conference papers [61, 62, 63, 64].

Journal articles:

- L. Blanco and M. Nájar, "Joint distributed beamforming design and relay subset selection in multi-user wireless relay networks: A novel DC programming approach," submitted to IEEE Transactions on Wireless Communications.
- L. Blanco and M. Nájar, "Sparse multiple relay selection for network beamforming with individual power constraints using semidefinite relaxation," IEEE Transactions on Wireless Communications, vol. 15, no.2, pp. 1206-1217, Feb. 2016.
- L. Blanco and M. Nájar, "Sparse covariance fitting for direction of arrival estimation," EURASIP Journal on Advances in Signal Processing, May 2012.

Conference papers:

- L. Blanco and M. Nájar, "Relay subset selection in cognitive networks with imperfect CSI and individual power constraints," in Proceedings of the European Signal Processing Conference (EUSIPCO 2015), 31 Aug. - 4 Sept. 2015, Nice, Cote d'Azur (France).
- L. Blanco and M. Nájar, "Subset relay selection in wireless cooperative networks using sparsity-inducing norms," in Proceedings of the 11th International Symposium on Wireless Communications Systems (ISWCS), 26-29 Aug. 2014, Barcelona (Spain).
- L. Blanco, M. Nájar, "Multiple relay selection in underlay cognitive networks with per-relay power constraints," 23rd European Conference on Networks and Communications (EuCNC), 23-26 June 2014, Bologna (Italy).
- L. Blanco, M. Nájar, F. Rubio, "Estimation of superimposed complex exponentials using covariance matching and sparsity," Presentation at the International Conference on Trends and Perspectives in Linear Statistical Inference (LinStat), 27-31 July 2010, Tomar (Portugal).

1.4 Other research contributions

Besides the main contributions of this thesis outlined in the previous sections, a number of other research works have been carried out before and while this thesis was prepared. Even though some of them are not in the scope of the thesis, it is worth mentioning the contributions in scientific journals:

- L. Blanco, D. Tarchi, A. Biasson, Jesús Alonso-Zárate, Michele Zorzi, "On the Gains of Using variable Spreading Factors in Satellite-based IoT Networks using E-SSA with Energy Harvesting," submitted to Journal on Selected Areas in Communications (JSAC).
- M.A. Vázquez, L. Blanco, A.I. Pérez-Neira, "Spectrum sharing backhaul satellite-terrestrial systems via phase-only beamforming," submitted to IEEE Transactions on signal processing.
- M. A. Vázquez, L. Blanco, A.I. Pérez-Neira,"Hybrid Analog-Digital Transmit Beamforming for Spectrum Sharing Backhaul Systems," submitted to IEEE Transactions on wireless communications.

- O. Font-Bach, N. Bartzoudis, A. Pascual-Iserte, M. Payaro, L. Blanco, D. López, M. Molina, "Interference management in LTE-based HetNets: a Practical Approach," Transactions on Emerging Telecommunications Technologies, Vol. 26, No. 2, pp. 195-215, Feb. 2015.

- L. Blanco, J. Serra, M. Nájar, "Minimum variance time of arrival estimation for positioning," Elsevier Signal Processing, Vol. 90, No. 8, Pages 2611-2620, August 2010.

and international conferences:

- M. Á. Vázquez, A. Konnar, L. Blanco, N. D. Sidiropoulos, A. I. Pérez-Neira, "Non-convex consensus ADMM for Satellite Precoder Design," in Proceedings of IEEE International Conference on Acoustics, Speech and Signal Processing (ICASSP'17), March 5-9, 2017, New Orleans, Louisiana, March 2017.

- M. Á. Vázquez, L. Blanco, A. I. Pérez-Neira, "Multiuser Downlink Hybrid Analog-Digital Beamforming with Individual SINR Constraints," in Proceedings of International ITG Workshop on Smart Antennas (WSA 2017), 15-17 March 2017 Berlin, (Germany), March 2017.

- M. Á. Vázquez, L. Blanco, X. Artiga, A. I. Pérez-Neira, "Hybrid Analog-Digital Transmit Beamforming for Spectrum Sharing Satellite-Terrestrial Systems," in Proceedings of the IEEE International Workshop on Signal Processing Advances for Wireless Communications (SPAWC 2016), 3-6 July 2016, Edinburgh (UK).

- M. Á. Vázquez, L. Blanco, A. I. Pérez-Neira, M. Á. Lagunas, "Phase-Only Transmit Beamforming for Spectrum Sharing Microwave Systems," in Proceedings of International ITG Workshop on Smart Antennas (WSA 2016), 9-11 March 2016 Munich, (Germany).

- J. Serra, L. Blanco, M. Nájar, "Cramer-Rao Bound for Time-Delay estimation in the Frequency domain," in Proceedings of the 17th European Signal Processing Conference (EUSIPCO 2009) 24-28 August 2009, Glasgow (Scotland, UK).

- L. Blanco, J. Serra, M. Nájar, "Conformal Transformation For Efficient Root-TOA Estimation," invited paper in Proceedings of 2nd International Symposium on Communications, Control and Signal Processing (ISCCSP 2008), 12-14 March 2008, Malta.

- L. Blanco, J. Serra, M. Nájar, "Root Minimum Variance TOA estimation for wireless location," XV European Signal Processing Conference, (EUSIPCO) September 2007.
- L. Blanco, J. Serra, M. Nájar, "Low Complexity TOA Estimation for Wireless Location," IEEE GLOBECOM 2006, San Francisco (California). November 2006.
- L. Blanco, J. Serra, M. Nájar, "Root spectral estimation for location based on TOA," European Signal Processing Conference, (EUSIPCO 06), Florence (Italy). September 2006.

Chapter 2

Sparse signal processing

The aim of this chapter is to describe linear ill-posed inverse problems. In the next chapter, the classical source location problem will be rewritten as a linear inverse problem that is ill-posed. The solutions of this type of problems are very sensitive to noise and regularization methods must be used to stabilize the solutions by considering some additional information about the data. The structure of the chapter is the following. Quadratic regularization, which is the classical tool for solving ill-posed problems, is mentioned first. Unfortunately, it does not lead to sparse solutions. Due to this reason, sparse regularization techniques are introduced and discussed in the context of signal representation with overcomplete basis.

2.1 Linear ill-posed inverse problems

Ill-posed problems appear frequently in many areas of science and engineering. This term was introduced in the early 20-th century by Jacques Hadamard. Consider the next linear system

$$\tilde{\mathbf{y}} = \mathbf{A}\mathbf{x}, \tag{2.1}$$

where $\tilde{\mathbf{y}} \in \mathbb{R}^{M\times 1}$ is the measured vector, $\mathbf{A} \in \mathbb{R}^{M\times N}$ is a known matrix and $\mathbf{x}$ is the unknown vector that we want to estimate. It models an inverse problem; that is, a situation where the hidden information is computed from external observations. This linear system is said to be well-posed if it satisfies the following three requirements:

1. Existence. For each $\tilde{\mathbf{y}}$, it exists a vector $\mathbf{x}$ such that $\tilde{\mathbf{y}} = \mathbf{A}\mathbf{x}$.

2. Uniqueness. The solution is unique. Formally, if $\mathbf{A}\mathbf{x}_1 = \mathbf{A}\mathbf{x}_2$, then $\mathbf{x}_1 = \mathbf{x}_2$.

3. Stability. The solution is stable with respect to perturbations in the measured vector $\tilde{\mathbf{y}}$, that is, small perturbations on $\tilde{\mathbf{y}}$ do not cause an arbitrary large perturbation in the solution. In other words, the solution depends continuously on the observed data vector $\tilde{\mathbf{y}}$ in some reasonable topology.

If one or more of these conditions are not fulfilled, the linear problem is said to be ill-posed. In practice this happens when the matrix $\mathbf{A}$ is theoretically or numerically rank deficient.

The model presented in (2.1) is noiseless. This is normally an oversimplification either because of a modeling error or because a non-negligible level of noise is normally present in the measurement. The addition of a noise term to the model (2.1) provides a mechanism for dealing with both situations. A model including an additive noise can be expressed as

$$\mathbf{y} = \tilde{\mathbf{y}} + \mathbf{n} = \mathbf{A}\mathbf{x} + \mathbf{n}. \tag{2.2}$$

Many problems in signal processing can be formulated as an underdetermined linear system of equations and this is the case of the problem that is addressed in the next chapter. For this reason, our discussion on ill-posed problems will be focused on the underdetermined framework.

Consider a linear system of equations that has more unknowns than equations, i.e. $N > M$. In this case, the system either has no solution or infinitely many solutions. These two situations violate the first and the second of the Hadamard's conditions exposed above and as a consequence, an underdetermined linear system is, by definition, an ill-posed problem. To avoid the possibility of having no solution, we shall hereafter consider that the matrix $\mathbf{A}$ is full-rank, implying that its columns span the entire space $\mathbb{R}^M$. If we have infinitely many possible solutions $\mathbf{x}$ of (2.1), among which there are some that may "look" better than the others. Then, how can we find the suitable $\mathbf{x}$? As the matrix $\mathbf{A}$ cannot be directly inverted, an alternative objective function must be defined to solve the inverse problem. The goal is to find a functional that measures how close the predicted data fits the measurement. The standard approach is to minimize the Euclidean distance between the observed data and the predicted data from the model. Formally, this can be expressed as

$$\hat{\mathbf{x}} = \min_{\mathbf{x}} \|\mathbf{y} - \mathbf{A}\mathbf{x}\|_2^2 . \tag{2.3}$$

The solution of this problem is well-known and is given by

$$\hat{\mathbf{x}} = \mathbf{A}^{\#}\mathbf{y}, \tag{2.4}$$

where $\mathbf{A}^{\#}$ denotes the Moore-Penrose pseudo-inverse $\mathbf{A}^{\#} = (\mathbf{A}^T\mathbf{A})^{-1}\mathbf{A}^T$. Unfortunately, in presence of noise in the measurement, if the condition number of $\mathbf{A}^{\#}$ (the ratio between the largest and the smallest singular value) is too large, the application of the pseudo-inverse could lead to a solution dominated by noise. Let us analyze hereafter this effect in more detail. First of all, consider the Singular Value Decomposition (SVD) of the matrix $\mathbf{A}$

$$\mathbf{A} = \mathbf{U}\mathbf{\Sigma}\mathbf{V}^T = \sum_{i=1}^{M} \lambda_i \mathbf{u}_i \mathbf{v}_i^T, \tag{2.5}$$

where $\mathbf{U}$ and $\mathbf{V}$ are square matrices of dimensions M and N, respectively, and $\mathbf{\Sigma}$ is a $M \times N$ matrix. Furthermore, $\mathbf{U}$ and $\mathbf{V}$ are unitary matrices. Therefore, $\mathbf{U}\mathbf{U}^T = \mathbf{I}_M$ and $\mathbf{V}\mathbf{V}^T = \mathbf{I}_N$, where $\mathbf{I}_M$ and $\mathbf{I}_N$ denote identity matrices of size M and N, respectively. Bearing in mind (2.5), the pseudo-inverse of the matrix $\mathbf{A}$ is given by

$$\mathbf{A}^{\#} = \sum_{i=1}^{M} \lambda_i^{-1} \mathbf{v}_i \mathbf{u}_i^T. \tag{2.6}$$

By applying the pseudo-inverse, we can find the minimum least squares solution. Recalling (2.2), (2.5) and (2.6), it yields:

$$\hat{\mathbf{x}} = \mathbf{A}^{\#}\mathbf{y} = \left[\sum_{j=1}^{M} \lambda_j^{-1} \mathbf{v}_j \mathbf{u}_j^T\right] \left[\sum_{i=1}^{M} \lambda_i \mathbf{u}_i \mathbf{v}_i^T\right] \mathbf{x} + \sum_{i=1}^{M} \lambda_i^{-1} \mathbf{v}_i \mathbf{u}_i^T \mathbf{n}. \tag{2.7}$$

Let us analyze this expression. If the noise is white, the power distribution of the projection of the noise on all the left singular vectors of $\mathbf{A}$ is uniform and, as consequence, $E\{\left|\mathbf{u}_i^T\mathbf{n}\right|^2\}$ is not a function of i. By applying the pseudo-inverse, the noise components are multiplied by the inverses of the eigenvalues of the matrix $\mathbf{A}$. This issue is critical if the condition number of $\mathbf{A}^{\#}$ is large, because the amplification of the noise components will dominate the final solution and the signal of interest will become hidden under the noise level.

To obtain a meaningful solution of an ill-posed problem, we need to consider regularization methods. Much effort has been devoted in the field of discrete ill-posed problems

to find an appropriate solution less sensitive to noise. These methods incorporate some *a priori* information about the problem. A possible way of regularizing ill-posed inverse problems is to impose a constraint on the norm of the solution. If the coefficients of $\mathbf{x}$, denoted by x_i, with $i = 1, ..., N$, remain unconstrained they are more susceptible to exhibit a high variance. By controlling the norm of the solution, we can control how large the coefficients grow. This problem can be formulated as

$$\min_{\mathbf{x}} \quad \|\mathbf{y} - \mathbf{A}\mathbf{x}\|_2^2 \quad \text{s.t.} \quad \|\mathbf{x}\|_p^p \leq \beta, \tag{2.8}$$

where $\|\mathbf{x}\|_p = \left[\sum_i |x_i|^p\right]^{1/p}$, with $p \geq 0$, denotes the so-called l_p-norm. Consequently, $\|\mathbf{x}\|_p^p = \sum_i |x_i|^p$. Figure 2.1 shows the geometry of l_p norm for $p = 0.5, 1, 2, 3$.

The classical approach to regularize ill-posed problems is to control the energy of the solution using the squared Euclidean norm ($p = 2$):

$$\min_{\mathbf{x}} \quad \|\mathbf{y} - \mathbf{A}\mathbf{x}\|_2^2 \quad \text{s.t.} \quad \|\mathbf{x}\|_2^2 \leq \beta. \tag{2.9}$$

This problem is the so-called Tykhonov regularization or ridge regression [28]. Introducing the Lagrangian, it is easy to obtain the next closed-form solution

$$\mathbf{x}_\lambda^{Tikhonov} = \left(\mathbf{A}^T\mathbf{A} + \lambda\mathbf{I}_N\right)^{-1}\mathbf{A}^T\mathbf{y}, \tag{2.10}$$

where λ is a Lagrange multiplier. Note that inclusion of λ makes the problem non-singular even if $\mathbf{A}^T\mathbf{A}$ is not invertible. The use of the Euclidean norm is widespread in a plethora of fields of engineering. This is principally due to its simplicity as it has been shown in the closed-form solution exposed above. Nevertheless, the following question arises: is $\|\mathbf{x}\|_2^2$ the best choice in (2.8)? It depends. The selection of a proper regularizer depends on the property of the solution that we want to promote and, consequently, it depends on the particular application. The traditional approach is to consider energy constraints (as in the Tykhonov problem) or to promote different forms of smoothness in the solution, yielding regularizers based on the l_2-norm of $\mathbf{x}$ or its derivatives. Unfortunately, Tykhonov regularization leads to non-sparse solutions which typically have non-zero values associated to all the coefficients. While the Tykhonov is an effective way of achieving numerical

stability and increasing the predictive performance, it does not address any problem related to the parsimony of the model or the interpretability of the coefficient values. On the contrary, in the last decade, the use of sparsity-promoting norms [5, 16] has attracted the interest of researchers in many areas. This is the case of l_p-norms with $0 \leq p \leq 1$ in the problem (2.8), which enforce sparsity and promote solutions few non-zero entries. Unfortunately, the problem (2.8) is not convex for $p < 1$ and therefore, the l_1-norm ($p = 1$) is preferred. l_1 regularization has many of the beneficial properties of the l_2 regularization, but yields sparse solutions that can be more easily interpreted.

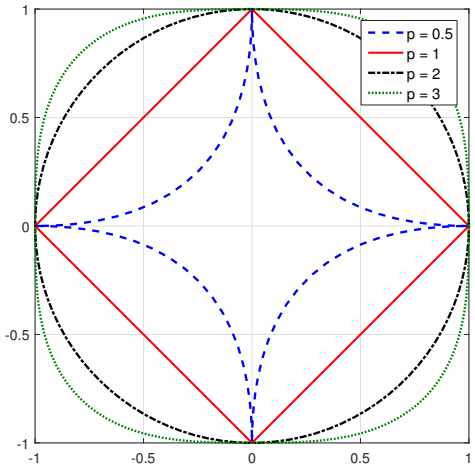

Figure 2.1: Geometry of the l_p norm in two dimensions for different values of p.

2.2 Sparse signal representation

Sparse representation of signals over redundant dictionaries is a hot topic that has attracted the interest of researchers in many fields during the last decade, such as image reconstruction [65], variable selection [66] and compressed sensing [67]. The most basic problem aims to find the sparsest vector $\mathbf{x}$ such that $\mathbf{y} = \mathbf{A}\mathbf{x}$, where $\mathbf{y}$ is the measured vector and $\mathbf{A}$ is known. This matrix $\mathbf{A}$ is called dictionary and is overcomplete, i.e. it has more columns that rows. As a consequence, without imposing a sparsity prior on $\mathbf{x}$, the set of equations $\mathbf{y} = \mathbf{A}\mathbf{x}$ is underdetermined and admits many solutions. Formally, this can be expressed as

$$\min_{\mathbf{x}} \|\mathbf{x}\|_0 \qquad \text{s.t. } \mathbf{y} = \mathbf{A}\mathbf{x}, \tag{2.11}$$

where $\|\cdot\|_0$ denotes the l_0-norm [1]. In presence of noise, the equality constraint can be relaxed in order to allow some error tolerance

$$\min_{\mathbf{x}} \|\mathbf{x}\|_0 \quad \text{subject to} \quad \|\mathbf{y} - \mathbf{A}\mathbf{x}\|_2^2 \leq \varepsilon. \tag{2.12}$$

If there are no restrictions on $\mathbf{A}$ and $\mathbf{y}$ these problems are intractable NP-hard combinatorial problems, in general [14]. Nonetheless, the development of computationally tractable algorithms for solving sparse approximation problems have deserved a lot of attention. These methods can be classified into five major families of techniques:

1. *Brute force*: Solve the combinatorial problem by searching through all possible support sets. In general, this approach is not feasible in terms of computational complexity, even for optimization problems of moderate size.

2. *Non-convex optimization*: Transform the original problem involving the l_0-norm into another related non-convex problem and find a stationary point [3, 23, 68].

3. *Bayesian framework*: Assume a prior distribution of the coefficients that promotes sparsity [69, 70].

4. *Greedy pursuit methods*: Iteratively refine the solution of the sparse approximation problem by successively identifying the coefficients that achieve the greatest improvement in the approximation [17, 71].

5. *Convex relaxations*: Replace the NP-hard combinatorial problem with a convex optimization problem. The traditional approach is to replace the non-convex l_0-norm with a convex surrogate [6, 72, 73].

Among all these techniques greedy pursuit methods and convex relaxations have attracted a special interest. Both families of techniques provide computationally feasible algorithms which are able to obtain the correct solution under some well-defined conditions. If the vector $\mathbf{x}$ is sufficiently sparse, the problem in (2.11) can be relaxed by replacing the l_0-norm by a l_1-norm, defined as $\|\mathbf{x}\|_1 = \sum_i |x_i|$, leading to a convex optimization problem with a lower computational burden

$$\min_{\mathbf{x}} \|\mathbf{x}\|_1 \qquad \text{s.t. } \mathbf{y} = \mathbf{A}\mathbf{x}. \tag{2.13}$$

The conditions that ensure the uniqueness of the solution were studied in [19]. If the observation vector is contaminated by noise, the aforementioned equality constraint can be relaxed as

$$\min_{\mathbf{x}} \|\mathbf{x}\|_1 \quad \text{subject to} \quad \|\mathbf{y} - \mathbf{A}\mathbf{x}\|_2^2 \leq \varepsilon. \tag{2.14}$$

This problem can be alternatively expressed as

$$\min_{\mathbf{x}} \|\mathbf{y} - \mathbf{A}\mathbf{x}\|_2^2 \quad \text{subject to} \quad \|\mathbf{x}\|_1 \leq \beta, \tag{2.15}$$

where the constraint $\|\mathbf{x}\|_1 \leq \beta$, with $\beta \geq 0$, promotes sparsity. This formulation is known as LASSO (Least Absolute Shrinkage and Selector Operator) and was originally proposed by Tibishirani in [74]. The augmented formulation of (2.15) is well-known in signal processing and is commonly called Basis Pursuit Denoising (BPDN) [73]:

$$\min_{\mathbf{x}} \|\mathbf{y} - \mathbf{A}\mathbf{x}\|_2^2 \ + \tau \ \|\mathbf{x}\|_1 \quad \text{with} \ \ \tau \geq 0 \ . \tag{2.16}$$

The three formulations (2.14)-(2.16) are equivalent in the sense that the sets of solutions are the same for all the possible choices of the parameters τ, ε, β. To go from one formulation to the other we only need a proper correspondence of the parameters. Nevertheless, even if the mapping between the regularization parameters exists, this correspondence is not trivial and it is possibly nonlinear and discontinuous [75].

When the vector $\mathbf{x}$ is real, the LASSO problem (2.15), or its equivalent formulation (2.16), can be solved with standard quadratic programming techniques [74]. However, these techniques are time demanding and faster methods are preferred. Osborne et al. [76] and later Efron et al. [46] proposed an efficient algorithm for solving the LASSO. This algorithm is known as "homotopy method" [76] or LARS (Least Angle Regression) [46]. In this thesis this technique will be referred to as LARS/homotopy. A variant of the traditional LASSO, that will be specially useful for the covariance fitting problem that will be addressed later in Chapter 3, is the so-called positive LASSO. In this case, an additional constraint on the entries of the vector $\mathbf{x}$ is considered in the LASSO problem to enforce the components of the vector to be non-negative:

$$\begin{aligned} &\min_{\mathbf{x}} \|\mathbf{y} - \mathbf{A}\mathbf{x}\|_2^2 \\ &\text{subject to} \quad \|\mathbf{x}\|_1 \leq \beta \quad \text{and} \quad x_i \geq 0 \ \forall i. \end{aligned} \tag{2.17}$$

The positive LASSO problem (2.17) can be solved in a efficient way introducing some slight modifications in the traditional LARS/homotopy. This approach was proposed by

Efron et al. in [46], but is not as widely known as the traditional one. Briefly, the algorithm starts with a very large value of τ, and gradually decreases the regularization parameter, until the desired value is attained. As τ evolves, the optimal solution for a given τ, $\mathbf{x}(\tau)$ moves on a piecewise affine path. As the minimizer $\mathbf{x}(\tau)$ is a piecewise-linear function of τ we only need to find the critical regularization parameters $\tau_0, \tau_1, \tau_2, ..., \tau_{stop}$ where the slope changes [75], these values are the so-called breakpoints. The algorithm starts with $\mathbf{x} = \mathbf{0}$ and operates in an iterative fashion calculating the critical regularization parameters $\tau_0 > \tau_1 > \cdots > \tau_{stop} \geq 0$ and the associated minimizers $\mathbf{x}(\tau_0)$, $\mathbf{x}(\tau_1), ..., \mathbf{x}(\tau_{stop})$ where an inactive component of $\mathbf{x}$ becomes positive or an active element becomes equal to zero. Normally, the number of active components increases as τ decreases. Nevertheless, this fact cannot be guaranteed: at some breakpoints, some entries may need to be removed from the active set.

Chapter 3

Sparse covariance fitting for source location

This chapter proposes a new algorithm for finding the angles of arrival of multiple uncorrelated sources impinging on a uniform linear array of sensors. The method is based on sparse signal representation and does not require either the knowledge of the number of the sources or a previous initialization. The proposed technique considers a covariance matrix model based on overcomplete basis representation and tries to fit the unknown signal powers to the sample covariance matrix. Sparsity is enforced by means of an l_1-norm penalty. The final problem is reformulated as an l_1-penalized least-squares functional with non-negative constraints that can be solved efficiently using the LARS/homotopy algorithm. The method described herein is able to provide high resolution with a very low computational burden. It proceeds in an iterative fashion, solving at each iteration a small linear system of equations until a stopping condition is fulfilled. The proposed stopping criterion is based on the residual spectrum and arises in a natural way when the LARS/homotopy is applied to the considered objective function.

3.1 State of the art

3.1.1 Classical methods for finding the angles of arrival

The estimation of the Directions of Arrival (DoA) of multiple sources using sensor arrays is an old problem and plays a key role in array signal processing. During the last five

decades, a plethora of methods have been proposed for finding the directions of arrival of different narrowband signals impinging on a passive array of sensors. These methods can be divided into two categories: parametric and nonparametric estimators.

Nonparametric methods include beamforming and subspace methods. The former relies on scanning the power from different locations. Exponents of this category are conventional beamformer [77] and Capon's method [78]. Conventional beamformer, a.k.a. Bartlett beamformer, suffers from poor spatial resolution and cannot resolve sources within the Rayleigh resolution limit [77]. As it is well known, this lack of resolution can be mitigated only by increasing the number of sensors of the array because improving the SNR or increasing the number of time observations does not increase the resolution. On the contrary, Capon's minimum variance method can resolve sources within the Rayleigh cell if the SNR is high enough, the number of observations is sufficient and the sources are not correlated. Unfortunately, in practice, Capon's power profile is strongly dependent on the beamwidth, which, on its turn, depends on the explored direction and in some scenarios this could lead to a resolution loss. To counteract this drawback, an estimator of the spectral density obtained from the Capon's power estimate was derived in [79] achieving better resolution properties. Here, this method will be referred as Normalized Capon. Another well-known category of nonparametric DoA estimators is the one composed by subspace methods. These algorithms are able to provide high-resolution and outperform beamforming methods. The most prominent member of this family is MUSIC (MUltiple SIgnals Classification) [80], it relies on an appropriate separation between signal and noise subspaces. This characterization is costly and needs a previous estimation of the number of incoming signals.

Parametric methods based on the Maximum Likelihood criterion [81] exhibit a good performance at expenses of a high computational cost. These techniques estimate the parameters of a given model instead of searching the maxima of the spatial spectrum. Unfortunately, they often lead to difficult multidimensional optimization problems with a heavy computational burden.

An interesting algorithm that lies in between the class of parametric and nonparametric techniques is the CLEAN algorithm. This method was firstly introduced by Högbom in [82] and have applications in several areas: array signal processing, image processing, radar and astronomy. Recently, Stoica and Moses have shed light on the semiparametric nature of the algorithm [83]. Broadly speaking, it operates in a recursive manner subtracting at each iteration a fraction of the strongest signal from the observed spatial spectrum.

For those readers interested on a more detailed and comprehensive summary of angle of arrival estimators, the authors refer them to [77] and [84].

3.1.2 Sparse representation in source location

Although there are some pioneering studies carried out in the late nineties, e.g. [85] and [86], the application of sparse representation to direction finding has gained noticeable interest during the last decade. Recent techniques based on sparse representation show promising results that outperform conventional high-resolution methods such as MUSIC. In [85] a recursive weighted minimum-norm algorithm called FOCUSS was presented. This algorithm considers a single snapshot and requires a proper initialization. The extension to the multiple-snapshot case was carried out in [87] and it is known as M-FOCUSS. Unfortunately, as it is described in [88], this technique is computationally expensive and requires the tuning of two hyperparameters that can affect the performance of the method significantly.

If multiple snapshots can be collected in an array of sensors, they can be used to improve the estimation of the angles of arrival. Several approaches for summarizing multiple observations have been proposed in the literature. The first of these approaches is the so-called l_1-SVD presented by Malioutov et al. in [89]. This method is based on the application of a Singular Value Decomposition (SVD) over the received data matrix and leads to a second-order cone optimization problem. This algorithm requires an initial estimation of the number of sources. Although it does not have to be exact, a small error is needed for a good performance. An underestimation or an overestimation of the number of sources provokes a degradation in the performance of the method. Even if the effect of an incorrect determination of the number of sources has no catastrophic consequences, such as the disappearance of the sources in MUSIC, the performance of the algorithm can be considerably degraded. Another important drawback is that l_1-SVD depends on a user-defined parameter which is not trivial to select. An alternative approach to summarize multiple snapshots is the use of mixed norms over Multiple Measurement Vectors (MMV) that share the same sparsity pattern [87], [90]. This formulation is useful in array signal processing, specially, when the number of snapshots is smaller than the number of sensors. If we assume that the snapshots are collected during the coherence time of the angles, the position of the sources keep identical among the snapshots; the only difference between them resides in the amplitudes of the impinging rays. Basically, this approach, which is out of the scope of this chapter, tries to combine multiple snapshots using the l_2 norm and to promote sparsity on the spatial dimension by means of the l_1-norm. Unfortunately, this joint optimization problem is complex and requires a high computational burden. When the number of snapshots increases, the computational load becomes too high for practical real-time source location. Recently, new techniques based on a covariance matrix fitting approach have been considered to summarize multiple snapshots, e. g. [91], [92] and [93].

Basically, these methods try to fit the covariance matrix to a certain model. The main advantage of covariance fitting approaches is that they lead to convex optimization problems with an affordable computational burden. Moreover, they do not require a previous estimation of the number of incoming sources or heavy computations such as SVD of the data. It should be also pointed out that since these methods work directly with the covariance matrix, less storage space is needed because they do not need to store huge amounts of real-time data. The technique proposed by T. Yardibi et al. in [91] leads to an optimization problem that can be solved efficiently using Quadratic Programming (QP). In the case of the approach exposed by J. S. Picard et al. in [92], the solution is obtained by means of Linear Programming (LP). The main drawback of this last method is that it depends on a user defined parameter that is difficult to adjust. In the same way, the authors of [94] propose a new method which is based on a hyperparameter that has been heuristically determined. On the contrary, Stoica et al. propose in [93] and [95] an iterative algorithm named SPICE (SParse Iterative Covariance-based Estimation approach), that can be used in noisy data scenarios without the need for choosing any hyperparameter. The major drawback of this method is that it needs to be initialized.

3.2 Chaper contribution

This chapter proposes a simple, fast and accurate algorithm for finding the angles of arrival of multiple sources impinging on a uniform linear array. In contrast to other methods in the literature, the proposed technique does not depend on user-defined parameters and does not require either the knowledge of the number of sources or initialization. It assumes white noise and that the point sources are uncorrelated.

The method considers a structured covariance matrix model based on over-complete basis representation and tries to fit the unknown signal powers of the model to the sample covariance. Sparsity is promoted by means of a l_1-norm penalty imposed on the powers. The final problem is reduced to an objective function with a non-negative constraint that can be solved efficiently using the LARS/homotopy algorithm, which is, in general, faster than QP [46] and LP [75]. The method described herein proceeds in an iterative manner solving at each iteration a small linear system of equations until a stopping condition is fulfilled. The proposed stopping criterion is based on the residual spectrum and arises in a natural way when the LARS/homotopy is applied to the considered objective function. To the best of our knowledge this stopping condition has never been considered before in sparse signal representation.

3.3 The proposed method

Consider L narrowband signals $\{x_i[k]\}_{i=1}^{L}$ impinging on an array of M sensors. The kth observation can be expressed as:

$$\mathbf{y}[k] = \mathbf{S}(\boldsymbol{\theta})\,\mathbf{x}[k] + \mathbf{w}[k] \qquad k = 1, \ldots, N, \tag{3.1}$$

where $\mathbf{x}[k] = \begin{bmatrix} x_1[k] & \cdots & x_L[k] \end{bmatrix}^T$ is the vector of unknown source signals, the matrix $\mathbf{S}(\boldsymbol{\theta}) \in \mathbb{C}^{M\times L}$ is the collection of the steering vectors corresponding to the angles of arrival of the sources $\boldsymbol{\theta} = [\theta_1, \ldots, \theta_L]^T$, that is, $\mathbf{S}(\boldsymbol{\theta}) = [\mathbf{s}(\theta_1) \cdots \mathbf{s}(\theta_L)]$; and $\mathbf{w}[k] \in \mathbb{C}^{M\times 1}$ denotes a zero-mean additive noise, spatially, and temporally white, independent of the sources with covariance matrix $\sigma_w^2\mathbf{I}_M$, where $\mathbf{I}_M$ denotes the identity matrix of size M.

Taking into account (3.1) the spatial covariance matrix can be expressed as

$$\mathbf{R} = E\left\{\mathbf{y}[k]\,\mathbf{y}^H[k]\right\} = \mathbf{S}(\boldsymbol{\theta})\,\mathbf{P}\mathbf{S}^H(\boldsymbol{\theta}) + \sigma_w^2\mathbf{I}_M, \tag{3.2}$$

where $\mathbf{P} = E\left\{\mathbf{x}[k]\,\mathbf{x}^H[k]\right\}$. The classical direction finding problem can be reformulated as a sparse representation problem. With this aim, let us consider an exploration grid of G equally spaced angles $\boldsymbol{\Phi} = \{\phi_1, \ldots, \phi_G\}$ with $G \gg M$ and $G \gg L$. If the set of angles of arrival of the impinging signals $\boldsymbol{\theta}$ is a subset of $\boldsymbol{\Phi}$, the received signal model (3.1) can be rewritten in terms of an overcomplete matrix $\mathbf{S}_G$ constructed by the horizontal concatenation of the steering vectors corresponding to all the potential source locations.

$$\mathbf{y}[k] = \mathbf{S}_G\mathbf{x}_G[k] + \mathbf{w}[k], \tag{3.3}$$

where $\mathbf{S}_G \in \mathbb{C}^{M\times G}$ contains the steering vectors corresponding to the angles of the grid $\mathbf{S}_G = [\mathbf{s}_1 \cdots \mathbf{s}_G]$, with $\mathbf{s}_i = \mathbf{s}(\phi_i)$, and $\mathbf{x}_G[k] \in \mathbb{C}^{G\times 1}$ is a sparse vector. The non-zero entries of $\mathbf{x}_G[k]$ are the positions that corresponds to the source locations. In other words, the nth element of $\mathbf{x}_G[k]$ is different from zero and equal to the qth component of the vector $\mathbf{x}[k]$ defined in (3.1), denoted by $x_q[k]$, if and only if $\phi_n = \theta_q$. It is important to point out that the matrix $\mathbf{S}_G$ is known and does not depend on the source locations.

The assumption that the set of angles of arrival is a subset of $\boldsymbol{\Phi}$ is only required for the derivation of the algorithm. Obviously, it does not always hold. Actually, this is a common assumption in many exploration methods in the direction finding literature (e.g., Capon, Normalized Capon, MUSIC, etc). In the case that $\boldsymbol{\theta} \nsubseteq \boldsymbol{\Phi}$, the contribution of the sources leaks into the neighboring elements of the grid.

Bearing in mind (3.3) and assuming a white noise with covariance matrix $\sigma_w^2\mathbf{I}_M$, the spatial covariance matrix of (3.1) can be rewritten in terms of $\mathbf{S}_G$

$$\mathbf{R} = E\left\{\mathbf{y}\left[k\right]\mathbf{y}^{H}\left[k\right]\right\} = \mathbf{S}_G\mathbf{D}\mathbf{S}_G^{H} + \sigma_w^2\mathbf{I}_M, \tag{3.4}$$

with $\mathbf{D} = E\left\{\mathbf{x}_G\left[k\right]\mathbf{x}_G^{H}\left[k\right]\right\}$. An important remark is that $\mathbf{D} \in \mathbb{C}^{G\times G}$ is different to the source covariance matrix $\mathbf{P} \in \mathbb{C}^{L\times L}$ introduced in (3.2). Actually, since only L^2 entries out of G^2 can differ from zero, $\mathbf{D}$ is a sparse matrix.

A common assumption in many direction finding problems is that sources are uncorrelated. Under this assumption, the matrix $\mathbf{D}$ is a diagonal matrix with only L non-zero entries given by $\text{diag}\left(\mathbf{D}\right) = \left[\begin{array}{ccc} p_1 & \cdots & p_G \end{array}\right]^T = \mathbf{p}$, where $\mathbf{p} \in \mathbb{R}_+^{G\times 1}$. Note that $\mathbf{p}$ is a $G\times 1$ sparse vector with non-zero entries at positions corresponding to source locations. Furthermore, the elements of $\mathbf{p}$ are real-valued and non-negative.

To cast the problem into a positive LASSO with real variables let us make some manipulations on (3.4). Applying the next property of vectorization $\text{vec}\left\{\mathbf{ABC}\right\} = \mathbf{A}^T\otimes\mathbf{B}\,\text{vec}\left\{\mathbf{B}\right\}$ to (3.4), it yields

$$\text{vec}\left\{\mathbf{R}\right\} = \mathbf{S}_G^{*}\otimes\mathbf{S}_G\,\text{vec}\left\{\mathbf{D}\right\} + \sigma_w^2\ \ \text{vec}\left\{\mathbf{I}_M\right\}, \tag{3.5}$$

where $\otimes$ and $\text{vec}\left\{\cdot\right\}$ denote the Kronecker product and the vectorization operator, respectively. It should be remarked that the result of $\mathbf{S}_G^{*}\otimes\mathbf{S}_G \in \mathbb{C}^{M^2\times G^2}$.

Since $\mathbf{D}$ is a diagonal matrix because the sources are uncorrelated, only G columns of $\mathbf{S}_G^{*}\otimes\mathbf{S}_G$ have to be taken into account. Using this fact, the dimensionality of the problem can be reduced. Hence, it is straightforward to rewrite the expression (3.5) in terms of vector $\mathbf{p}$ just removing some columns of $\mathbf{S}_G^{*}\otimes\mathbf{S}_G$:

$$\text{vec}\left\{\mathbf{R}\right\} = \tilde{\mathbf{A}}\mathbf{p} + \sigma_w^2\ \ \text{vec}\left\{\mathbf{I}_M\right\}, \tag{3.6}$$

with $\tilde{\mathbf{A}} = \left[\begin{array}{cccc} \mathbf{s}_1^{*}\otimes\mathbf{s}_1 & \mathbf{s}_2^{*}\otimes\mathbf{s}_2 & \cdots & \mathbf{s}_G^{*}\otimes\mathbf{s}_G \end{array}\right]$. Note that $\tilde{\mathbf{A}} \in \mathbb{C}^{M^2\times G}$.

The complex-valued equality in (3.6), can be transformed into a real-valued one by separating the real and the imaginary parts of the matrices involved in expression (3.6). The last equation can be reformulated as

$$\left[\begin{array}{c} \mathbf{r}_r \\ \mathbf{r}_i \end{array}\right] = \left[\begin{array}{c} \tilde{\mathbf{A}}_r \\ \tilde{\mathbf{A}}_i \end{array}\right]\mathbf{p} + \left[\begin{array}{cc} \sigma_w^2 & \text{vec}\left\{\mathbf{I}_M\right\} \\ & \mathbf{0}_{M^2} \end{array}\right], \tag{3.7}$$

where

$$\begin{array}{ll} \mathbf{r}_r = \Re\left\{\text{vec}\left[\mathbf{R}\right]\right\} & \tilde{\mathbf{A}}_r = \Re\{\tilde{\mathbf{A}}\} \\ \mathbf{r}_i = \Im\left\{\text{vec}\left[\mathbf{R}\right]\right\} & \tilde{\mathbf{A}}_i = \Im\{\tilde{\mathbf{A}}\} \end{array}.$$

In the expression (3.7), vec$\{\mathbf{I}_M\}$ denotes the vectorization of the identity matrix of dimensions $M \times M$ and $\mathbf{0}_{M^2}$ is a column vector of zeros of length M^2. The operators $\Re\{\cdot\}$ and $\Im\{\cdot\}$ denote the real and the imaginary part of its argument, respectively.

More compactly, the expression (3.7) can be rewritten as

$$\mathbf{r} = \mathbf{A}\mathbf{p} + \mathbf{n}, \tag{3.8}$$

with obvious definitions for $\mathbf{r}$, $\mathbf{A}$, $\mathbf{p}$, and $\mathbf{n}$. Note that $\mathbf{r}$ and $\mathbf{n} \in \mathbb{R}^{2M^2 \times 1}$ and $\mathbf{A} \in \mathbb{R}^{2M^2 \times G}$.

Unfortunately, the spatial covariance matrix is unknown in practice and is normally replaced by the sample covariance matrix $\hat{\mathbf{R}}$ obtained from a set of N observations $\{\mathbf{y}[k]\}_{i=1}^{N}$, given by $\hat{\mathbf{R}} = \frac{1}{N}\sum_{k=1}^{N} \mathbf{y}[k]\,\mathbf{y}^H[k]$. To estimate $\mathbf{p}$, let us consider the following constrained least-squares problem

$$\begin{aligned} &\min_{\mathbf{p}} \|\hat{\mathbf{r}} - \mathbf{A}\mathbf{p}\|_2^2 \\ &\text{subject to} \quad p_i \geq 0 \quad i = 1, \ldots, G \\ &\|\mathbf{p}\|_1 = \sum_{j=1}^{G} p_j \leq \beta \quad \text{with} \quad \beta \geq 0, \end{aligned} \tag{3.9}$$

where $\hat{\mathbf{r}} = \begin{bmatrix} \Re\left\{\text{vec}(\hat{\mathbf{R}})\right\} \\ \Im\left\{\text{vec}(\hat{\mathbf{R}})\right\} \end{bmatrix}$.

Note that (3.9) is a positive LASSO problem. The main idea behind the formulation presented in (3.9) is to fit the unknown powers to the model such that the solution is sparse. The method tries to minimize the residual, or in other words, tries to maintain the fidelity of the sparse representation with the estimated sample covariance matrix subject to a non-negative constraint on the powers and $\sum_{j=1}^{G} p_j \leq \beta$. This last constraint promotes sparsity, as it was exposed in (2.15), but also imposes a bound on the received signal power. Unfortunately, the parameter β is unknown and has to be estimated.

The solution of the problem (3.9) is very sensitive to the value of β, a little error in the estimation of this parameter can lead to a wrong solution vector. To overcome this drawback, instead of solving (3.9), let us consider the next equivalent formulation

$$\begin{aligned} &\min_{\mathbf{p}} \|\hat{\mathbf{r}} - \mathbf{A}\mathbf{p}\|_2^2 + \tau \|\mathbf{p}\|_1 \\ &\text{s.t.} \quad \tau \geq 0, \quad p_i \geq 0 \quad i = 1, \ldots, G. \end{aligned} \tag{3.10}$$

Problems (3.9) and (3.10) are equivalent in the sense that the path of solutions of (3.9) parameterized by a positive β matches with the solution path (3.10) as τ varies. To go

from one formulation to the other one, we need to find the proper correspondence between the parameters τ and β.

The problem (3.10) can be solved with the LARS/homotopy algorithm for the positive LASSO problem. This method operates in an iterative fashion computing the critical regularization parameters $\tau_0 > \tau_1 > \cdots > \tau_{\text{stop}} \geq 0$ and the associated minimizers $\mathbf{p}(\tau_0)$, $\mathbf{p}(\tau_1)$,$\cdots$, $\mathbf{p}(\tau_{\text{stop}})$, where an inactive component of $\mathbf{p}$ becomes positive or an active element becomes equal to zero. Let us remark that there is only one new candidate to enter or leave the active set at each iteration (this is the 'one at a time condition' exposed by Efron et al. in reference [46]).

The algorithm is based on the computation of the so-called vector of residual correlations, or just residual correlation, $\mathbf{b}(\tau) = \mathbf{A}^T(\hat{\mathbf{r}} - \mathbf{A}\mathbf{p}(\tau))$ at each iteration. The method starts with $\mathbf{p} = \mathbf{0}$, which is the solution of (3.10) for all the $\tau \geq \tau_0 = 2\max_i \left(\mathbf{A}^T\hat{\mathbf{r}}\right)_i$, where $\left(\mathbf{A}^T\hat{\mathbf{r}}\right)_i$ denotes the ith component of the vector $\mathbf{A}^T\hat{\mathbf{r}}$, and proceeds in an iterative manner, solving at each iteration a linear system of equations with a reduced order. The whole algorithm is described in Appendix 3.A.3 and summarized in Algorithm 1 (See the references [46,96,97,28] for further details). This iterative procedure must be halted when a stopping condition is satisfied. This stopping criterion, will be presented in the next Section.

It should be pointed out that the least squares error of the covariance fitting method exposed in (3.10) decreases at each iteration of the LARS/homotopy algorithm. This result is justified by the next two theorems.

Theorem 3.1 *The sum of the powers increases monotonically at each iteration of the algorithm. Given two vectors with non-negative elements* $\mathbf{p}(\tau_{n+1})$ *and* $\mathbf{p}(\tau_n)$ *that are minimizers of (3.10) for two breakpoints* τ_{n+1} *and* τ_n*, respectively, with* $\tau_n > \tau_{n+1}$*, it can be stated that* $\left\|\mathbf{p}(\tau_{n+1})\right\|_1 \geq \left\|\mathbf{p}(\tau_n)\right\|_1$.

Proof*: See Appendix 3.A.1.*

Theorem 3.2 *The least squares error* $\|\hat{\mathbf{r}} - \mathbf{A}\mathbf{p}(\tau)\|_2^2$ *decreases at each iteration of the LARS/homotopy algorithm. Given two vectors with non-negative elements* $\mathbf{p}(\tau_n)$ *and* $\mathbf{p}(\tau_{n+1})$ *that are minimizers of (3.10) for two consecutive breakpoints* τ_n *and* τ_{n+1} *of the LARS/homotopy, with* $\tau_n > \tau_{n+1}$*, it can be stated that* $\|\hat{\mathbf{r}} - \mathbf{A}\mathbf{p}(\tau_{n+1})\|_2^2 \leq \|\hat{\mathbf{r}} - \mathbf{A}\mathbf{p}(\tau_n)\|_2^2$.

Proof*: See Appendix 3.A.2.*

Algorithm 1 Proposed method

INITIALIZATION: $\mathbf{p} = \mathbf{0}$, $\tau_0 = 2 \max_i \left(\mathbf{A}^T \hat{\mathbf{r}}\right)_i$, $n = 0$

$J = active\ set = \varnothing$, $I = inactive\ set = J^c$

while $\neq$stopping criterion and $\exists\ i \in I$ such that $b_i > 0$ **do**

1) Compute the residual correlation $\mathbf{b} = \mathbf{A}^T (\hat{\mathbf{r}} - \mathbf{A}\mathbf{p})$

2) Determine the maximal components of $\mathbf{b}$. These will be the non-zero elements of $\mathbf{p}(\tau_n)$ (active components).

$$J = \arg\max \{b_j\}, \quad I = J^c$$

3) Calculate the update direction $\mathbf{u}$ such that all the active components lead to an uniform decrease of the residual correlation (equiangular direction).

$$\mathbf{u}_J = \left(\mathbf{A}_J^T \mathbf{A}_J\right)^{-1} \mathbf{1}_J$$

4) Compute the step size γ such that a new element of the $\mathbf{b}$ becomes equal to the maximal ones ($\exists\ i \in I$ such that $b_i(\tau_{n+1}) = b_{j \in J}(\tau_{n+1})$) or one non-zero component of $\mathbf{p}$ becomes zero ($\exists\ j \in J$ such that $\mathbf{p}_j(\tau_{n+1}) = 0$).

5) Actualize $\mathbf{p} \leftarrow \mathbf{p} + \gamma \mathbf{u}$, $\tau_{n+1} = \tau_n - 2\gamma$, $n = n + 1$

end while

3.3.1 Stopping criterion: the cumulative spectrum

The definition of an appropriate stopping criterion is of paramount importance because it determines the final regularization parameter τ_{stop} and consequently the number of active positions in the solution vector. In general, larger values of τ produce sparser solutions. Nevertheless, this fact cannot be guaranteed: at some breakpoints, some entries may need to be removed from the active set.

Most of the traditional approaches exposed in the literature for choosing the regularization parameter in discrete ill-posed problems are based on the norm of the residual error in one way or another, e. g. discrepancy principle, cross validation and the L-curve. Nevertheless, recent publications [98], [99] suggest the use of a new parameter-choice method based on the residual spectrum. This technique is based on the evaluation of the shape of the Fourier transform of the residual error. To the best of our knowledge, this approach has never been used as a stopping criterion in sparse representation problems. The method exposed herein is inspired in the same idea with some slight modifications. The main difference resides in the fact that no Fourier transform needs to be computed over the residual, as it will be exposed later on, the spatial spectrum of the residual arises in a natural way when the LARS/homotopy is applied to (3.10). The following result is the key point of the stopping criterion proposed in this chapter.

Theorem 3.3 *When the LARS/homotopy is applied to the problem (3.10), the residual correlation at the k-th iteration of the algorithm, expressed as* $\mathbf{b}\left(\tau_k\right)=\mathbf{A}^T(\hat{\mathbf{r}}-\mathbf{A}\mathbf{p}(\tau_k))$*, is equivalent to the Bartlett estimator applied to the residual covariance matrix* $\hat{\mathbf{C}}_k = \hat{\mathbf{R}} - \sum_{i=1}^{G} p_i\left(\tau_k\right)\mathbf{s}_i\mathbf{s}_i^H$*. Then, the ith component of the vector of residual correlations satisfies* $\mathbf{b}_i(\tau_k) = \mathbf{s}_i^H\hat{\mathbf{C}}_k\mathbf{s}_i$.

Proof: *See Appendix 3.A.4*

This theorem provides an alternative interpretation of the residual correlation at the kth iteration $\mathbf{b}\left(\tau_k\right)$ which can be seen as a residual spatial spectrum. Bearing in mind this idea and under the assumption that the noise is zero-mean and spatially white, the following parameter-choice method is proposed: to stop as soon as the residual correlation resembles white noise.

Under the assumption that the noise is spatially white, the power is distributed uniformly over all the angles of arrival and the spatial spectrum has to be flat. To determine whether the residual correlation corresponds to a white noise spectrum a statistical tool has to be considered. Several tests are available in the literature to test the hypothesis of white noise. Herein, the metric that will be considered to see if the residual looks like noise is:

$$c_k\left(l\right) = \frac{\sum_{i=1}^{l}\left|b_i\left(\tau_k\right)\right|}{\sum_{i=1}^{G}\left|b_i\left(\tau_k\right)\right|} \qquad l = 1, \cdots, G, \tag{3.11}$$

where the subindex k denotes the kth iteration of the LARS/homotopy algorithm, with $k = 0, \cdots, k_{stop}$. The metric c_k is a slight modification of the conventional normalized cumulative periodogram proposed by Bartlett in [100] and later by Durbin in [101] . Traditionally, the cumulative periodogram has been defined for real-valued time series. In the real case, the spectrum is symmetric and only half of the spectrum needs to be computed. However, it can be easily extended to embrace complex-valued vectors as it is shown in (3.11). Throughout this entire chapter, the metric presented in (3.11) will be referred to as Normalized Cumulative Spectrum (NCS).

For an ideal white noise the plot of the NCS is a straight line and resembles the cumulative distribution of a uniform distribution. Thus, any distributional test, such as the Kolmogorov-Smirnov (K-S) test, can be considered to determine the 'goodness of fit'

between the cumulative spectrum and the theoretical straight line. In [100] Bartlett proposed the use of the Kolmogorov-Smirnov test which is based on the largest deviation in absolute value between the cumulative spectrum and the theoretical straight line. The K-S test rejects the hypothesis of white noise whenever the maximum deviation between the cumulative spectrum and the straight line is too large. On the contrary, the cumulative spectrum is considered white noise if it lies within the Kolmogorov-Smirnov limits. The upper and the lower K-S limits, as a function of index l, are given by

$$\frac{l}{G} \pm \frac{\delta}{\sqrt{MN}}, \tag{3.12}$$

where $\delta = 1.36$ for the 95% confidence band and $\delta = 1.63$ for the 99% band.

Notice that the NCS does not require an accurate estimation of the noise power at the receiver. Since the cumulative spectrum (3.11) is normalized with respect to the average power at each kth iteration, the decision metric only depends on the shape of the spatial spectrum.

The proposed stopping condition is: to stop as soon as the residual correlation resembles white noise, that is, when the NCS lies within the Kolmogorov-Smirnov limits.

3.4 Numerical results

The aim of this Section is to analyze the performance of the covariance fitting method proposed in this chapter. To carry out this objective, some simulations have been done in Matlab. Throughout the simulations, a uniform grid with 1^o of resolution has been considered for all the analyzed techniques. Furthermore, a zero-mean white Gaussian noise with power $\sigma_w^2 = 1$ has been considered. The generated source signals are uncorrelated and distributed as circularly symmetric i.i.d. complex Gaussian variables with zero mean. Since the same power P will be considered for all the sources, throughout this entire section the signal to noise ratio (SNR) is defined by $SNR(dB) = 10\log_{10}(\frac{P}{\sigma_w^2})$.

To illustrate the algorithm and the new stopping condition based on the cumulative spectrum, we have considered four uncorrelated sources located at -36^o, -30^o, 30^o, 50^o that impinge on a uniform linear array (ULA) with $M = 10$ sensors separated by half the wavelength. The SNR is set to 0 dB and the sample covariance matrix is computed with $N = 600$ snapshots. Figure 3.1 and Figure 3.2 show the evolution of the normalized cumulative spectrum and the vector of residual correlations, respectively. As it is shown in Figure 3.1, the algorithm stops after 16 iterations, when the NCS lies within the

Kolmogorov-Smirnov limits of the 99% confidence band. The final solution $\mathbf{p}$ is shown in the Figure 3.3. Note that the residual spectrum of the final solution in Figure 3.2 is almost flat and the residual correlation resembles white noise.

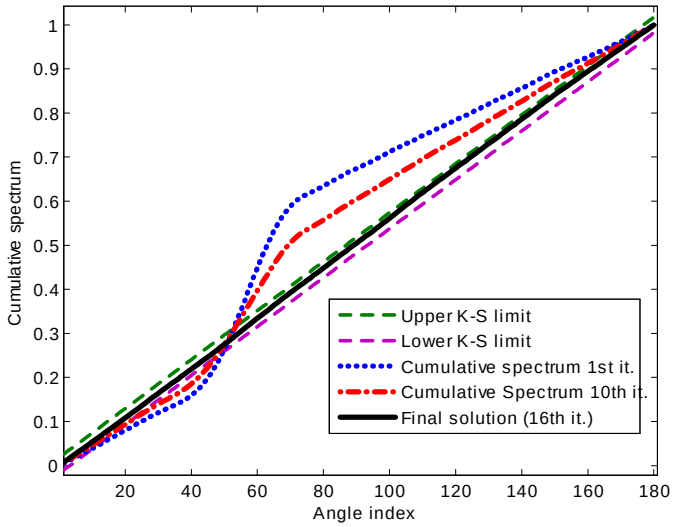

Figure 3.1: Cumulative Spectrum as a function of the angle index. The scenario is composed by four sources located at $\boldsymbol{\theta} = [-36^o, -30^o, 30^o, 50^o]$, $M = 10$ sensors, $N = 600$ snapshots, SNR = 0 dB. The final solution is achieved after 16 iterations of the LARS/homotopy and it is chosen as the first one that lies within the Kolmogorov-Smirnov limits of the 99% confidence band.

Next, the probability of resolution of the covariance fitting method as a function of the SNR is investigated. With this aim, we have considered two uncorrelated sources located at -36^o and -30^o that impinge on a ULA with $M = 9$ sensors. Both sources transmit with the same power and the sample covariance has been computed with $N = 1000$ snapshots. Figure 3.4 shows the results of the covariance fitting method compared to other classical estimators: MUSIC [80], Capon [78] and Normalized Capon [79]. In order to make a fair comparison between the different techniques, the number of sources of the MUSIC algorithm has been estimated with the Akaike Information Criterion (AIC) [83]. The curves in Figure 3.4 are averaged over 300 independent simulation runs. From this figure, it is clear that the proposed covariance fitting technique outperforms the other classical estimators and it is about 6 dB better than the MUSIC algorithm and about 12 dB better than the Normalized Capon method.

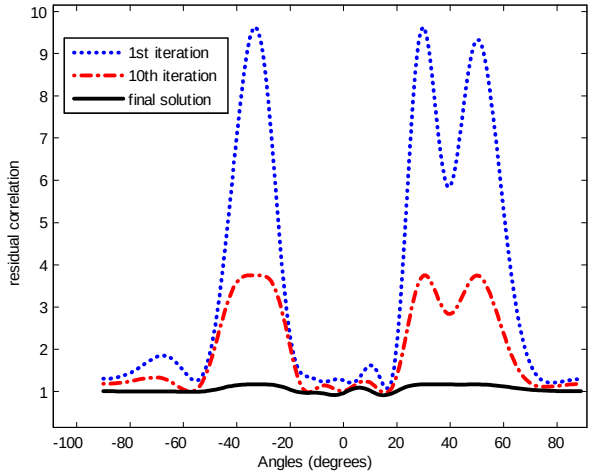

Figure 3.2: Evolution of the vector of residual correlations $\mathbf{b}$ with the iterations. The final solution is achieved after 16 iterations and is chosen as the first one that lies within the Kolmogorov-Smirnov limits of the 99%. Note that residual correlation is almost flat.

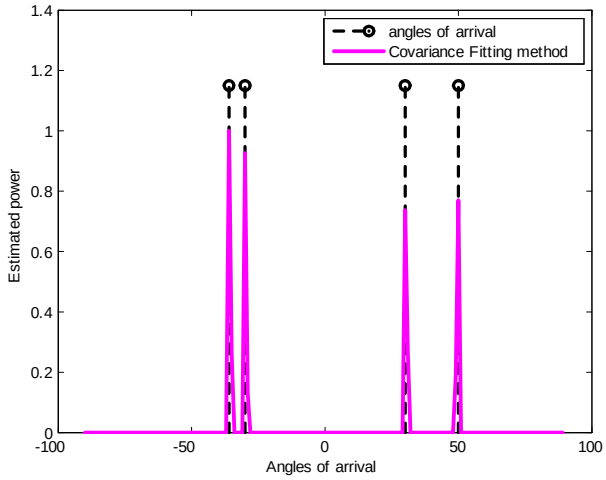

Figure 3.3: The power estimate of the proposed covariance matrix fitting method. Final solution $\mathbf{p}$ obtained by the LARS/homotopy after 16 iterations. The settings are: four sources located at $\boldsymbol{\theta} = [-36^o, -30^o, 30^o, 50^o]$, $M = 10$ sensors, $N = 600$ snapshots, SNR = 0 dB.

Next, the performance of the proposed method in terms of Root Mean Square Error (RMSE) is analyzed and presented in Figure 3.5. Two uncorrelated sources separated by $\Delta\theta = 6^o$ that impinge on an array of $M = 9$ sensors were taken into account in the simulations. In this case, the positions of the sources do not correspond to the angles of the grid. With this aim, the angle of the first source θ_1 is generated as a random variable following a uniform distribution between -80^o and 80^o and the angle of the second source is generated as $\theta_2 = \theta_1 + \Delta\theta$. The sample covariance has been computed with 900 snapshots. Figure 3.5 shows the RMSE of the proposed method and MUSIC as a function of the SNR as long as the two sources are resolved with a probability equal to 1. In the case of MUSIC the determination of the number of signal sources is performed by the AIC. The two curves are based on the average of 300 independent runs. From Figure 3.5 it can be concluded that at low SNR the proposed method outperforms MUSIC. When the SNR increases both methods tends to exhibit the same performance.

Finally, the resolution capability of the method as a function of the number of snapshots is investigated. The scenario considered for this purpose is the following: two sources located at $\theta_1 = -36^o$ and $\theta_1 = -30^o$ that impinge on a ULA with $M = 9$ sensors. In this case, the transmitted signals have constant modulus, which is a common situation in communications applications, $s_1(t) = e^{j\varphi_1(t)}$ and $s_2(t) = e^{j\varphi_2(t)}$. The signal phases $\{\varphi_k(t)\}_{k=1}^2$ are independent and follow a uniform distribution in $[0, 2\pi]$. Figure 3.6 shows the probability of resolution of the proposed method and MUSIC as a function of the number of snapshots N. In this case the signal to noise ratio is fixed to 1 dB. As in the previous cases, in order to make a fair comparison between the two techniques, the number of sources of the MUSIC algorithm has been determined using AIC. The curves were obtained by averaging the results of 500 independent trials. Note that the covariance fitting method clearly outperforms MUSIC and is able to resolve the two sources with a probability greater than 95% if $N \geq 30$.

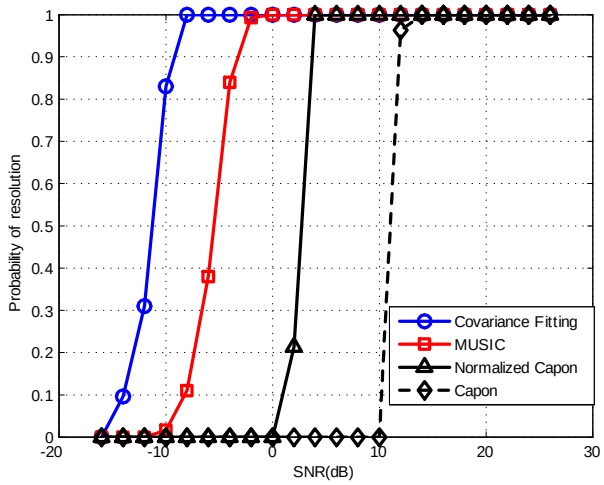

Figure 3.4: Probability of resolution against SNR. $\boldsymbol{\theta} = [-36^o, -30^o]$, $M = 9$ sensors, $N = 1000$ snapshots. The curves were obtained by averaging the results of 300 independent simulation runs.

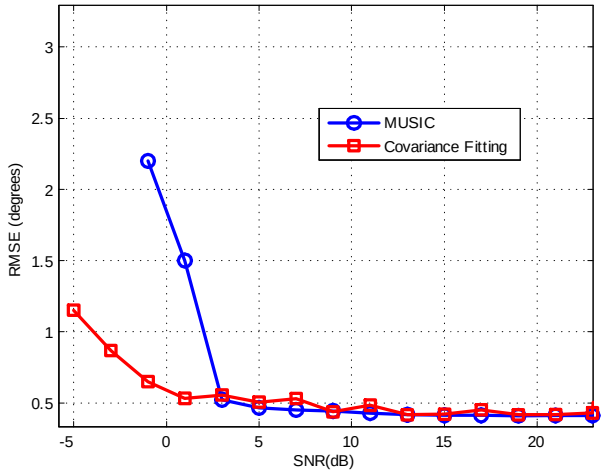

Figure 3.5: Root mean square error as a function of the signal-to-noise ratio. Two uncorrelated sources separated by $\Delta\theta = 6^o$. $M = 10$ sensors, $N = 900$ snapshots, SNR = 0 dB. The curves were obtained by averaging the results of 300 independent simulation runs.

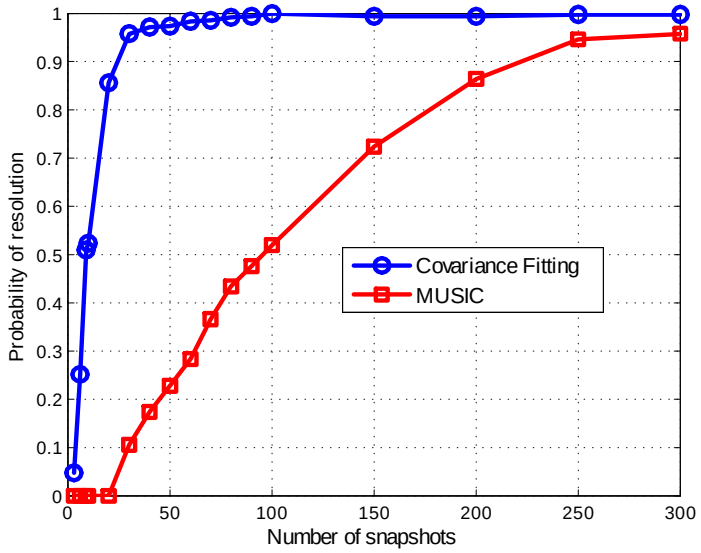

Figure 3.6: Probability of resolution as a function of the number of snapshots. Two uncorrelated sources located at $\boldsymbol{\theta} = [-36^o, -30^o]$, $M = 9$ sensors. The curves were obtained by averaging the results of 500 independent trials.

3.5 Conclusions

A new method for finding the directions of arrival of multiple sources that impinge on a ULA has been presented in this chapter. The proposed technique is based on sparse signal representation and outperforms classical direction finding algorithms, even subspace methods, in terms of RMSE and probability of resolution. The proposed technique assumes white noise and uncorrelated point sources. Furthermore, it does not require either the knowledge of the number of sources or a previous initialization.

3.A Appendix

3.A.1 Proof of Theorem 3.1

The LARS/homotopy provides all the breakpoints $\tau_0 > \tau_1 > \cdots > \tau_{\text{stop}} \geq 0$ and the associated solutions $\mathbf{p}(\tau_0), \mathbf{p}(\tau_1), \ldots, \mathbf{p}(\tau_{\text{stop}})$ where a new component enter or leaves the support (the set of active elements) of $\mathbf{p}(\tau)$. It can be proved that the sum of powers increases monotonically at each iteration of the algorithm. Suppose two non-negative vectors $\mathbf{p}(\tau_n)$ and $\mathbf{p}(\tau_{n+1})$ that are minimizers of (3.10) for the regularization parameters τ_n and τ_{n+1}, respectively, with $\tau_n > \tau_{n+1} \geq 0$. The following inequality holds for the breakpoint τ_n

$$\|\hat{\mathbf{r}} - \mathbf{A}\mathbf{p}(\tau_n)\|_2^2 + \tau_n \|\mathbf{p}(\tau_n)\|_1 \leq \|\hat{\mathbf{r}} - \mathbf{A}\mathbf{p}(\tau_{n+1})\|_2^2 + \tau_n \|\mathbf{p}(\tau_{n+1})\|_1 . \tag{3.13}$$

Note that the regularization parameter τ_n is the same on both sides of the inequality. The expression on the right-hand side of the inequality (3.13) is equal to $\|\hat{\mathbf{r}} - \mathbf{A}\mathbf{p}(\tau_{n+1})\|_2^2 + \tau_{n+1} \|\mathbf{p}(\tau_{n+1})\|_1 + (\tau_n - \tau_{n+1}) \|\mathbf{p}(\tau_{n+1})\|_1$. Therefore, the expression (3.13) can be rewritten as

$$\|\hat{\mathbf{r}} - \mathbf{A}\mathbf{p}(\tau_n)\|_2^2 + \tau_n \|\mathbf{p}(\tau_n)\|_1 \leq \|\hat{\mathbf{r}} - \mathbf{A}\mathbf{p}(\tau_{n+1})\|_2^2 + \tau_{n+1} \|\mathbf{p}(\tau_{n+1})\|_1 + (\tau_n - \tau_{n+1}) \|\mathbf{p}(\tau_{n+1})\|_1 . \tag{3.14}$$

By using minimization properties, if $\mathbf{p}(\tau_{n+1})$ is the minimizer of (3.10) for the regularization parameter τ_{n+1}. Then, next inequality holds

$$\|\hat{\mathbf{r}} - \mathbf{A}\mathbf{p}(\tau_{n+1})\|_2^2 + \tau_{n+1} \|\mathbf{p}(\tau_{n+1})\|_1 \leq \|\hat{\mathbf{r}} - \mathbf{A}\mathbf{p}(\tau_n)\|_2^2 + \tau_{n+1} \|\mathbf{p}(\tau_n)\|_1 . \tag{3.15}$$

Note that the regularization parameter τ_{n+1} is the same on both sides of the inequality. Bearing in mind (3.15) and (3.14), it is straightforward to obtain

$$\|\hat{\mathbf{r}} - \mathbf{A}\mathbf{p}(\tau_n)\|_2^2 + \tau_n \|\mathbf{p}(\tau_n)\|_1 \leq \|\hat{\mathbf{r}} - \mathbf{A}\mathbf{p}(\tau_n)\|_2^2 + \tau_{n+1} \|\mathbf{p}(\tau_n)\|_1 + (\tau_n - \tau_{n+1}) \|\mathbf{p}(\tau_{n+1})\|_1 . \tag{3.16}$$

If the term $\tau_n \|\mathbf{p}(\tau_n)\|_1$ is added and subtracted from expression on the right-hand side of the inequality (3.16), the next expression is obtained

$$\begin{aligned} \|\hat{\mathbf{r}} - \mathbf{A}\mathbf{p}(\tau_n)\|_2^2 + \tau_n \|\mathbf{p}(\tau_n)\|_1 \quad \leq \quad & \|\hat{\mathbf{r}} - \mathbf{A}\mathbf{p}(\tau_n)\|_2^2 + \tau_n \|\mathbf{p}(\tau_n)\|_1 \\ & + (\tau_n - \tau_{n+1}) \left(\|\mathbf{p}(\tau_{n+1})\|_1 - \|\mathbf{p}(\tau_n)\|_1 \right) . \end{aligned} \tag{3.17}$$

Therefore, we can conclude that $(\tau_n - \tau_{n+1})(\|\mathbf{p}(\tau_{n+1})\|_1 - \|\mathbf{p}(\tau_n)\|_1) \geq 0$. As $\tau_n > \tau_{n+1} \geq 0$, then $\|\mathbf{p}(\tau_{n+1})\|_1 - \|\mathbf{p}(\tau_n)\|_1 \geq 0$. Finally, we obtain $\|\mathbf{p}(\tau_{n+1})\|_1 \geq \|\mathbf{p}(\tau_n)\|_1$.

3.A.2 Proof of Theorem 3.2

If $\mathbf{p}(\tau_{n+1})$ is a vector with non-negative components that minimizes the problem (3.10) for $\tau_{n+1} > 0$, then the following inequality is fulfilled

$$\|\hat{\mathbf{r}} - \mathbf{A}\mathbf{p}(\tau_{n+1})\|_2^2 + \tau_{n+1} \|\mathbf{p}(\tau_{n+1})\|_1 \leq \quad \|\hat{\mathbf{r}} - \mathbf{A}\mathbf{p}(\tau_n)\|_2^2 + \tau_{n+1} \|\mathbf{p}(\tau_n)\|_1 , \tag{3.18}$$

which can be rewritten as

$$\tau_{n+1}(\|\mathbf{p}(\tau_{n+1})\|_1 - \|\mathbf{p}(\tau_n)\|_1) \;\leq\; \|\hat{\mathbf{r}} - \mathbf{A}\mathbf{p}(\tau_n)\|_2^2 - \|\hat{\mathbf{r}} - \mathbf{A}\mathbf{p}(\tau_{n+1})\|_2^2 . \tag{3.19}$$

Since $\tau_{n+1} > 0$ and $\|\mathbf{p}(\tau_{n+1})\|_1 - \|\mathbf{p}(\tau_n)\|_1 \geq 0$, as it was proved in Theorem 3.1, the following inequality is fulfilled $\|\hat{\mathbf{r}} - \mathbf{A}\mathbf{p}(\tau_n)\|_2^2 - \|\hat{\mathbf{r}} - \mathbf{A}\mathbf{p}(\tau_{n+1})\|_2^2 \geq 0$. Finally, we obtain $\|\hat{\mathbf{r}} - \mathbf{A}\mathbf{p}(\tau_n)\|_2^2 \geq \|\hat{\mathbf{r}} - \mathbf{A}\mathbf{p}(\tau_{n+1})\|_2^2$.

3.A.3 The LARS/homotopy for source location

The method operates in an iterative fashion computing the critical regularization parameters $\tau_0 > \tau_1 > \cdots > \tau_{stop} \geq 0$ and the associated minimizers $\mathbf{p}(\tau_0)$, $\mathbf{p}(\tau_1), ..., \mathbf{p}(\tau_{stop})$ where an inactive component of $\mathbf{p}$ becomes positive or an active element becomes equal to zero. The algorithm is based on the computation of the so-called vector of residual correlations, or just residual correlation, $\mathbf{b}(\tau) = \mathbf{A}^T(\hat{\mathbf{r}} - \mathbf{A}\mathbf{p}(\tau))$ at each iteration.

By considering the subgradient, it straightforward to obtain the variational equations that describe the minimizer $\mathbf{p}(\tau)$ of the problem (3.10) [28, 97], which are given by

$$\begin{cases} (\mathbf{A}^T(\hat{\mathbf{r}} - \mathbf{A}\mathbf{p}(\tau)))_i & = \frac{\tau}{2} \quad \text{if} \quad p_i(\tau) \neq 0 \\ \left|(\mathbf{A}^T(\hat{\mathbf{r}} - \mathbf{A}\mathbf{p}(\tau)))_i\right| & \leq \frac{\tau}{2} \quad \text{if} \quad p_i(\tau) = 0, \end{cases} \tag{3.20}$$

where $(\mathbf{A}^T(\hat{\mathbf{r}} - \mathbf{A}\mathbf{p}(\tau)))_i$ is the ith entry of the vector $\mathbf{A}^T(\hat{\mathbf{r}} - \mathbf{A}\mathbf{p}(\tau))$.

Let $J = \{i \;: p_i \neq 0\}$ denote the support of $\mathbf{p}(\tau)$ or active set and let $I = \{i \;:\; p_i = 0\}$ denote the inactive set. Residual correlations on the support J must all have equal magnitude $\frac{\tau}{2}$, i.e. $b_j(\tau) = \frac{\tau}{2}$ for $j \in J$, whereas the residual correlations for the inactive elements satisfy $b_i \leq \frac{\tau}{2}$ for $i \in I$.

The LARS/homotopy starts with $\mathbf{p} = \mathbf{0}$, which is the solution of (3.10) for all the $\tau \geq \tau_0 = 2 \max_i \left(\mathbf{A}^T \hat{\mathbf{r}}\right)_i$, where $\left(\mathbf{A}^T \hat{\mathbf{r}}\right)_i$ denotes the ith component of the vector $\mathbf{A}^T \hat{\mathbf{r}}$, and proceeds in an iterative manner, solving at each iteration a small linear system of equations. Given the solution at one breakpoint τ_n, denoted by $\mathbf{p}(\tau_n)$, it is possible to construct the solution at the next breakpoint $\mathbf{p}(\tau_{n+1})$ as follows

$$\mathbf{p}(\tau_{n+1}) = \mathbf{p}(\tau_n) + \gamma \mathbf{u}(\tau_{n+1}), \tag{3.21}$$

where $\mathbf{u}(\tau_{n+1})$ denotes the update direction and $\gamma > 0$ is the walking step. It is important to remark that γ depends also on τ_{n+1}. However, herein this dependency is omitted for notational convenience. This step results in a change in the residual correlation given by

$$b(\tau_{n+1}) = b(\tau_n) - \gamma A^T A u(\tau_{n+1}) = b(\tau_n) - \gamma v(\tau_{n+1}). \tag{3.22}$$

The update direction for the subset of active entries $\mathbf{u}_J$ is given by the solution of the following reduced-order linear system

$$\mathbf{A}_J^T \mathbf{A}_J \mathbf{u}_J(\tau_{n+1}) = \mathbf{1}_J, \tag{3.23}$$

and $u_i(\tau_{n+1}) = 0$ for the components off of the active set ($u_i(\tau_{n+1}) = 0$ for $i \notin J$ at τ_n). Where $\mathbf{A}_J$ denotes a submatrix of $\mathbf{A}$ consisting of the columns of the elements of the set J and $\mathbf{1}_J$ denotes a column vector of ones with length equal to the cardinality of the set J. The update direction $\mathbf{u}_J(\tau_{n+1}) = \left(\mathbf{A}_J^T \mathbf{A}_J\right)^{-1} \mathbf{1}_J$, which is called equiangular direction by Efron et al. in [46], ensures that the maximal components of the residual correlation, those corresponding to the active set, decline equally.

The step size $\gamma > 0$ is calculated as the smallest real number that makes a component of the new residual (3.22) become equal in size to the maximal ones or an active component of $\mathbf{p}$ become equal to zero. Formally, the step size is determined by (see [75] and [96] for further details)

$$\gamma = \min\{\gamma_1, \gamma_2\}, \tag{3.24}$$

γ_1 is defined as $\gamma_1 = \min_{i \in I} \frac{\frac{\tau_n}{2} - \mathbf{b}_i(\tau_n)}{1 - \mathbf{v}_i(\tau_{n+1})}$ and is the minimum step that implies the activation of a zero component of $\mathbf{p}$. The parameter γ_2 is related with the second scenario leading to a breakpoint: when an active component crosses zeros. This occurs when $\gamma_2 = \min_{j \in J} \left\{ -\frac{\mathbf{p}_j(\tau_n)}{\mathbf{u}_j(\tau_{n+1})} \right\}$. It is important to remark that there is only one new candidate

to enter or leave the active set at each iteration of the algorithm (this condition is the so-called 'one at a time condition' [46]).

Once the new step size γ is computed, the next breakpoint can be obtained as $\tau_{n+1} = \tau_n - 2\gamma$ (since $\gamma > 0$, then $\tau_n > \tau_{n+1}$) and the associated minimizer as $\mathbf{p}(\tau_{n+1}) = \mathbf{p}(\tau_n) + \gamma \mathbf{u}(\tau_{n+1})$. This iterative procedure must be halted when a stopping condition is satisfied.

3.A.4 Proof of Theorem 3.3: An alternative interpretation of the residual

The residual correlation $\mathbf{b}$ that appears when the LARS/homotopy algorithm is applied to the problem (3.10) has a clear physical interpretation.

Recall (3.7). The residual correlation $\mathbf{b}$ of the LARS/homotopy applied to the problem presented in (3.10) is given by

$$\mathbf{b}(\tau) = \mathbf{A}^T(\hat{\mathbf{r}} - \mathbf{A}\mathbf{p}(\tau)) = \begin{bmatrix} \tilde{\mathbf{A}}_r^T & \tilde{\mathbf{A}}_i^T \end{bmatrix} \left(\begin{bmatrix} \hat{\mathbf{r}}_r \\ \hat{\mathbf{r}}_i \end{bmatrix} - \begin{bmatrix} \tilde{\mathbf{A}}_r \\ \tilde{\mathbf{A}}_i \end{bmatrix} \mathbf{p}(\tau) \right), \tag{3.25}$$

which can be rewritten in terms of the complex matrix $\tilde{\mathbf{A}}$ exposed in (3.6) and the sample covariance $\hat{\mathbf{R}}$

$$\mathbf{b}(\tau) = \Re\left\{ \tilde{\mathbf{A}}^H \left(\mathrm{vec}\left[\hat{\mathbf{R}}\right] - \tilde{\mathbf{A}}\mathbf{p}(\tau) \right) \right\}. \tag{3.26}$$

The term $\tilde{\mathbf{A}}\mathbf{p}(\tau)$ in (3.26) can be expressed as

$$\tilde{\mathbf{A}}\mathbf{p}(\tau) = \begin{bmatrix} \mathbf{s}_1^* \otimes \mathbf{s}_1 & \mathbf{s}_2^* \otimes \mathbf{s}_2 & \cdots & \mathbf{s}_G^* \otimes \mathbf{s}_G \end{bmatrix} \begin{bmatrix} p_1(\tau) \\ p_2(\tau) \\ \vdots \\ p_G(\tau) \end{bmatrix} = \sum_{i=1}^{G} p_i(\tau)\, \mathbf{s}_i^* \otimes \mathbf{s}_i. \tag{3.27}$$

Since $\mathbf{s}_i^* \otimes \mathbf{s}_i = \mathrm{vec}(\mathbf{s}_i \mathbf{s}_i^H)$, then $\tilde{\mathbf{A}}\mathbf{p}(\tau) = \mathrm{vec}\left\{ \sum_{i=1}^{G} p_i(\tau)\, \mathbf{s}_i \mathbf{s}_i^H \right\}$. By applying this equality to (3.26), the residual correlation evaluated at τ is given by

$$\mathbf{b}(\tau) = \Re\left\{ \tilde{\mathbf{A}}^H \left(\mathrm{vec}\left[\hat{\mathbf{R}}\right] - \mathrm{vec}\left[\sum_{i=1}^{G} p_i(\tau)\, \mathbf{s}_i \mathbf{s}_i^H \right] \right) \right\} = \Re\left\{ \tilde{\mathbf{A}}^H \,\mathrm{vec}\left(\hat{\mathbf{R}} - \sum_{i=1}^{G} p_i(\tau)\, \mathbf{s}_i \mathbf{s}_i^H \right) \right\}. \tag{3.28}$$

Bearing in mind the matrix $\tilde{\mathbf{A}}$ presented in (3.6), the last expression can be reformulated as

$$\mathbf{b}(\tau) = \Re\left\{ \begin{bmatrix} \mathbf{s}_1^T \otimes \mathbf{s}_1^H \\ \mathbf{s}_2^T \otimes \mathbf{s}_2^H \\ \vdots \\ \mathbf{s}_G^T \otimes \mathbf{s}_G^H \end{bmatrix} \operatorname{vec}\left[\hat{\mathbf{C}}_\tau\right] \right\} = \Re\left\{ \begin{bmatrix} \left(\mathbf{s}_1^T \otimes \mathbf{s}_1^H\right) \operatorname{vec}\left[\hat{\mathbf{C}}_\tau\right] \\ \left(\mathbf{s}_2^T \otimes \mathbf{s}_2^H\right) \operatorname{vec}\left[\hat{\mathbf{C}}_\tau\right] \\ \vdots \\ \left(\mathbf{s}_G^T \otimes \mathbf{s}_G^H\right) \operatorname{vec}\left[\hat{\mathbf{C}}_\tau\right] \end{bmatrix} \right\} = \Re\left\{ \begin{bmatrix} \mathbf{s}_1^H \hat{\mathbf{C}}_\tau \mathbf{s}_1 \\ \mathbf{s}_2^H \hat{\mathbf{C}}_\tau \mathbf{s}_2 \\ \vdots \\ \mathbf{s}_G^H \hat{\mathbf{C}}_\tau \mathbf{s}_G \end{bmatrix} \right\}, \quad (3.29)$$

where $\hat{\mathbf{C}}_\tau = \hat{\mathbf{R}} - \sum_{i=1}^{G} p_i(\tau)\, \mathbf{s}_i \mathbf{s}_i^H$.

The ith component of $\mathbf{b}(\tau)$ fulfills $\mathbf{s}_i^H \hat{\mathbf{C}}_\tau \mathbf{s}_i = \mathbf{s}_i^H \hat{\mathbf{C}}_\tau^H \mathbf{s}_i$ and, as a consequence, is real. Hence, the residual correlation $\mathbf{b}(\tau)$ can be expressed as

$$\mathbf{b}(\tau) = \left[\begin{array}{cccc} \mathbf{s}_1^H \hat{\mathbf{C}}_\tau \mathbf{s}_1, & \mathbf{s}_2^H \hat{\mathbf{C}}_\tau \mathbf{s}_2, & \cdots, & \mathbf{s}_G^H \hat{\mathbf{C}}_\tau \mathbf{s}_G \end{array} \right]^T. \quad (3.30)$$

This result provides an alternative interpretation of the residual correlation. At each breakpoint τ, the corresponding residual $\mathbf{b}(\tau)$ can be seen as the Bartlett estimator applied to the residual covariance matrix $\hat{\mathbf{C}}_\tau = \hat{\mathbf{R}} - \sum_{i=1}^{G} p_i(\tau)\, \mathbf{s}_i \mathbf{s}_i^H$.

Chapter 4

Sparse multiple relay selection and network beamforming with individual power constraints using semidefinite relaxation

This chapter deals with the multiple relay selection problem in two-hop wireless cooperative networks with individual power constraints at the relays. In particular, it addresses the problem of selecting the best subset of K cooperative nodes and their corresponding beamforming weights so that the signal-to-noise ratio (SNR) is maximized at the destination. This problem is computationally demanding and requires an exhaustive search over all the possible combinations. In order to reduce the complexity, a new sub-optimal method is proposed. This technique exhibits a near-optimal performance with a computational burden that is far less than the one needed in the combinatorial search. The proposed method is based on the use of the l_1-norm squared and the Charnes-Cooper transformation and naturally leads to a semidefinite programming relaxation with an affordable computational cost. Contrary to other approaches in the literature, the technique exposed herein is based on the knowledge of the second-order statistics of the channels and the relays are not limited to cooperate with full power.

4.1 Introduction

As it is well-known, relay systems increase the spatial diversity and the reliability of wireless communications systems. The simplest relay network consists of a single source and N relays that cooperate to send to a destination node the message transmitted by the source. Relay communications systems can be classified taking into account how the relays process the information received from the source node. The most popular cooperative schemes available in the wireless relay literature are: amplify-and-forward (AF), decode-and-forward [102], compress-and-forward and coded-cooperation [103]. Nonetheless, amplify-and-forward has attracted special interest due to its simplicity. In this context, distributed relay beamforming, also known as cooperative beamforming, has been shown to be a powerful technique which provides power efficiency and is able to increase the communications reliability. In general terms, in distributed beamforming the relays cooperate acting as virtual antenna and adjust their transmission weights to form a beam to the destination. Since each relay multiplies its received signal by a complex weight and retransmits it, the beamforming weights have to be determined according to some optimality criterion. Different beamforming approaches have been considered in the literature [104]. One such criteria is the minimization of the total transmitted power subject to a given constraint on the quality of service at the receiver. The second approach is the maximization of the received SNR subject to certain power constraints, i.e., individual power constraints in each relay or on the total power transmitted by the relays. Due to the fact that relay nodes have particular constraints on the battery lifetimes, individual power constraints in each relay are of practical interest. It is worth noting that the optimal solution of this maximization problem results in relay powers which do not correspond, in general, to their maximum allowable values, i.e., to achieve the maximum SNR at the receiver, the relays may not use their maximum allowable power.

In the conventional cooperation strategies exposed above, all the relays cooperate in relaying the signals. This is the optimal strategy from the point of view of the end-to-end performance. Nevertheless, in practical scenarios, the benefits of the cooperation could be offset by the cost of the cooperation and the consumption of additional system resources. In many cases, it is impractical or even unfeasible to activate all (or many) relays (see the references [47, 48, 49, 50, 51, 52]). For instance, in many practical situations the number of potential cooperating nodes could be large, e.g., in device-to-device communication networks or in wireless sensor networks, and the benefits of the cooperation with all the relays can be outweighed by the costs of the cooperation. These costs include the signaling overhead and the efforts needed to maintain the synchronization between all the

nodes [47, 48, 49, 50]. In this context, by considering relay selection, the overall processing in the network can be simplified achieving a significant reduction in the implementation complexity [47, 49, 50, 51, 52].

There exist a vast literature devoted to relay selection. Most of these schemes are based on single relay selection, i.e., only one of the relay nodes can be selected to cooperate in the retransmission, e.g. [105] and [106]. Nevertheless, in adverse environments, transmitting over a single relay may not be sufficient to achieve the desired performance at the destination. This has motivated the generalization of this idea, allowing more than one node to cooperate. Multiple relay selection for a single source-destination pair has attracted attention in some references [107, 108, 52, 109]. In all these approaches, for simplicity, the relays are not allowed to adjust their transmit power arbitrarily, i.e., each relay has only two choices: to cooperate with full power or not to cooperate at all. In [52], the authors propose several SNR-suboptimal multiple relay selection techniques based on some ordering functions. In [108], Laneman et al. proposed a Decode-and-Forward protocol that allow the relays to cooperate if the channel between the source and the relays, the so-called backward channel, exceeds a fixed threshold. On the contrary, the scheme proposed in [107] is based on the full Channel State Information (CSI) of the backward and the forward channels of each relay. Therein two different problems have been tackled: the minimization of the end-to-end error performance under a total power constraint, and the dual problem, the minimization of the total power consumption constrained to a maximum error probability. These problems fall within the class of the so-called 0-1 Knapsack problems and are solved by taking use of several greedy algorithms. A similar approach was proposed for cognitive relay networks in [109].

This chapter deals with problem of multiple relay selection for distributed beamforming under individual power constraints at the relay nodes. In particular, it addresses the problem of finding the best subset of cooperative nodes, and their beamformer weights, so that the SNR is maximized at the destination. The selection of the best subset of K nodes out of a set of N potential relays with individual relay power constraints is a NP-hard problem which requires an exhaustive search over all the possible sparsity patterns. In order to reduce the computational burden, this chapter proposes a sub-optimal method which exhibits a performance which is very close to the SNR-optimal multiple relay scheme with a reduced complexity. The proposed method is based on the knowledge of the second-order statistics of the CSI and in contrast to other approaches in the relay selection literature [107, 108, 52, 109], in the technique proposed herein, the relays are not limited to cooperate only with full power. Interestingly enough, this optimization leads to results in which the powers of the selected set of relays do not correspond to the maximum allowable values. The proposed algorithm is based on the Charnes-Cooper transformation and the l_1-norm

squared [39], a surrogate of the l_0-norm which enforces zeros in the relay powers, and naturally yields a semidefinite programming problem (SDP).

It is important to remark that the sparse multiple relay selection problem described in this chapter does not belong to the class of the so-called *sparse recovery problems* in which a solution vector with few non-zero elements has to be estimated and the conditions that ensure the exact recovery of the true sparsity pattern need to be studied. The adjective sparse herein relates to the fact that the algorithm proposed for the selection of the relays uses a sparsity-inducing norm, the l_1-norm squared, that promotes the appearance of zeros in the final solution and consequently performs the subset selection.

The chapter is organized as follows. Section 4.2 describes the signal model and presents the multiple relay selection problem. The algorithm proposed for the selection of the cooperating nodes is derived in Section 4.3 and the analysis of its performance is shown in Section 4.4. Finally, some concluding remarks are provided in Section 4.5.

4.2 System model and problem formulation

Consider a two-hop wireless cooperative network which consists of a source, a destination and N potential relays as it is shown in Fig. 4.1. Each of the nodes of this scheme is equipped with a single antenna. For sake of simplicity it is assumed that due to the poor quality of the channel between the source and the destination, there is no direct link between them. The channel between the source and the ith relay and the channel between the ith relay and the destination are denoted by h_i and g_i, respectively.

Even though, the pioneering studies on network relay beamforming have assumed that the instantaneous CSI is perfectly known at the relays or at the destination node [110]. Unfortunately, this assumption is often violated in practical scenarios. To avoid the need to know the instantaneous CSI, the flat fading channel coefficients $\{h_i\}_{i=1}^N$ and $\{g_i\}_{i=1}^N$ can be modeled as random values. Similar to [104], [111], [112] and [113], in this chapter it is assumed that the joint second-order statistics of these channels are known at a central node, for instance, at the destination node, which is the one in charge of computing the relay weights taking into account past observations, and then distributing them to the relay nodes via a dedicated channel. This assumption allows us to consider some uncertainty in the channel models through introducing the covariance matrices of the channel gains. Since the coefficients of the channels are relatively stable in stationary environments and can be estimated using past observations, it is reasonable to assume the availability of the second order statistics of the channels.

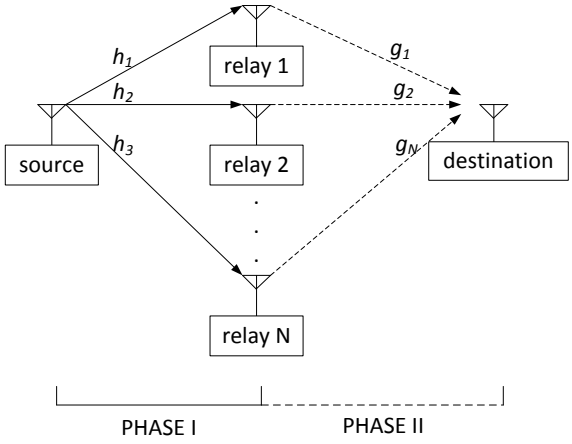

Figure 4.1: Wireless relay network

In the scheme presented herein, we have considered a two-step amplify-and-forward protocol for the communication between the source and the destination. During the first step (slot) the source broadcasts the signal $\sqrt{P_s}s$ to the relays, where P_s denotes the transmit power and s is the information symbol. Without loss of generality it is assumed that $E\{|s|^2\} = 1$. The signal received at the ith relay is given by

$$x_i = \sqrt{P_s}h_i s + \eta_i, \tag{4.1}$$

where η_i denotes the additive noise at the ith relay whose variance is known to be σ_r^2. In the second step the ith relay transmits a weighted version of its received signal. This can be expressed as

$$y_i = w_i x_i. \tag{4.2}$$

The received signal at the destination node is given by

$$r = \sqrt{P_s}\sum_{i=1}^{N} w_i h_i g_i s + \sum_{i=1}^{N} w_i g_i \eta_i + n_d, \tag{4.3}$$

where n_d is the noise at the destination which has a known variance σ_d^2. Note that whereas the first term in (4.3) corresponds to the desired signal component, the sum of the second and the third term is the total noise received at the destination.

4.2.1 SNR maximization with individual power constraints without relay selection

The aim of this subsection is to briefly describe the classical design problem presented in [104]. The maximization of the SNR at the destination under transmit power constraints at each relay is given by

$$\max_{\mathbf{w}} \ \text{SNR} \qquad \text{s.t.} \qquad p_i \leq P_i \qquad \forall i = 1, ..., N, \tag{4.4}$$

where $\mathbf{w} = [w_1 \dots w_N]^T$is the network beamforming vector and p_i and P_i are the actual transmit power and the maximum allowable transmit power of the ith relay, respectively. Note that in the problem exposed above relay selection is not considered.

The expected power of the desired signal component in the expression (4.3), that is, the expected power of the first term in the sum is given by

$$P_d = E\left\{\left|\sqrt{P_s}\sum_{i=1}^{N} w_i h_i g_i s\right|^2\right\} = \mathbf{w}^H \mathbf{A} \mathbf{w}, \tag{4.5}$$

where $\mathbf{A} = P_s E\left\{(\mathbf{h} \odot \mathbf{g})(\mathbf{h} \odot \mathbf{g})^H\right\}$. In the latter expression, the operator $\odot$ represents the Schur-Hadamard product and $\mathbf{h} = [h_1 \dots h_N]^T$, $\mathbf{g} = [g_1 \dots g_N]^T$. This matrix can be decomposed as a diagonal matrix plus a rank-one matrix [112] (DPR1). Assuming that the coefficients of the backward and the forward channels, $\{h_i\}_{i=1}^N$ and $\{g_i\}_{i=1}^N$, are statistically independent, the (i, j)th element of $\mathbf{A}$, denoted by $A_{i,j}$, can be expressed as follows

$$A_{ij} = \begin{cases} P_s E\{|h_i|^2\} E\{|g_i|^2\} & \text{if } i = j \\ P_s E\{h_i\} E\{g_i\} E\{h_j^*\} E\{g_j^*\} & \forall i \neq j. \end{cases} \tag{4.6}$$

Let $\bar{h}_i = E\{h_i\}$, $\bar{g}_i = E\{g_i\}$, $\alpha_i = E\{|h_i - \bar{h}_i|^2\}$ and $\beta_i = E\{|g_i - \bar{g}_i|^2\}$. It is straightforward to rewrite $\mathbf{A}$ as

$$\mathbf{A} = \mathbf{\Lambda} + \mathbf{v}\mathbf{v}^H, \tag{4.7}$$

with $\mathbf{\Lambda} = P_s \text{diag}(\beta_1 |\bar{h}_1|^2 + \alpha_1 |\bar{g}_1|^2 + \alpha_1\beta_1, ..., \beta_N |\bar{h}_N|^2 + \alpha_N |\bar{g}_N|^2 + \alpha_N\beta_N)$ and $\mathbf{v} = \sqrt{P_s}[\bar{h}_1\bar{g}_1, ..., \bar{h}_N\bar{g}_N]^T$.

The total noise power, denoted as P_n, is defined as

$$P_n{=}E\left\{\left(\sum_{i=1}^{N} w_i g_i \eta_i{+}n_d\right)\left(\sum_{j=1}^{N} w_j g_j \eta_j{+}n_d\right)^*\right\}. \tag{4.8}$$

Assuming that η_i is a zero-mean additive noise and that $\{\eta_i\}_{i=1}^{N}$ and n_d are mutually independent random variables, then the noise power can be formulated as

$$P_n{=}\mathbf{w}^H\mathbf{B}\mathbf{w} + \ \sigma_d^2. \tag{4.9}$$

where

$$\mathbf{B}{=}\ \sigma_r^2\text{diag}(E\{\,|g_1|^2\,\},\ E\{\,|g_2|^2\,\},\ldots,E\{\,|g_N|^2\,\}). \tag{4.10}$$

Hence, the SNR at destination node is defined as

$$\text{SNR} = \frac{P_d}{P_n} = \frac{\mathbf{w}^H\mathbf{A}\mathbf{w}}{\mathbf{w}^H\mathbf{B}\mathbf{w}{+}\sigma_d^2}. \tag{4.11}$$

In order to specify the power constraints at the relays in (4.4), the average transmit power of the ith relay, denoted as p_i, is defined as follows

$$p_i{=}\ E\left\{|x_i|^2\right\}|w_i|^2 = D_{ii}\,|w_i|^2\,, \tag{4.12}$$

where D_{ii} is the ith element of diagonal of the matrix $\mathbf{D}$ given by

$$\mathbf{D}{=}\ P_s\ \text{diag}\left(E\left\{|h_1|^2\right\},\ldots,E\{\,|h_N|^2\,\}\right)\quad + \sigma_r^2\mathbf{I}. \tag{4.13}$$

The maximization of the SNR under individual relay power constraints exposed in (4.4) can be formally expressed as

$$\begin{aligned} \max_{\mathbf{w}} \quad & \frac{\mathbf{w}^H\mathbf{A}\mathbf{w}}{\mathbf{w}^H\mathbf{B}\mathbf{w}{+}\sigma_d^2} \\ \text{s.t.} \quad & D_{ii}\,|w_i|^2 \le P_i \qquad \forall i = 1,...,N. \end{aligned} \tag{4.14}$$

Note that since $\mathbf{B}$ is diagonal and $\mathbf{A}$ is a diagonal plus rank-one matrix, the phases of the optimal beamformer only depend on the entries of the vector $\mathbf{v}$ defined in (4.7). In particular, the phases of the optimal weights can be obtained as $\angle w_i = \angle v_i$, where v_i denotes the ith element of $\mathbf{v}$.

Considering $\mathbf{X} = \mathbf{w}\mathbf{w}^H$, the problem (4.14) can be rewritten as

$$\begin{aligned} \max_{\mathbf{X}} \quad & \frac{\mathrm{Tr}\{\mathbf{A}\mathbf{X}\}}{\mathrm{Tr}\{\mathbf{B}\mathbf{X}\}+\sigma_d^2} \\ \text{s.t.} \quad & X_{ii} \leq P_i/D_{ii} \quad \forall i = 1, ..., N \\ & \mathbf{X} \succeq 0;\ \mathrm{rank}(\mathbf{X}) = 1, \end{aligned} \tag{4.15}$$

where X_{ii} denotes the ith diagonal element of $\mathbf{X}$. Following the idea of semidefinite relaxation and dropping the non-convex rank constraint, the problem presented above can be relaxed as follows

$$\begin{aligned} \max_{\mathbf{X},t} \quad & t \\ \text{s.t.} \quad & \mathrm{Tr}\{\mathbf{X}(\mathbf{A}-t\mathbf{B})\} \geq \sigma_d^2 t \\ & X_{ii} \leq P_i/D_{ii} \quad \forall i = 1, ..., N\ ;\ \ \mathbf{X} \succeq 0. \end{aligned} \tag{4.16}$$

The latter problem is quasiconvex and the standard approach is to solve it by means of a bisection search method in which the optimal solution is obtained iteratively after solving a sequence of (often many) semidefinite programming problems (for further information see reference [104]).

4.2.2 Multiple relay selection for SNR optimization with individual constraints

Let us consider the joint problem of selecting the best subset of K nodes out of the set of N potential relays and the estimation of the weights which maximize the SNR at the destination, subject to individual power constraints at the relays. Mathematically, this problem can be expressed as

$$\begin{aligned} \max_{\mathbf{w}} \quad & \frac{\mathbf{w}^H\mathbf{A}\mathbf{w}}{\mathbf{w}^H\mathbf{B}\mathbf{w}+\sigma_d^2} \\ \text{s.t.} \quad & D_{ii}\,|w_i|^2 \leq P_i \qquad \forall i = 1, ..., N \\ & \mathrm{card}(\mathbf{w}) = K, \end{aligned} \tag{4.17}$$

where $K > 0$ is a given constant and $\mathrm{card}(\mathbf{w}) = K$ is the number of non-zero coefficients in the vector $\mathbf{w}$. It is worth mentioning that adding zeros in the network beamforming vector is equivalent to selecting the best subset of relays. Note that the kth relay is excluded

from the transmission if the kth component of the solution vector $\mathbf{w}$ is equal to zero. The problem in (4.17) is a NP-hard problem and requires an exhaustive search over all the possible $\binom{N}{K}$ sparsity patterns. This search is computationally unaffordable and this fact motivates the pursuit of an efficient algorithm with a near-optimal performance.

4.3 The proposed method

4.3.1 Selection of the subset of relays

The problem considered in (4.17) is non-convex and the aim of this subsection is to derive a convex relaxation of this problem in order to obtain a new algorithm with a lower computational complexity. The traditional way of deriving convex approximations of cardinality-constrained problems in combinatorial optimization is to replace the cardinality operator by the l_1-norm [72], [4], defined as $\|\mathbf{w}\|_1 = \sum_{i=1}^{i=N} |w_i|$. As it is well-known, the l_1-norm is the tightest convex relaxation of the cardinality operator [4] and has a sparsifying effect that has long been observed in statistics and signal processing [25]. Nonetheless, a different approach is considered in this chapter. Similar to [39] and [38], the l_1-norm squared, denoted as $\|\mathbf{w}\|_1^2$, is considered instead of the traditional l_1-norm. The rationale behind the use of the l_1-norm squared as a surrogate of the cardinality is twofold. First, it is a sparsity-inducing norm which encourages the appearance of null components in the network beamforming vector and, consequently, performs the subset selection. Second, the problem that results after considering the l_1-norm squared naturally yields a semidefinite programming relaxation, something that is not obvious when the l_1-norm is considered instead. Therefore, let us relax the problem presented in (4.17) rewriting it in terms of the l_1-norm squared

$$\max_{\mathbf{w}} \quad \frac{\mathbf{w}^H \mathbf{A} \mathbf{w}}{\mathbf{w}^H \mathbf{B} \mathbf{w} + \sigma_d^2} \tag{4.18a}$$

$$\text{s.t.} \quad D_{ii} \left| w_i \right|^2 \leq P_i \qquad \forall i = 1, ..., N \tag{4.18b}$$

$$\|\mathbf{w}\|_1^2 \leq \gamma, \tag{4.18c}$$

where γ is a positive parameter that controls the sparsity of the beamforming vector, i.e., the number of active components in $\mathbf{w}$. Let us skip now the discussion about how to adjust the parameter γ to properly perform the subset selection. Later, in the following subsection, this problem will be addressed and it will be explained how to adjust the parameter γ to obtain a solution of (4.18) with only K active entries.

Unfortunately, the problem in (4.18) is still NP-hard and this motivates the use of a semidefinite relaxation to handle it. First, let us define $\mathbf{X} \triangleq \mathbf{w}\mathbf{w}^H \in H_N^+$, i.e., a $N \times N$ Hermitian positive semidefinite matrix. Then, the constraint (4.18c) can be rewritten as

$$\|\mathbf{w}\|_1^2 = \left(\sum_{i=1}^{N} |w_i|\right)^2 = \mathbf{1}_N^T |\mathbf{X}| \mathbf{1}_N, \tag{4.19}$$

where $|\mathbf{X}|$ denotes the element-wise absolute value of the matrix $\mathbf{X}$ and $\mathbf{1}_N$ the all-one column vector of length N. By substituting the l_1-norm squared by its equivalent formulation (4.19), the problem in (4.18) can be expressed as

$$\begin{aligned} \max_{\mathbf{X}} \quad & \frac{\mathrm{Tr}\{\mathbf{A}\mathbf{X}\}}{\mathrm{Tr}\{\mathbf{B}\mathbf{X}\}+\sigma_d^2} \\ \text{s.t.} \quad & X_{ii} \leq q_i \ \forall i = 1, ..., N \\ & \mathbf{1}_N^T |\mathbf{X}| \mathbf{1}_N \leq \gamma; \quad \mathbf{X} \succeq 0 \\ & \mathrm{rank}\,(\mathbf{X}) = 1, \end{aligned} \tag{4.20}$$

where q_i is the ith component of the vector $\mathbf{q}$ defined as $\mathbf{q} = [P_1/D_{11}, ..., P_N/D_{NN}]^T$. By dropping the rank-one constraint the following problem is obtained

$$\max_{\mathbf{X}} \quad \frac{\mathrm{Tr}\{\mathbf{A}\mathbf{X}\}}{\mathrm{Tr}\{\mathbf{B}\mathbf{X}\}+\sigma_d^2} \tag{4.21a}$$

$$\text{s.t.} \quad X_{ii} \leq q_i \ \ \forall i = 1, ..., N \tag{4.21b}$$

$$\mathbf{1}_N^T |\mathbf{X}| \mathbf{1}_N \leq \gamma; \quad \mathbf{X} \succeq 0. \tag{4.21c}$$

Unfortunately, the semidefinite relaxation does not immediately yield a semidefinite programming. Due to the fractional structure of its objective (4.21a), this problem is a quasi-convex problem in the variable $\mathbf{X}$. The standard approach for solving this type of problems in the signal processing literature is to use a bisection search method [104], [114] in which the solution is sequentially searched by solving a sequence of (often many) semidefinite programming problems. A different approach has been considered herein. The main idea is to reformulate the quasi-convex problem presented in (4.21) into a convex semidefinite problem using a slight modification of the conventional Charnes-Cooper transformation [115]. Consider the following transformation of variables:

$$z = \frac{1}{\mathrm{Tr}\{\mathbf{B}\mathbf{X}\}+\sigma_d^2}, \quad \mathbf{Y} = \frac{\mathbf{X}}{\mathrm{Tr}\{\mathbf{B}\mathbf{X}\}+\sigma_d^2} = z\mathbf{X}. \tag{4.22}$$

By using (4.22), the quasi-convex problem (4.21) can be rewritten as the following semidefinite program (SDP)

$$\max_{\mathbf{Y},\, z} \quad \mathrm{Tr}\{\mathbf{AY}\} \tag{4.23a}$$

$$\text{s.t.} \quad Y_{ii} \leq z\, q_i \quad \forall i = 1, ..., N \tag{4.23b}$$

$$\mathbf{1}_N^T\, |\mathbf{Y}|\, \mathbf{1}_N \leq z\gamma \tag{4.23c}$$

$$\mathrm{Tr}\{\mathbf{BY}\} + \sigma_d^2 z \;=\; 1 \tag{4.23d}$$

$$\mathbf{Y} \succeq 0; \;\; z \geq 0, \tag{4.23e}$$

with $z \in \mathbb{R}$ and $\mathbf{Y} \in H_N^+ = \left\{\mathbf{Y} \in \mathbb{C}^{N\mathrm{x}N} | \mathbf{Y} = \mathbf{Y}^H, \mathbf{Y} \succeq 0\right\}$, under the assumption that the optimal solution, denoted by $(\mathbf{Y}^*, z^*)$, has $z^* > 0$. Actually, $z^* = 0$ cannot be a solution of this problem, because if $z^* = 0$, then according to (4.23c), we have $\mathbf{Y}^* = \mathbf{0}$, which violates the constraint (4.23d). This proves the equivalence between the quasi-convex problem in (4.21) and the SDP presented in (4.23). Hence, if $(\mathbf{Y}^*, z^*)$ is the optimal solution of (4.23), then $\mathbf{X}^* = \mathbf{Y}^*/z^*$ is the optimal solution of (4.21). The problem presented in (4.23) can be solved using the standard interior point methods implemented in solvers such as SeDuMi [116].

To determine the subset of selected nodes the following procedure is considered. The non-zero elements of diagonal $\mathbf{Y}^*$ correspond the selected relays. On the contrary, the null diagonal entries correspond to the relays that should be left out of the transmission. Note that since the active elements of the diagonal of $\mathbf{Y}^*$ are the same than those of the matrix $\mathbf{X}^*$, then the change of variables does not need to be undone.

4.3.2 Computation of the network beamforming weights

Once the subset of K relays is selected, the network beamforming weights which maximize the SNR have to be computed. Due to the influence of the l_1-norm squared behind the constraint (4.23c), these weights cannot be directly extracted from the solution of (4.23). To compute the beamformer weights this constraint and the subset of inactive relays have to be removed from this problem. Let us denote by $S \subseteq \{1, \ldots, N\}$ the subset of K nodes selected for the retransmission and by $\tilde{\mathbf{w}} = \left[w_{S(1)}, ..., w_{S(K)}\right]^T$ the weights of the active relays. To find the coefficients of the optimal beamforming, the following reduced-size

problem has to be solved:

$$\begin{aligned}
\max_{\tilde{\mathbf{Y}},\, z} \quad & \mathrm{Tr}\{\tilde{\mathbf{A}}\tilde{\mathbf{Y}}\} && \text{(4.24a)}\\
\text{s.t.} \quad & \tilde{Y}_{ii} \leq z\, \tilde{q}_i \quad \forall i = 1, ..., K && \text{(4.24b)}\\
& \mathrm{Tr}\{\tilde{\mathbf{B}}\tilde{\mathbf{Y}}\} + \sigma_d^2 z \;=\; 1 && \text{(4.24c)}\\
& \tilde{\mathbf{Y}} \succeq 0 && \text{(4.24d)}\\
& z \geq 0, && \text{(4.24e)}
\end{aligned}$$

where $\tilde{\mathbf{A}}$ and $\tilde{\mathbf{B}}$ are the submatrices of $\mathbf{A}$ and $\mathbf{B}$ formed by selecting the rows and columns which correspond to the active relays. Note that $\tilde{\mathbf{B}}$ and $\tilde{\mathbf{A}}$ preserve the special structure of the original matrices, i.e., $\tilde{\mathbf{B}}$ is a diagonal matrix and $\tilde{\mathbf{A}}$ is DPR1 which can be decomposed as $\tilde{\mathbf{A}} = \tilde{\mathbf{\Lambda}} + \tilde{\mathbf{v}}\tilde{\mathbf{v}}^H$, with obvious definitions of $\tilde{\mathbf{\Lambda}}$ and $\tilde{\mathbf{v}}$. In the same way, $\tilde{q}_i$ denotes the ith entry of the vector $\tilde{\mathbf{q}}$ which is obtained by removing the inactive relays from the vector $\mathbf{q}$. Note that $\tilde{\mathbf{Y}}$ is a square matrix of size K formed by the active rows and columns of $\mathbf{Y}$.

Theorem 4.1 *At least one of the inequalities in (4.24b) has to be fulfilled with equality.*

Proof: *See Appendix 4.A.1.*

Due to the semidefinite relaxation, the solution of the problem described above may not be rank-one in general. Interestingly, it can be proved that: i) when $\tilde{\mathbf{A}}$ is a diagonal matrix the solution of the problem (4.24) can be computed exactly by means of a linear programming problem (LP); ii) when the matrix $\tilde{\mathbf{A}}$ is not diagonal the beamformer weights can be extracted from the diagonal elements of the solution. Notice that no eigendecomposition or randomization is needed to extract the coefficients. In what follows both cases are analyzed.

When the matrix $\tilde{\mathbf{A}}$ is diagonal, it is straightforward to rewrite the problem in (4.24) as the following linear programming problem

$$\begin{aligned}
\max_{\mathbf{u}\in\mathbb{R}^K, z} \quad & \mathbf{a}^T\mathbf{u}\\
\text{s.t.} \quad & u_i \leq z\, \tilde{q}_i \quad \forall i = 1, ..., K\\
& \mathbf{b}^T\mathbf{u} + \sigma_d^2 z \;=\; 1\\
& u_i \geq 0 \quad \forall i = 1, ..., K; \quad z \geq 0, && \text{(4.25)}
\end{aligned}$$

where vectors $\mathbf{a}$ and $\mathbf{b}$ contain the diagonal entries of the matrices $\tilde{\mathbf{A}}$ and $\tilde{\mathbf{B}}$ respectively, i. e., $\mathbf{a} = [\tilde{A}_{11}, ..., \tilde{A}_{KK}]^T$, $\mathbf{b} = [\tilde{B}_{11}, ..., \tilde{B}_{KK}]^T$ and the ith entry of the vector $\mathbf{u}$ is given by $u_i = z\left|w_{S(i)}\right|^2$. Note that when $\tilde{\mathbf{A}}$ is a diagonal matrix, the maximization of the SNR does not depend on the phase of the beamforming vector. Thus, the optimal beamformer can be directly obtained as $\tilde{\mathbf{w}} = [\sqrt{u_1/z}, ..., \sqrt{u_K/z}]^T$.

If the matrix $\tilde{\mathbf{A}}$ is not diagonal but fulfills the condition exposed in the following theorem, the solution of the problem exposed in (4.24) always has rank one.

Theorem 4.2 *If the matrix $\tilde{\mathbf{A}}$ is not diagonal, but all the elements of the vector $\tilde{\mathbf{v}}$ are different from zero and $(\tilde{\mathbf{Y}}^*, z^*)$ is the solution of the problem in (4.24), then $\tilde{\mathbf{Y}}^*$ has rank one.*

Proof: *See Appendix 4.A.2.*

If the conditions exposed in the last theorem are fulfilled, $\tilde{\mathbf{w}}$ can be obtained directly from the eigendecomposition of the rank-one matrix $\mathbf{Q} = \tilde{\mathbf{Y}}^*/z^*$. Nonetheless, the computational cost of the eigendecomposition can be avoided as is described next. Since the phase of the complex weights can be obtained from $\tilde{\mathbf{v}}$ by considering $\angle\tilde{w}_i = \angle\tilde{v}_i$, where $\tilde{w}_i$ and $\tilde{v}_i$ denote the ith entries of the vectors $\tilde{\mathbf{w}}$ and $\tilde{\mathbf{v}}$, respectively, then it only remains to compute their moduli. These can be obtained from the elements of the diagonal of the matrix $\mathbf{Q}$. Therefore, it is straightforward to show that the ith entry of $\tilde{\mathbf{w}}$ is given by

$$\tilde{w}_i = \sqrt{\frac{\tilde{Y}^*_{ii}}{z^*}} e^{j\angle\tilde{v}_i} \qquad \forall i = 1, ..., K, \tag{4.26}$$

If some of the entries of $\tilde{\mathbf{v}}$ are zero, the optimal weights can be obtained in a similar way. This is justified by the following theorem.

Theorem 4.3 *If some of the elements of $\tilde{\mathbf{v}}$ are zero and $(\tilde{\mathbf{Y}}^*, z^*)$ is the solution of (4.24), then the ith entry of $\tilde{\mathbf{w}}$ is given by:*

$$\tilde{w}_i = \begin{cases} \sqrt{\frac{\tilde{Y}^*_{ii}}{z^*}} & \text{if } \tilde{v}_i = 0 \\ \sqrt{\frac{\tilde{Y}^*_{ii}}{z^*}} e^{j\angle\tilde{v}_i} & \text{if } \tilde{v}_i \neq 0. \end{cases} \tag{4.27}$$

Proof: *See Appendix 4.A.3.*

This result can be seen as a generalization of (4.26) if one assume that $\angle\tilde{v}_i = 0$ when $\tilde{v}_i = 0$. Notice that even if $\tilde{\mathbf{A}}$ is not diagonal the entries of the vector can be directly obtained from the solution of (4.24) and no randomization or eigendecomposition is needed.

A direct consequence of the Theorems 4.1 - 4.3 is that at least one of the relays has to transmit with the maximum allowable power.

4.3.3 Parameter selection

A crucial part of the algorithm is the proper choice of the parameter γ in (4.23c) because it performs the selection of the subset of relays. This parameter controls the amount of shrinkage applied to the estimates and, consequently, the number of the active nodes in the optimal beamformer. It is worth noting that sparser solutions are obtained when γ is decreased. The goal of this subsection is to propose a method based on a binary search over the parameter γ that successively increase the sparsity of the vector $\mathbf{w}$ until the desired number of relays is selected.

Recall the inequality in (4.18c), i.e., $\|\mathbf{w}\|_1^2 \leq \gamma$ and consider the following useful bounds on the l_1-norm squared [117]

$$\|\mathbf{w}\|_2^2 \leq \|\mathbf{w}\|_1^2 \leq K \|\mathbf{w}\|_2^2 . \tag{4.28}$$

This last expression connects the l_1-norm squared with the l_2-norm and the desired cardinality of the vector $\mathbf{w}$, which is K. First of all, we need to determine an initial value of the parameter γ in the binary search procedure. This value, which is denoted by $\gamma_{\max}$, has to ensure that the obtained solution will have, at least, K active relays. With this aim in mind let us focus on the right side of the inequality, i.e., $\|\mathbf{w}\|_1^2 \leq K \|\mathbf{w}\|_2^2$. If an upper bound on l_2-norm squared of $\mathbf{w}$ can be determined, it can be used to compute $\gamma_{\max}$. To obtain this bound consider the problem in (4.24) assuming that all the relays are active, i.e., consider $\tilde{\mathbf{A}} = \mathbf{A}$ and $\tilde{\mathbf{B}} = \mathbf{B}$ and $\tilde{\mathbf{q}} = \mathbf{q}$ and let $\mathbf{w}^{(0)}$ be the optimal beamformer obtained from the solution of this problem. From (4.18c) and (4.28), it is clear that $\gamma = K \left\|\mathbf{w}^{(0)}\right\|_2^2$ ensures that at least K relays will be active. This is due to the fact that by decreasing γ one is also decreasing $\|\mathbf{w}\|_1^2$ and, consequently, $\|\mathbf{w}\|_2^2$. Thus, $\gamma_{\max} = K \left\|\mathbf{w}^{(0)}\right\|_2^2$ will be used as initial value in the search process. Unfortunately, $\gamma = \gamma_{\max}$ often enforces solutions with more than K active entries in the solution vector. Therefore, we need to decrease the parameter γ by considering a binary search until a solution with the desired number of active relays is obtained. The whole algorithm is summarized in the following subsection. Note that this

binary search requires solving the problem in (4.23) for different values of γ until a solution with the desired degree of sparsity is obtained. Nevertheless, the number of semidefinite programming problems which needs to be solved with this binary search is far less than in the exhaustive search which requires solving $\binom{N}{K}$ problems of type (4.24). This fact will be further analyzed in Section 4.4.

4.3.4 Description of the algorithm

The whole method is summarized in Algorithm 2.

Algorithm 2 Proposed method

STEP 1) INITIALIZATION: Solve (4.24) assuming that all the relays are active and obtain $\mathbf{w}^{(0)}$. Initialize the values for the binary search: $\gamma_{\max} = K \left\|\mathbf{w}^{(0)}\right\|_2^2$, $\gamma_{low} = 0$, $\gamma = \gamma_{\max}$.

STEP 2) SELECTION OF THE SUBSET OF RELAYS:
while number of active relays$\neq K$ **do**

A) Solve (4.23) for the corresponding γ and determine the active relays (non-zero entries of the diagonal of $\mathbf{Y}$)
B) Compute the new value of γ as follows
if number of active relays $> K$ **then**
$\gamma_{up} = \gamma$ and $\gamma \leftarrow (\gamma_{low} + \gamma)/2$
else
if number of active relays $< K$ **then**
$\gamma_{low} = \gamma$ and $\gamma \leftarrow (\gamma_{up} + \gamma)/2$
end if
end if
end while

STEP 3) COMPUTATION OF THE WEIGHTS: Solve the reduced-size problem (4.24) with the selected subset and extract the weights $\tilde{\mathbf{w}}$.

The extension of this algorithm to cognitive relay networks has been proposed by the authors in [63]. Compared to the problem addressed in this chapter, it requires the addition of new constraints in order to keep the interference radiated to the users of the primary network below the maximum tolerable level. Since the extension is straightforward, the details are omitted in this chapter.

4.3.5 Relationship between total relay transmit power and parameter γ

To analyze this relationship let us explore the expression of the total relay transmit power which is given by

$$P_T = \sum_{i=1}^{i=N} |y_i|^2 = \sum_{i=1}^{i=N} E\left\{|x_i|^2\right\} |w_i|^2 = \mathbf{w}^H \mathbf{D} \mathbf{w}, \tag{4.29}$$

where y_i and the diagonal matrix $\mathbf{D}$ have been defined in (4.2) and (4.13) respectively. Applying the Cauchy-Schwarz inequality

$$P_T = \mathbf{w}^H \mathbf{D} \mathbf{w} = \left\|\mathbf{D}^{1/2}\mathbf{w}\right\|_2^2 \leq \left\|\mathbf{D}^{1/2}\right\|_2^2 \|\mathbf{w}\|_2^2 . \tag{4.30}$$

Bearing in mind (4.30), the left side inequality in (4.28) and (4.18c), it is straightforward to show

$$P_T \leq \left\|\mathbf{D}^{1/2}\right\|_2^2 \|\mathbf{w}\|_2^2 \leq \left\|\mathbf{D}^{1/2}\right\|_2^2 \|\mathbf{w}\|_1^2 \leq \left\|\mathbf{D}^{1/2}\right\|_2^2 \gamma. \tag{4.31}$$

From this inequality one can conclude that if the parameter γ is shrunk to promote the desired degree of sparsity, the power transmitted by the relays P_T is also decreased.

4.4 Numerical Results

The goal of this section is to analyze the performance of the algorithm exposed above by numerical simulations. To solve the semidefinite problems presented in (4.23) and (4.24), CVX [118], a MATLAB package for disciplined convex programming, is used. Next, we describe the set of parameters considered throughout the simulations.

The first scenario under consideration is a wireless network composed of a source, which transmits with a power $P_s = 0$ dBW, a destination and $N = 20$ potential relays whose individual power constraints are uniformly given by

$$P_i = \frac{P}{N} \quad \text{(in W)} \qquad \text{for } i = 1, ..., N. \tag{4.32}$$

with $P = 20$ W (which implies $P_i = 0$ dBW). The noise variances are set to $\sigma_d^2 = \sigma_r^2 = -3$ dBW.

Figure 4.2 plots the achieved SNR as a function of the number of selected relays K. The curves were obtained by averaging the results of 500 independent simulation runs. In each

trial, the means and the variances of the flat fading channels were generated randomly as follows:

$$\begin{array}{rcll} \bar{h}_i, \bar{g}_i & \sim & \mathcal{CN}(0,1) & \text{for } i = 1, ..., N \\ \alpha_i, \beta_i & \sim & \frac{1}{2}\mathcal{X}^2(2) & \text{for } i = 1, ..., N \end{array} \tag{4.33}$$

where $\mathcal{X}^2(2)$ denotes the chi-square distribution with two degrees of freedom. The parameters $\bar{h}_i$, α_i, $\bar{g}_i$ and β_i denote the mean and the variance of the i-th element of $\mathbf{h}$ and $\mathbf{g}$, respectively, as has been exposed in (4.7). In each trial, the matrices $\mathbf{A}$, $\mathbf{B}$ and $\mathbf{D}$ have been generated according to the values of the paramaters presented above. In particular, the matrix $\mathbf{A}$ is generated following the expression (4.7) and $\mathbf{B}$ is created according to (4.10), with $E\{|g_i|^2\} = |\bar{g}_i|^2 + \beta_i$. Regarding the matrix $\mathbf{D}$, it is formed as in (4.13), with $E\{|h_i|^2\} = |\bar{h}_i|^2 + \alpha_i$.

As can be seen from Figure 4.2, the proposed method clearly outperforms the random selection of the relays and achieves a performance in terms of end-to-end SNR that is very close to that of the exhaustive search, requiring far less computational complexity. This fact will be analyzed later.

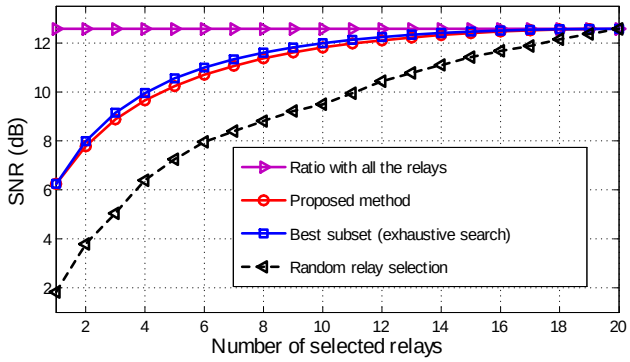

Figure 4.2: SNR at the receiver as a function of the number of selected relays K with uniform power constraints. $P_i = 0$ dBW, $\sigma_d^2 = \sigma_r^2 = -3$ dBW. Average of the results of 500 independent trials.

To gain further insight into the approximation quality of the solution described in this chapter, Figure 4.3 plots the averaged and the maximum approximation ratios as a function of the number of selected relays. The approximation ratio is a common way to measure the quality of convex approximations in combinatorial problems and is defined as the ratio between the optimal SNR, obtained by computing the exhaustive search, and the SNR

obtained by the solution of the relaxed problem $\tilde{\mathbf{w}}$. Note that the approximation ratio parameter is always greater than or equal to one and is equal to one if the relaxed problem attains the same objective value as the optimal-SNR scheme. The proposed method clearly provides high quality approximate solutions, in terms of both the averaged and the worst case perfomance, and is close to the optimal for the all the possible cooperative sizes.

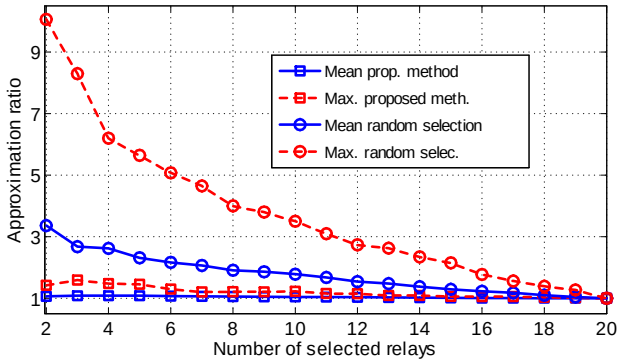

Figure 4.3: Empirical approximation ratio as a function of the number of selected relays.

Regarding the computational complexity, Table 4.1a shows the mean number of semi-definite programming problems required to select the appropriate number of relays during the binary search procedure. Note that the number of iterations for each K is always less than the total number of potential relays N. To get further insight about the reduction of the computational complexity, consider, for instance, the selection of the best subset of 12 nodes out of a potential set of 20 relays. An exhaustive search in this case requires solving 125970 SDP. Nonetheless, the proposed technique needs to solve less than 7 SDP problems in mean (less than 6 for the selection of the subset plus 1 for the computation of the optimal weights). Furthermore, the worst case required the computation of 15 SDP problems which is far less than the number of SDP needed by the exhaustive search.

In order to analyze the performance of the method for different individual power values, Figure 4.4 plots the achieved SNR versus the individual power constraints for different values of K. In this case, the value of the uniform power constraints presented in (4.32) is varied. Note that the proposed algorithm exhibits a good performance and is close to the optimal solution for all the possible individual power levels.

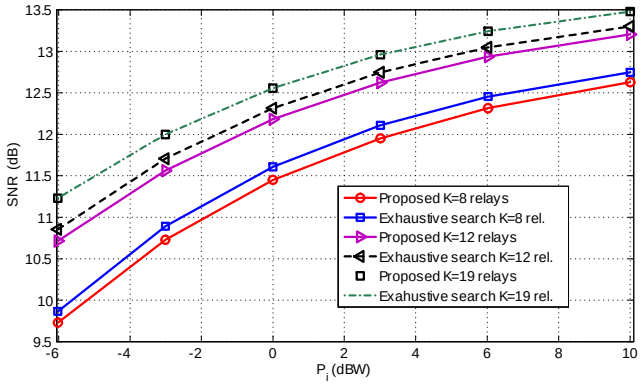

Figure 4.4: SNR measured at the receiver as a function of the individual power constraints for different values of K

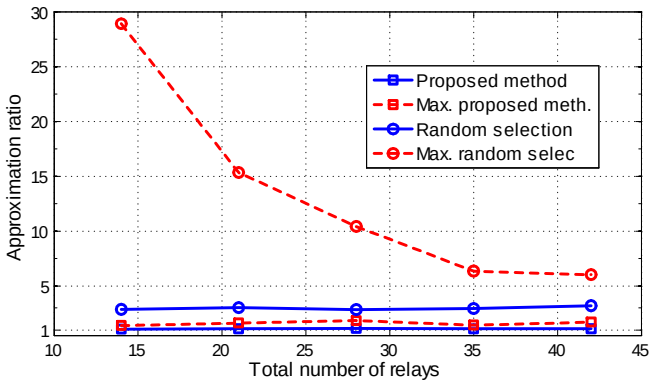

Figure 4.5: Approximation ratio as a function of the total number of potential relays. $N \in [14,\ 21,\ 28,\ 35,\ 42]$, $K = \frac{N}{7}$ and $P = 10$ dBW.

K	Mean num. it. Prop. meth.	Num. SDP Exhaustive
2	6.35	190
3	7.08	1140
4	7.11	4845
5	6.94	15504
6	6.63	38760
7	6.46	77520
8	6.14	125970
9	6.09	167960
10	6.13	184756
11	6.09	167960
12	5.66	125970
13	5.52	77520
14	4.99	38760
15	4.96	15504
16	4.52	4845
17	4.19	1140
18	3.56	190
19	3.56	20

(a) $N = 20$ potential relays and uniform power constraints

K	Mean num. it. prop. meth.	Num. SDP Exhaustive
2	5.27	45
3	5.40	120
4	5.15	210
5	4.96	252
6	4.65	210
7	4.51	120
8	4.12	45
9	3.67	10

(b) $N = 10$ potential relays and non-uniform power constraints

Table 4.1: Mean number of SDP problems which needs to be solved during the binary process as a function of the number of relays.

Next, we investigate the performance of the algorithm when the number of potential relay nodes increases. With this aim, we have considered a wireless cooperative network composed of a source, which transmits with a power $P_s = 0$ dBW, N potential relays, with the aforementioned uniform power constraints and $P = 10$ dBW, and the noise variances σ_d^2, σ_r^2 are set to -3 dBW. Figure 4.5 shows the averaged and the maximum approximation ratio as a function of the total number of potential relays N when the size of the cooperative group is fixed to $K = N/7$. As can be seen from Figure 4.5, the described technique is close to the optimal solution for all the network sizes and delivers high approximate solutions in both the averaged and the worst case perfomance.

In order to illustrate the high performance of the algorithm, Figure 4.6 shows the empirical Cumulative Distribution Function (CDF) of the approximation ratios in the

previous scenario for the case $N = 35$ and $K = 5$. Notice that the proposed algorithm achieves ratios that are close to the optimal value with a high probability and clearly outperforms the random selection of the subset of cooperative nodes.

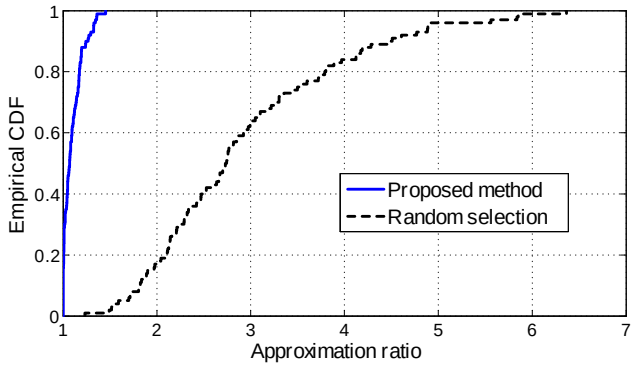

Figure 4.6: Empirical cumulative distribution function of the approximation ratios. $P_s = 0$ dBW, $N = 35$, $K = 5$, uniform power constraints with $P = 10$ dBW and $\sigma_d^2 = \sigma_r^2 = -3$ dBW.

Next, we consider a numerical example with non-uniform power constraints. In this case the individual constraints are set to

$$P_i = i\frac{2P}{N(N+1)} \quad \text{(in W)} \qquad \text{for } i = 1, ..., N. \tag{4.34}$$

Notice that the sum of individual power constraints is equal to P, as in the previous examples. For the new scenario the number of potential relays is $N = 10$, the rest of parameters are set to $P_s = 3$ dBW, $\sigma_d^2 = \sigma_r^2 = 0$ dBW and $P = 20$W. The results presented below are obtained by averaging the results of 1000 simulation runs and at each trial the matrices $\mathbf{A}$, $\mathbf{B}$ and $\mathbf{D}$ have been generated according to the procedure described above.

Figure 4.7 and Table 4.1b show the achieved SNR and the mean number of SDP problems which needs to be solved as a function of the number of selected relays, respectively. As in the uniform-constrained case, the described technique achieves a near-optimal performance with a low computational burden. Regarding the computational complexity, the worst-case scenario required 14 iterations and was obtained for $K = 6$.

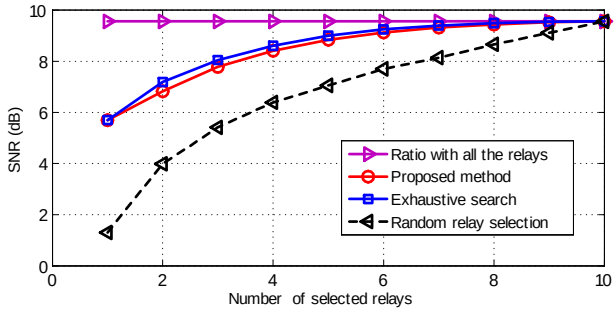

Figure 4.7: SNR measured at the receiver as a function of the number of selected relays K. 10 relays and non-uniform power constraints.

4.5 Conclusions

A new method which deals with the problem of multiple relay selection under per-relay power constraints was presented in this chapter. In particular, we have addressed the joint problem of selecting the best subset of cooperative nodes and their corresponding beamforming weights so that the end-to-end SNR is maximized. The optimal solution of this problem is computationally demanding and requires an exhaustive combinatorial search. In order to reduce the computational burden, this chapter has proposed a sub-optimal method with a near-optimal performance and a feasible computational complexity. Our approach is based on the knowledge of the second-order statistics of the CSI and the relays are not limited to cooperate at full power.

4.A Appendix

4.A.1 Proof of Theorem 4.1

Since the maximization problem presented in (4.24) is convex and feasible, the KKT conditions [114] are necessary and sufficient conditions for the optimality. Let $\left(\tilde{\mathbf{Y}}^*, z^*\right)$ be the solution to (4.24), then the KKT conditions of this problem are

$$-\tilde{\mathbf{A}} + \sum_{i=1}^{K} \lambda_i \mathbf{J}_i + \mu \tilde{\mathbf{B}} - \mathbf{\Phi} = \mathbf{0} \tag{4.35a}$$

$$-\sum_{i=1}^{K} \lambda_i \tilde{q}_i + \mu \sigma_d^2 - \delta = 0 \tag{4.35b}$$

$$\mathrm{Tr}\{\mathbf{J}_i \tilde{\mathbf{Y}}^*\} - z^* \tilde{q}_i \leq \mathbf{0} \qquad \forall i = 1, ..., K \tag{4.35c}$$

$$\mathrm{Tr}\{\tilde{\mathbf{B}} \tilde{\mathbf{Y}}^*\} + \sigma_d^2 z^* \ - 1 = 0; \tilde{\mathbf{Y}}^* \succeq 0; \ z^* \geq 0 \tag{4.35d}$$

$$\lambda_i \geq 0 \ \ \forall i; \quad \mathbf{\Phi} \succeq 0 \tag{4.35e}$$

$$\lambda_i \left[\mathrm{Tr}\{\mathbf{J}_i \tilde{\mathbf{Y}}^*\} - \ z^* \tilde{q}_i \right] = 0 \qquad \forall i = 1, ..., K \tag{4.35f}$$

$$\mathrm{Tr}\{\mathbf{\Phi} \tilde{\mathbf{Y}}^*\} = 0 \tag{4.35g}$$

$$\delta z^* = 0, \tag{4.35h}$$

where $\mathbf{J}_i$ is a single-entry matrix, with zeros in all the entries except for the (i,i)th element which is equal to one. The parameters λ_i, μ, $\mathbf{\Phi}$ and δ are the Lagrange multipliers associated with the constraints (4.24b)-(4.24e) respectively.

As it was discussed in the subsection 4.3.1, $z^* = 0$ cannot be a solution of the problem (4.23), and this imposes $\delta = 0$ in the equation (4.35h). Consider that all the relays do not use their maximum power in the retransmission. Taking into account (4.35f), this implies $\lambda_i = 0 \quad \forall i$. Consequently, as $\delta = 0$, $\lambda_i = 0 \ \forall i$, it is clear from (4.35b) that $\mu = 0$. Bearing in mind these values, equation (4.35a) can be rewritten as $\mathbf{\Phi} = -\tilde{\mathbf{A}}$ which does not make sense because $\mathbf{\Phi} \succeq 0$ and $\tilde{\mathbf{A}} \succeq 0$.

4.A.2 Proof of Theorem 4.2

Recall the KKT conditions presented in Appendix 4.A.1 (4.35a) - (4.35h). Taking into account (4.35g), as $\mathbf{\Phi} \succeq 0$ and $\tilde{\mathbf{Y}}^* \succeq 0$, then it is clear that $\mathbf{\Phi} \tilde{\mathbf{Y}}^* = \mathbf{0}$. As the matrices $\tilde{\mathbf{Y}}^*$ and $\mathbf{\Phi}$ are square matrices of size $K \times K$, then the Sylvester's rank inequality holds (Section 10.5.1 of [119])

$$\mathrm{rank}(\mathbf{\Phi} \tilde{\mathbf{Y}}^*) \geq \mathrm{rank}(\mathbf{\Phi}) + \mathrm{rank}(\tilde{\mathbf{Y}}^*) - K. \tag{4.36}$$

As the $\text{rank}(\boldsymbol{\Phi}\tilde{\mathbf{Y}}^*) = 0$, then

$$\text{rank}(\tilde{\mathbf{Y}}^*) \leq \ K - \text{rank}(\boldsymbol{\Phi}). \tag{4.37}$$

To determine the $\text{rank}(\tilde{\mathbf{Y}}^*)$ we need to compute the $\text{rank}(\boldsymbol{\Phi})$. With this aim let us recall (4.35a). As the matrix $\tilde{\mathbf{A}}$ can be expressed in terms of the sum of diagonal matrix plus a rank-one matrix (4.7) $\tilde{\mathbf{A}} = \tilde{\boldsymbol{\Lambda}} + \tilde{\mathbf{v}}\tilde{\mathbf{v}}^H$. Then equation in (4.35a) can be rewritten as

$$\left[\sum_{i=1}^{K} \lambda_i \mathbf{J}_i - \tilde{\boldsymbol{\Lambda}} + \mu\tilde{\mathbf{B}}\right] - \tilde{\mathbf{v}}\tilde{\mathbf{v}}^H = \boldsymbol{\Phi}. \tag{4.38}$$

Note that the matrix $\sum_{i=1}^{K} \lambda_i \mathbf{J}_i - \tilde{\boldsymbol{\Lambda}} + \mu\tilde{\mathbf{B}}$ is a diagonal matrix. Now let us prove that the entries of this matrix are all greater than zero. To prove that fact, consider that the ith element of diagonal of the matrix $\sum_{i=1}^{K} \lambda_i \mathbf{J}_i - \tilde{\boldsymbol{\Lambda}} + \mu\tilde{\mathbf{B}}$ is less than or equal to zero and consider a single-entry vector $\mathbf{s}_i$ with all the elements equal to zero except for the ith element which is equal to one. If all the entries of the vector $\tilde{\mathbf{v}}$ are different from zero, then $\mathbf{s}_i^H \tilde{\mathbf{v}}\tilde{\mathbf{v}}^H \mathbf{s}_i > 0$ and consequently,

$$\mathbf{s}_i^H \boldsymbol{\Phi} \mathbf{s}_i = \mathbf{s}_i^H \ \left[\sum_{i=1}^{K} \lambda_i \mathbf{J}_i - \tilde{\boldsymbol{\Lambda}} + \mu\tilde{\mathbf{B}}\right] \mathbf{s}_i - \mathbf{s}_i^H \tilde{\mathbf{v}}\tilde{\mathbf{v}}^H \mathbf{s}_i < 0. \tag{4.39}$$

However, this violates $\boldsymbol{\Phi} \succeq 0$. Therefore, $\boldsymbol{\Psi} = \sum_{i=1}^{K} \lambda_i \mathbf{J}_i - \tilde{\boldsymbol{\Lambda}} + \mu\tilde{\mathbf{B}} \succ 0$ because $\boldsymbol{\Psi}$ is a diagonal matrix with positive entries. Furthermore, it follows from this statement that

$$\text{rank}(\boldsymbol{\Psi}) = K. \tag{4.40}$$

This result will be important in the computation of $\text{rank}(\boldsymbol{\Phi})$. At this point let us recall the expression (4.38). Using the following result in matrix theory [119] $\text{rank}(\mathbf{U} + \mathbf{V}) \leq \text{rank}(\mathbf{U}) + \text{rank}(\mathbf{V})$, it is straightforward to rewrite $\text{rank}(\boldsymbol{\Phi})$ in terms of the next inequality

$$\text{rank}(\boldsymbol{\Phi}) \geq \text{rank}(\boldsymbol{\Psi}) - \text{rank}(\tilde{\mathbf{v}}\tilde{\mathbf{v}}^H) = K - 1 \tag{4.41}$$

Thus, from the expressions (4.37) and (4.41) it follows that

$$\text{rank}(\tilde{\mathbf{Y}}^*) \leq K - \text{rank}(\boldsymbol{\Phi}) \leq K - K + 1. \tag{4.42}$$

Therefore, since $\tilde{\mathbf{Y}}^* = \mathbf{0}$ cannot maximize the objective function (4.24), we can conclude that $\text{rank}(\tilde{\mathbf{Y}}^*) = 1$.

4.A.3 Proof of Theorem 4.3

If some of the elements of $\tilde{\mathbf{v}}$ are zero, the SDP problem in (4.24) can have a solution $(\tilde{\mathbf{Y}}^*,z^*)$ where the rank of $\tilde{\mathbf{Y}}^*$ is greater than one. Nevertheless, if the solution has a rank greater than one, the rank-one solution can be recovered as it is proved in this Appendix.

Denote by J the set of inactive components of $\tilde{\mathbf{v}}$, i. e., $J=\{l \mid \tilde{v}_l=0\}$ and let $(\tilde{\mathbf{Y}}^*,z^*)$ be the solution of (4.24). Consider a matrix $\mathbf{C}$ defined as

$$C_{lk}=\begin{cases}\tilde{Y}^*_{lk} & \text{if } \ l=k \ \text{ or } \ l,k\notin J\\ 0 & \text{otherwise,}\end{cases} \tag{4.43}$$

where C_{lk} denotes the (l,k)th element of the matrix $\mathbf{C}$. It can be proved that $(\mathbf{C},z^*)$ is also a feasible point of (4.24) that achieves the same objective value as $(\tilde{\mathbf{Y}}^*,z^*)$. To prove this, first of all, let us decompose $\mathbf{C}$ as follows:

$$\mathbf{C}=\mathbf{E}+\mathbf{F}, \tag{4.44}$$

where $\mathbf{E}$ is a sparse matrix whose active components are the entries of the diagonal corresponding to the elements of the set J

$$E_{ll}=\begin{cases}\tilde{Y}^*_{ll} & \text{if } \ l\in J\\ 0 & \text{otherwise,}\end{cases} \tag{4.45}$$

and $\mathbf{F}$ a matrix whose (l,k)th entry is given by

$$F_{lk}=\begin{cases}\tilde{Y}^*_{lk} & \text{if } \ l\notin J,\ k\notin J\\ 0 & \text{otherwise.}\end{cases} \tag{4.46}$$

Recall that the aim of this appendix is to prove that even if $\tilde{\mathbf{Y}}^*$ has a rank greater than one, the rank-one solution can be recovered directly from $\tilde{\mathbf{Y}}^*$ and z^* and no randomization or eigendecomposition is needed. The following lemma is the key point of the proof.

Lemma 4.1 *If $(\tilde{\mathbf{Y}}^*,z^*)$ is the solution of the SDP in (4.24), then $(\mathbf{C},z^*)$ is a feasible point which achieves the same objective value as $(\tilde{\mathbf{Y}}^*,z^*)$. Furthermore, $\mathbf{C}$ can be decomposed as $\mathbf{C}=\mathbf{E}+\mathbf{F}$, where $\mathbf{E}$ and $\mathbf{F}$ the matrices exposed above, and $\mathbf{F}$ is a rank-one matrix.*

Proof: *See Appendix 4.A.4.*

The proof of the first part of the lemma is based on fact that $\mathbf{C}$ differs from $\tilde{\mathbf{Y}}^*$ only at the entries given by (l,k) with $l,k \in J$ and $l \neq k$. Due to this fact, ($\mathbf{C}$,z^*) is a feasible point which attains the same objective function. Furthermore, since $\mathbf{F}$ is a rank-one matrix, it can be decomposed as $\mathbf{F} = \mathbf{f}\mathbf{f}^H$.

Consider $\mathbf{H} \triangleq \mathbf{h}\mathbf{h}^H$, where $\mathbf{h}$ is a vector whose lth entry is given by

$$h_l = \begin{cases} \sqrt{\tilde{Y}_{ll}^*} & \text{if } \ l \in J \\ f_l & \text{otherwise,} \end{cases} \tag{4.47}$$

where f_l denotes the lth element of $\mathbf{f}$. Following an analysis similar to the proof of Lemma4.1 it is straightforward showing that ($\mathbf{H}$,z^*) is a feasible point that achieves the same objective value as ($\tilde{\mathbf{Y}}^*$,z^*). The key point of this proof is that $\mathbf{H}$ differs from $\tilde{\mathbf{Y}}^*$ only at the entries given by (l,k) with $l,k \in J$ and $l \neq k$. Bearing in mind that fact and since $\mathbf{H}$ is rank one, the optimal beamformer can be recovered from the eigendecomposition of $\mathbf{H}/z^*$, i. e., $\tilde{\mathbf{w}} = h/\sqrt{z^*}$. Thus, the optimal weights can be obtained as

$$\tilde{w}_l = \begin{cases} \sqrt{\frac{\tilde{Y}_{ll}^*}{z^*}} & \text{if } \ l \in J \\ \frac{f_l}{\sqrt{z^*}} & \text{otherwise.} \end{cases} \tag{4.48}$$

Notice that the moduli of the diagonal entries of $\mathbf{F}$ (4.46) not belonging to J can be directly extracted from $\tilde{\mathbf{Y}}^*$. As a consequence, $|f_l| = \sqrt{\tilde{Y}_{ll}^*}$ for $l \notin J$. It only remains to compute the phases and they can be obtained from the components of $\tilde{\mathbf{v}}$. Therefore, the next result is obtained:

$$\tilde{w}_l = \begin{cases} \sqrt{\frac{\tilde{Y}_{ll}^*}{z^*}} & \text{if } \ l \in J \\ \sqrt{\frac{\tilde{Y}_{ll}^*}{z^*}} e^{j\angle \tilde{v}_l} & \text{otherwise,} \end{cases} \tag{4.49}$$

where $\tilde{v}_l$ denotes the lth element of $\tilde{\mathbf{v}}$. This concludes the proof of the theorem.

4.A.4 Proof of Lemma 4.1

To prove the first part of the lemma, i.e., to prove that ($\mathbf{C}$,z^*) is a feasible point that achieves the same objective value as ($\tilde{\mathbf{Y}}^*$,z^*) we need to show that:

1. $\text{Tr}\{\tilde{\mathbf{A}}\tilde{\mathbf{Y}}^*\} = \text{Tr}\{\tilde{\mathbf{A}}\mathbf{C}\}$
2. $C_{ii} = \tilde{Y}_{ii}^* \leq z^* \ \tilde{q}_i \quad \forall i = 1, ..., K$

3. $\text{Tr}\{\tilde{\mathbf{B}}\tilde{\mathbf{Y}}^*\} + \sigma_d^2 z^* = \text{Tr}\{\tilde{\mathbf{B}}\mathbf{C}\} + \sigma_d^2 z^* = 1$

4. $\mathbf{C} \succeq 0$

Let us analyze it point by point:

1. $\text{Tr}\{\tilde{\mathbf{A}}\tilde{\mathbf{Y}}^*\} = \text{Tr}\{\tilde{\mathbf{A}}\mathbf{C}\}$ implies $\text{Tr}\{\tilde{\mathbf{A}}(\tilde{\mathbf{Y}}^* - \mathbf{C})\} = 0$. Considering (4.7), this can be rewritten as follows $\text{Tr}\{(\tilde{\mathbf{\Lambda}} + \tilde{\mathbf{v}}\tilde{\mathbf{v}}^H)(\tilde{\mathbf{Y}}^* - \mathbf{C})\} = \text{Tr}\{(\tilde{\mathbf{\Lambda}}(\tilde{\mathbf{Y}}^* - \mathbf{C})\} + \text{Tr}\{\tilde{\mathbf{v}}\tilde{\mathbf{v}}^H(\tilde{\mathbf{Y}}^* - \mathbf{C})\} = 0$. The matrix $\tilde{\mathbf{Y}}^* - \mathbf{C}$ has all null entries except for the elements (l,k)th and (k,l)th $\forall k, l \in J$ with $k \neq l$. And it is straightforward to show that $\text{Tr}\{(\tilde{\mathbf{\Lambda}}(\tilde{\mathbf{Y}}^* - \mathbf{C})\} = 0$ and $\text{Tr}\{\tilde{\mathbf{v}}\tilde{\mathbf{v}}^H(\tilde{\mathbf{Y}}^* - \mathbf{C})\} = 0$.

2. The diagonals of the matrices $\tilde{\mathbf{Y}}^*$ and $\mathbf{C}$ have the same elements and then $C_{ii} = \tilde{Y}_{ii}^*$, then it is straightforward to show the inequality.

3. $\tilde{\mathbf{B}}$ is diagonal and the diagonals of $\tilde{\mathbf{Y}}^*$ and $\mathbf{C}$ have the same elements. Thus, $\text{Tr}\{\tilde{\mathbf{B}}\tilde{\mathbf{Y}}^*\} = \text{Tr}\{\tilde{\mathbf{B}}\mathbf{C}\}$, and then this point is proved.

4. Recall (4.44), $\mathbf{C} = \mathbf{E} + \mathbf{F}$. Since $\mathbf{E}$ is a diagonal matrix and the elements of the diagonal are zero or positive, then $\mathbf{E} \succeq 0$. Furthermore, $\mathbf{F}$ is obtained by putting to zero the rows and the columns of $\tilde{\mathbf{Y}}^*$ which correspond to the inactive components of $\tilde{\mathbf{v}}$. Since all the principal minors of the semidefinite matrix $\tilde{\mathbf{Y}}^*$ are also semidefinite. Then, $\mathbf{F} \succeq 0$ and as the sum of semidefinite matrices is also semidefinite, we obtain $\mathbf{C} = \mathbf{E} + \mathbf{F} \succeq 0$.

Once it has been proved that $(\mathbf{C}, z^*)$ is feasible solution, we need to prove that $\mathbf{F}$ is a rank-one matrix. With this aim in mind, let us define the following variables:

- $\breve{\mathbf{F}}$ is the matrix constructed by deleting the lth row and the lth column of $\mathbf{F}$ $\forall l \in J$.
- $\breve{\mathbf{\Lambda}}$ is the diagonal matrix formed by deleting the lth row and the lth column of $\tilde{\mathbf{\Lambda}} \forall l \in J$.
- $\breve{\mathbf{B}}$ is the diagonal matrix formed by deleting the lth row and the lth column of $\tilde{\mathbf{B}} \forall l \in J$.
- $\breve{\mathbf{v}}$ is the vector constructed by deleting lth element of $\tilde{\mathbf{v}}$ $\forall l \in J$.

Notice that $\breve{\mathbf{F}}$, $\breve{\mathbf{\Lambda}}$ and $\breve{\mathbf{B}}$ are square matrices of size $K-|J|$ and $\breve{\mathbf{v}}$ is a vector of length $K-|J|$. It can be shown that $\mathbf{F}$ is rank one because $\breve{\mathbf{F}}$ is rank one. With this end in mind, let us rewrite the objective function presented in (4.24a) in terms of $\breve{\mathbf{F}}$ and $\breve{\mathbf{v}}$. Using the point 1 exposed above and the equality in (4.44), the objective function can be rewritten as

$$\begin{aligned}\mathrm{Tr}\{\tilde{\mathbf{A}}\tilde{\mathbf{Y}}^*\} = \mathrm{Tr}\{\tilde{\mathbf{A}}\mathbf{C}\} = \mathrm{Tr}\{\tilde{\mathbf{A}}(\mathbf{E}+\mathbf{F})\} =& \mathrm{Tr}\{\tilde{\mathbf{A}}\mathbf{E}\}+\mathrm{Tr}\{\tilde{\mathbf{A}}\mathbf{F}\} \\ =& \mathrm{Tr}\{\tilde{\mathbf{A}}\mathbf{E}\}+\mathrm{Tr}\{(\breve{\mathbf{\Lambda}}+\breve{\mathbf{v}}\breve{\mathbf{v}}^H)\breve{\mathbf{F}}\}. \end{aligned} \tag{4.50}$$

The second line in (4.50) follows from the fact the matrix $\mathbf{F}$ has zeros in the rows and the columns corresponding to the elements of the set J. As a consequence, it is straightforward to show that $\mathrm{Tr}\{\tilde{\mathbf{A}}\mathbf{F}\} = \mathrm{Tr}\{(\breve{\mathbf{\Lambda}}+\breve{\mathbf{v}}\breve{\mathbf{v}}^H)\mathbf{F}\} =\mathrm{Tr}\{(\breve{\mathbf{\Lambda}}+\breve{\mathbf{v}}\breve{\mathbf{v}}^H)\breve{\mathbf{F}}\}$. In the same way, the constraint (4.24c) can be rewritten in terms of $\breve{\mathbf{F}}$. Consider the point 3 exposed above, then it is straightforward to show that

$$\begin{aligned}\mathrm{Tr}\{\tilde{\mathbf{B}}\tilde{\mathbf{Y}}^*\}+\sigma_d^2 z^* &= \mathrm{Tr}\{\tilde{\mathbf{B}}\mathbf{C}\}+\sigma_d^2 z^* \\ &= \mathrm{Tr}\{\tilde{\mathbf{B}}\mathbf{E}\}+\mathrm{Tr}\{\breve{\mathbf{B}}\breve{\mathbf{F}}\}+\sigma_d^2 z^*. \end{aligned} \tag{4.51}$$

Thus, the constraint (4.24c) can be expressed as

$$\mathrm{Tr}\{\tilde{\mathbf{B}}\mathbf{E}\}+\mathrm{Tr}\{\breve{\mathbf{B}}\breve{\mathbf{F}}\}+\sigma_d^2 z^* = 1. \tag{4.52}$$

Based on the analysis above and since ($\mathbf{C}$,z^*), with $\mathbf{C}=\mathbf{E}+\mathbf{F}$, is a feasible solution of (4.24), then $\breve{\mathbf{F}}$ can be obtained as the solution of the next problem

$$\max_{\breve{\mathbf{F}}} \quad \mathrm{Tr}\{\tilde{\mathbf{A}}\mathbf{E}\}+\mathrm{Tr}\{(\breve{\mathbf{\Lambda}}+\breve{\mathbf{v}}\breve{\mathbf{v}}^H)\breve{\mathbf{F}}\} \tag{4.53a}$$

$$\text{s.t.} \quad \breve{F}_{ii} + E_{\Theta(i)\Theta(i)} \leq z^*\ \tilde{q}_i \quad \forall i \in 1,...,K-|J| \tag{4.53b}$$

$$\mathrm{Tr}\{\tilde{\mathbf{B}}\mathbf{E}\}+\mathrm{Tr}\{\breve{\mathbf{B}}\breve{\mathbf{F}}\}+\sigma_d^2 z^* = 1 \tag{4.53c}$$

$$\breve{\mathbf{F}} \succeq 0\ , \tag{4.53d}$$

where Θ denotes the set of active components, i.e., $\Theta = \{l \mid \tilde{v}_l \neq 0\}$ and $\Theta(i)$ the ith element of the set Θ. Following an analysis similar to the one exposed in the proof of Theorem 4.2, we can show that since all the coefficients of $\breve{\mathbf{v}}$ differ from zero, then $\breve{\mathbf{F}}$ has rank one. Since $\mathbf{F}$ can be directly reconstructed from $\breve{\mathbf{F}}$ by adding some columns and rows of zeros and adding zero rows and zero columns does not change the rank of the matrix, the desired result is obtained.

Chapter 5

Joint distributed beamforming design and relay subset selection in multi-user wireless relay networks: A novel DC programming approach

This chapter deals with the joint relay subset selection and distributed beamforming optimization in multi-user multi-relay networks. In modern wireless cooperative networks the number of potential relays could be large, e.g. in device-to-device communications. In these scenarios it is impractical (or even unaffordable) to activate all the relays due to the communications and processing overhead required to maintain the synchronization amongst all the distributed nodes in the wireless network. In this context, the selection of the most suitable subset of relay nodes for the cooperation is of paramount importance because it has a great impact on the system performance. Two different problems are addressed in this chapter: i) the selection of the minimum number of relays that guarantees a predefined signal-to-interference-plus-noise-ratio (SINR) at the destination nodes in a multi-user peer-to-peer wireless cooperative network; and ii) the selection of the best subset of K nodes that minimizes the total relay transmit power satisfying the quality of service requirements at the destinations. Both problems are addressed taking into account individual power constraints at the relays. To solve these problems, several sub-optimal techniques based on the convex-concave procedure are proposed. Numerical results show that they achieve a near-optimal performance with a reduced computational complexity.

5.1 Introduction

Distributed beamforming in multi-user wireless relay networks has attracted a significant attention due to its ability to improve the service coverage, the spectral efficiency and the user's throughput [58, 120]. Within this context, the selection of the proper subset of spatially distributed relays is a key issue. Specially, for large-scale relay networks. In many practical situations the number of potential relay nodes could be large [50, 61], i.e., in device-to-device communications, and the proper selection of the subset of cooperative nodes is crucial, since it has dramatic effect in the overall system performance, e.g., in the network resources, user's throughput, power efficiency and system complexity.

5.1.1 Related work

The relay selection problem is a problem of combinatorial nature and has been intensively investigated during the past decade for single-user relay networks, i.e., for ad-hoc wireless networks with only one source-destination pair (see [50, 61] and references therein). However, the relay assignment problem in multi-user multi-relay networks is more challenging and all these techniques cannot be directly extended [121, 53]. The main problem is that the proper design of a relay subset selection method has to take into account the interference provoked by the simultaneous transmissions of multiple users and this requires the development of more sophisticated techniques. Relay selection in multi-user wireless relay networks has recently deserved a particular attention. The single relay selection problem has been addressed in [122]. This reference deals with the maximization of the network sum rate assuming that only one relay can help at most one user in its transmission. This approach is based on the fact the number of concurrent interfering source-to-destination communications is reduced and the proposed solution is formulated as a weighted bipartite problem that is solved using the Hungarian algorithm. Unfortunately, in adverse environments transmitting over a single relay may not be sufficient to achieve a desired performance at the destination nodes [53] and this fact motivates the multi-relay selection problem in multi-user wireless relay networks. The multiple relay assignment problem has been recently considered in [53] and [121]. Reference [53] considers the joint optimization of cooperative beamforming and the multiple relay selection problem that maximizes the minimum SINR at the destinations in a two-hop multi-user amplify-and-forward wireless network. Reference [121] addresses the maximization of the minimum user rate in a two-hop decode-and-forward network. In these works, the cooperation size, i.e., the number of selected relay nodes, is fixed and both lead to mathematical formulations where it is always possible to find a feasible solution.

5.1.2 Contributions of the chapter

This chapter considers two different relay subset selection problems:

1. The joint selection of the minimum number of relay nodes and the computation of the corresponding distributed beamforming weights that guarantee a predefined SINR at the destination nodes in a multi-user amplify-and-forward wireless relay network. This problem is addressed considering individual power constraints at the relays. To the best of authors' knowledge it has never been addressed in the literature. However, the selection of the minimum number of active links is of practical interest in wireless networks because it reduces the overall network complexity as well as the communications and processing overhead. Furthermore, by considering the selection of relay nodes, the links with the lowest quality are discarded and this fact increases the robustness against link failures. The mathematical formulation of the proposed problem involves a non-convex objective function with non-convex constraints. Herein, this problem is reformulated as a Difference-of-Convex-functions (DC) programming problem [45] and a low-complexity sub-optimal method, based on the Convex-Concave Procedure (CCP) [54], is proposed to solve it. The application of this procedure leads to an iterative reweighted l_1-norm [23] over the convexified set of SINR constraints.

2. The second problem considered in this chapter is the joint design of the distributed beamforming and the selection of the best subset of K cooperative nodes that minimize the total relay transmit power. This problem is addressed taking into account the SINR requirements at the destination nodes and individual power constraints at the relays. It involves non-convex constraints due to the SINR requirements and binary constraints and constitutes a very challenging non-convex mixed-integer nonlinear program (MINLP) [55]. It should be remarked that leaving aside the subset selection issue, finding the optimal beamforming weights that minimizes the total relay transmit power with SINR requirements and per-relay power constraints is an already hard non-convex Quadratically Constrained Quadratic Problem (QCQP) [56,57] that has been analyzed in [58]. As shown therein, the traditional Semidefinite Relaxation (SDR) [44] followed by a randomization often fails at providing a feasible solution. Here, the joint subset selection and distributed beamforming computation is rewritten as a DC program and solved with a new iterative algorithm based on the penalty convex-concave procedure which has been recently presented in references [59, 60].

Contrary to other approaches in the literature of subset selection problems in multi-user wireless relay networks, such as for instance [53] and [121], which are based on perfect

channel state information (CSI), the proposed techniques can be applied in scenarios with imperfect CSI as well.

5.1.3 Organization of the chapter

The chapter is structured as follows. Section 5.2 provides a fundamental background on DC programs and the penalty convex-concave procedure, the mathematical tool considered for the derivation of the techniques proposed in this chapter. Section 5.3 presents the system model. Section 5.4 deals with the minimum cardinality problem. The joint subset selection and beamforming computation that minimizes the total relay transmit power is addressed in Section 5.5. The performance of the proposed techniques is analyzed in Section 5.6. Finally, some concluding remarks are provided in Section 5.7.

5.2 Mathematical preliminaries: penalty convex-concave procedure

The aim of this section is to briefly summarize the penalty convex-concave procedure [59]. As it will be shown in the next sections, the subset selection problems addressed in this chapter can be recast as Difference of Convex (DC) programs [45]. Within this context, the convex-concave procedure (CCP) [54,123,59], a.k.a. Successive Convex Approximation (SCA), is a powerful method that has been found very effective for dealing with this kind of problems. The convex-concave procedure is a majorization-minorization algorithm [124] that solves DC programs as a sequence of convex problems. The general formulation of a DC program is given by

$$\min_{\mathbf{x}} \quad \alpha_0(\mathbf{x}) - \beta_0(\mathbf{x}) \tag{5.1a}$$

$$\text{s.t.} \quad \alpha_i(\mathbf{x}) - \beta_i(\mathbf{x}) \leq 0, \quad i = 1, ..., m \tag{5.1b}$$

where $\mathbf{x}$ can be a real- or a complex-valued vector ($\mathbf{x} \in \mathbb{R}^{n \times 1}$ or $\mathbb{C}^{n \times 1}$) and the functions $\{\alpha_i(\mathbf{x})\}_{i=0}^{i=m}$ and $\{\beta_i(\mathbf{x})\}_{i=0}^{i=m}$ are all real-valued convex functions. DC programs are not convex, unless the functions $\{\beta_i(\mathbf{x})\}_{i=0}^{i=m}$ are all affine and, hence, are hard to solve in general. Finding the global optimum of problems of the type (5.1) is computationally

expensive (or even intractable). The mathematical formulation in expression (5.1) models many non-convex problems in engineering [45]. For the sake of simplicity, it will be assumed that the functions $\{\beta_i(\mathbf{x})\}_{i=0}^{i=m}$ are differentiable. The extension to non-smooth functions is straightforward, but is out the scope of this chapter (interested readers are referred to [59]). CCP is an iterative procedure with low-complexity which has been proved to converge to KKT point of the problem (5.1). Starting from a initial feasible point $\mathbf{x}^{(0)}$, at each iteration, the CCP algorithm first linearizes the non-convex part of $\psi_i(\mathbf{x}) = \alpha_i(\mathbf{x}) - \beta_i(\mathbf{x})$ by replacing $\beta_i(\mathbf{x})$ by its affine approximation, for $i = 0, ..., m$, and then, solves the corresponding convexified problem. At the lth iteration, the algorithm approximates $\beta_i(\mathbf{x})$ by its first-order Taylor expansion $\hat{\beta}_i(\mathbf{x}, \mathbf{x}^{(l)})$ around the current point $\mathbf{x}^{(l)}$. For real-valued functions of complex variables, the first-order approximation $\hat{\beta}_i(\mathbf{x}, \mathbf{x}^{(l)})$ is given by

$$\hat{\beta}_i(\mathbf{x}, \mathbf{x}^{(l)}) = \beta_i(\mathbf{x}^{(l)}) + 2\Re\left\{\nabla_{\beta_i}(\mathbf{x}^{(l)})^H(\mathbf{x} - \mathbf{x}^{(l)})\right\}, \tag{5.2}$$

where $\Re\{\cdot\}$ denotes the real part of its argument and $\nabla_{\beta_i}(\mathbf{x}) = \frac{\partial \beta_i(\mathbf{x})}{\partial \mathbf{x}^H}$ denotes the conjugate derivative of the function $\beta_i(\mathbf{x})$ with respect to the complex-valued column-vector $\mathbf{x}$ [125]. For real vectors ($\mathbf{x} \in \mathbb{R}^{n\ x\ 1}$), the first-order Taylor expansion of $\beta_i(\mathbf{x})$ is computed as follows

$$\hat{\beta}_i(\mathbf{x}, \mathbf{x}^{(l)}) = \beta_i(\mathbf{x}^{(l)}) + \nabla_{\beta_i}\left(\mathbf{x}^{(l)}\right)^T(\mathbf{x} - \mathbf{x}^{(l)}), \tag{5.3}$$

where $\nabla_{\beta_i}(\mathbf{x}) = \frac{\partial \beta_i(\mathbf{x})}{\partial \mathbf{x}^T}$ denotes the gradient. The method is summarized in Algorithm 3. Let us remark that since the function $\beta_i(\mathbf{x})$ is convex in $\mathbf{x}$, it is minorized by its first-order Taylor approximation $\hat{\beta}_{i(\mathbf{x}, \mathbf{x}^{(l)})}$ [114], i.e, $\beta_i(\mathbf{x}) \geq \hat{\beta}_{i(\mathbf{x}, \mathbf{x}^{(l)})}\ \forall i$, and consequently

$$\alpha_i(\mathbf{x}) - \beta_i(\mathbf{x}) \ \leq \ \alpha_i(\mathbf{x}) - \hat{\beta}_i(\mathbf{x}, \mathbf{x}^{(l)}). \tag{5.4}$$

From this inequality, it is straightforward to see that by considering $\alpha_i(\mathbf{x}) - \hat{\beta}_i(\mathbf{x}, \mathbf{x}^{(l)}) \leq 0$ for $i = 1, ..., m$, in Algorithm 3, we are strengthening the original non-convex constraints in (5.1b). Since the new constraints are more conservative than the original ones, the feasible set of the convexified problem in Algorithm 3 is a subset of the original feasible set defined by the constraints in (5.1b).

As it has been introduced above, the CCP technique is a descendent algorithm that converges to a KKT point of the original problem in (5.1). The final solution depends on the selection of the initial feasible point. One option is to choose different starting (feasible) points and take the best solution. Unfortunately, in many practical problems, finding and initial feasible point for the CCP could be a difficult task. In order to overcome this drawback T. Lipp and S. Boyd have recently proposed in [59] an extension of the convex-concave procedure that removes the need for an starting point in the feasible region of the

original problem. This method, which is called penalty CCP, is based on the addition of some non-negative slack variables s_i to the constraints and the penalization of the sum of the constraint violations. A similar idea has been proposed by Mehanna et al. in [56] for solving non-convex Quadratically Constrained Quadratic Problems (QCQP). The penalty CCP is summarized in Algorithm 4.

Algorithm 3 Traditional CCP

Initialization: Start with a feasible point $\mathbf{x}^{(0)}$ and set $l = 0$
while convergence is not achieved **do**
1) ***Convexification*** of the objective function and the non-convex constraints by replacing $\beta_i(\mathbf{x})$ by its affine approximation $\hat{\beta}_i(\mathbf{x}, \mathbf{x}^{(l)})$ for $i = 0, ..., m$.

if $\mathbf{x} \in \mathbb{C}^{n \text{ x } 1}$ compute $\hat{\beta}_i(\mathbf{x}, \mathbf{x}^{(l)})$ as in (5.2)
if $\mathbf{x} \in \mathbb{R}^{n \text{ x } 1}$ compute $\hat{\beta}_i(\mathbf{x}, \mathbf{x}^{(l)})$ as in (5.3)

2) ***Solve the convexified problem***: Set the value of $\mathbf{x}^{(l+1)}$ to the solution of the following convex problem

$$\begin{aligned} \min_{\mathbf{x}} \quad & \alpha_0(\mathbf{x}) - \hat{\beta}_0(\mathbf{x}, \mathbf{x}^{(l)}) \\ \text{subject to} \quad & \alpha_i(\mathbf{x}) - \hat{\beta}_i(\mathbf{x}, \mathbf{x}^{(l)}) \leq 0, \ i = 1, \ldots, m. \end{aligned}$$

3) ***Update the iteration number:*** $l \leftarrow l + 1$
end while

It is worth noting that under the non-negative constraint on the vector of slack variables, the right-hand penalization of the sum of constraint violations in the objective of Algorithm 4 (step 2) is equivalent to penalizing the objective function with the l_1-norm of the vector of slack variables, defined as $\|\mathbf{s}\|_1 = \sum_{i=1}^{i=m} |s_i|$, which have a well-known sparsity-inducing effect [23, 26]. If the slack variables in the final solutions are all zeros, i.e., $\sum_{i=1}^{i=m} s_i \simeq 0$, then the algorithm has converged to a feasible solution.

Next, we expose some important remarks about the penalty CCP technique:

1. The algorithm always converges, although the convergence can be to an unfeasible point of the original problem (5.1) [59]. Since the algorithm is based on a local first-order approximation of the non-convex functions of the DC problem, the final solution depends on the starting point.

2. Depending on the problem under consideration, there are many possible variations in the way the constraints are handled in the method. In Algorithm 4, an initially

Algorithm 4 Penalty CCP

Initialization: Set $l = 0$. Define $\tau^{(0)} > 0$, τ_{max}, $\mu > 0$ and generate a random initial point $\mathbf{x}^{(0)}$

while convergence is not achieved **do**

1) ***Convexification*** of the non-convex functions by replacing $\beta_i(\mathbf{x})$ by its affine approximation $\hat{\beta}_i(\mathbf{x}, \mathbf{x}^{(l)})$ for $i = 0, ..., m$.

if $\mathbf{x} \in \mathbb{C}^{n \text{ x } 1}$ compute $\hat{\beta}_i(\mathbf{x}, \mathbf{x}^{(l)})$ as in (5.2)
if $\mathbf{x} \in \mathbb{R}^{n \text{ x } 1}$ compute $\hat{\beta}_i(\mathbf{x}, \mathbf{x}^{(l)})$ as in (5.3)

2) ***Solve the convexified problem***: Set the value of $\mathbf{x}^{(l+1)}$ to the solution of the following convex problem

$$\begin{aligned} \min_{\mathbf{x},\mathbf{s}} \quad & \alpha_0(\mathbf{x}) - \hat{\beta}_0(\mathbf{x}, \mathbf{x}^{(l)}) + \tau^{(l)} \sum_{i=1}^{m} s_i \\ \text{subject to} \quad & \alpha_i(\mathbf{x}) - \hat{\beta}_i(\mathbf{x}, \mathbf{x}^{(l)}) \leq s_i, \ i = 1, \ldots, m. \\ & s_i \geq 0, \ i = 1, \ldots, m. \end{aligned}$$

3) ***Update the penalty factor:*** $\tau^{(l+1)} \leftarrow \min(\mu\tau^{(l)}, \tau_{\max})$

4) ***Update the iteration number:*** $l \leftarrow l + 1$

end while

low penalty $\tau^{(0)}$ is imposed, allowing the violation of the constraints during the first iterations of the procedure with the aim of finding a more favorable region with a lower objective value. Note that the penalty on the violation of the constraints is increased at each iteration of Algorithm 4 by a factor μ, encouraging the fulfillment of the constraints in the subsequent steps of the procedure. Another possible modification of the method is to consider a large fixed value of τ in order to push the slack variables toward zero ($\sum_{i=1}^{i=m} s_i = 0$). This approach has been considered in [56]. Finally, yet another interesting variation is to choose different values of the penalty factor τ for each constraint, prioritizing the satisfaction of some constraints over the others. Interested readers are referred to Section 3 of [59] for a thorough discussion on the possible criteria for handling the constraints.

3. One possible variation of the method is to remove the slack variables for the constraints that are purely convex ($\beta_i(\mathbf{x}) = 0$). In this case, if a feasible point of the problem exists, it must satisfy all the convex constraints at each iteration. This approach, which has been considered in reference [56], reduces the total number of variables, reduces the search area for the solution and may lead to a faster convergence. However, the consideration of slack variables in the convex constraints may be

of interest. By considering this approach, the space of feasible solutions is enlarged and a temporal violation of the convex constraints is allowed with the aim of reaching in the following iterations a more favorable region of non-convex constraints. See Section 3.2 of [59] for a detailed discussion on this approach.

4. A reasonable stopping condition for the penalty convex-concave procedure is to halt the method when the improvement in the objective is small.

5.3 System model

Consider the ad-hoc wireless relay network presented in Fig. 5.1, composed of M source-destination pairs (denoted by $S_i - D_i,\ i = 1, ..., M$), communicating in a pairwise manner, with the help of N potential relays. All the nodes in this scheme are equipped with a single antenna and operate in the same frequency band in a half-duplex mode, i.e., they cannot receive and transmit at the same time. It is assumed that due to the severe path loss there is no direct link between any source and destination. Hence, in order to carry out its communication, each source-destination pair needs to be assisted by the set of N potential relays. The communication process takes place in two steps, during the first time slot the sources broadcast their signals simultaneously to the relays, which receive a noisy faded mixture of the signals of all the sources. In the second step, each relay multiplies its received signal by a complex coefficient (the beamforming weight) and forwards it to the destination nodes.

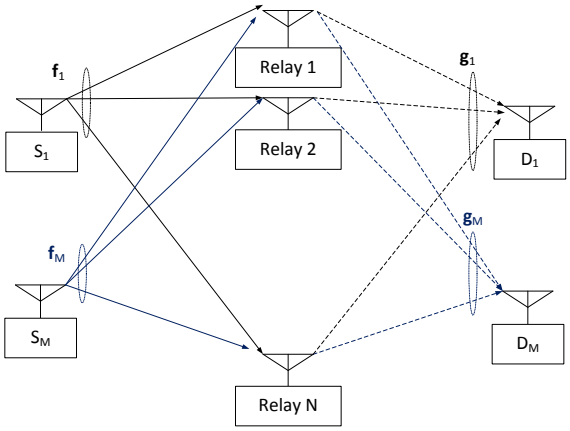

Figure 5.1: Amplify-and-forward multi-user multi-relay network

Let $\mathbf{a}=[a_1,...,a_M]^T$ be the vector of information symbols transmitted by the M source nodes, which is assumed to be zero-mean and component-wise independent with variance $E\{|a_i|^2\}=P_{S_i}$, and let $\mathbf{f}_k=[f_{k1},...,f_{kN}]^T$ denote the vector of complex channel coefficients between the kth source and the relays. The vector of received signals at the relays is given by

$$\mathbf{y}=\sum_{i=1}^{M}\mathbf{f}_i a_i+\boldsymbol{\eta}, \tag{5.5}$$

where $\boldsymbol{\eta}\in\mathbb{C}^N$ is the vector of Additive White Gaussian Noise (AWGN) components at the relay nodes, i.e., the ith entry denotes the noise component at the ith relay. The components of this vector are assumed to be zero-mean i.i.d. variables with variance σ_r^2. During the second phase of the transmission process each relay multiply its received signal by the corresponding complex weight w_i, with $i=1,...,N$. Thus, the vector of signals transmitted by all the relays can be expressed as $\mathbf{z}=\mathbf{W}\mathbf{y}$, where $\mathbf{W}=\text{diag}(w_1,...,w_N)$. The signal received at the kth destination node is given by

$$r_k=\mathbf{g}_k^T\mathbf{W}\mathbf{f}_k a_k+\sum_{i\neq k}^{M}\mathbf{g}_k^T\mathbf{W}\mathbf{f}_i a_i+\mathbf{g}_k^T\mathbf{W}\boldsymbol{\eta}+n_k, \tag{5.6}$$

where n_k denotes the AWGN at the destination node k, which has a known variance σ_d^2 and $\mathbf{g}_k=[g_{k1},...,g_{kN}]^T$ denotes the vector of channel coefficients between the relays and the kth destination. Note that only the first term of r_k is of interest for the kth destination. Let $\mathbf{h}_k=\mathbf{f}_k\odot\mathbf{g}_k$, where the operator $\odot$ denotes the Schur-Hadamard product, the SINR at the kth destination is given by

$$\text{SINR}_k(\mathbf{w})=\frac{\mathbf{w}^H\mathbf{A}_k\mathbf{w}}{\mathbf{w}^H(\mathbf{B}_k+\mathbf{C}_k)\mathbf{w}+\sigma_d^2}, \tag{5.7}$$

where $\mathbf{w}=[w_1,...,w_N]^T$ denotes the beamforming vector and the matrices $\mathbf{A}_k$,$\mathbf{B}_k$ and $\mathbf{C}_k$ are defined as follows:

$$\mathbf{A}_k=P_{S_k}E\{\mathbf{h}_k\mathbf{h}_k^H\},\ \mathbf{B}_k=\sum_{i\neq k}^{M}P_{S_i}E\{(\mathbf{f}_i\odot\mathbf{g}_k)(\mathbf{f}_i\odot\mathbf{g}_k)^H\},$$
$$\mathbf{C}_k=\sigma_r^2\ \text{diag}(E\{|g_{k1}|^2\},...,E\{|g_{kN}|^2\}).$$

The transmit power of the ith relay and the total power transmitted by all the relays, which are denoted by p_i and P_T, respectively, can be expressed as

$$p_i=D_{ii}\,|w_i|^2 \tag{5.8a}$$
$$P_T=\mathbf{w}^H\mathbf{D}\mathbf{w}, \tag{5.8b}$$

where $D_{ii} = \sum_{j=1}^{j=M} P_{S_j} E\{ |f_{ji}|^2 \} + \sigma_r^2$ denotes the ith entry of the diagonal matrix $\mathbf{D}$.

Regarding the Channel State Information (CSI), two different approaches have been considered in the multi-user peer-to-peer literature: i) the channel coefficients are perfectly known; ii) knowledge of the second-order statistics of the channel coefficients. Both cases are discussed below.

5.3.1 Perfect CSI available

In this case the channel coefficients are exactly known at the processing center where the beamforming weights are computed. This is the approach considered in the majority of previous works on distributed beamforming (see [58, 120, 53, 121] and references therein). In case of a perfect knowledge of the instantaneous CSI, the aforementioned matrices $\mathbf{A}_k$, $\mathbf{B}_k$, $\mathbf{C}_k$ and $\mathbf{D}$ are given by

$$\begin{aligned} &\mathbf{A}_k = P_{S_k} \mathbf{h}_k \mathbf{h}_k^H, \; \mathbf{B}_k = \sum_{i \neq k}^{M} P_{S_i} (\mathbf{f}_i \odot \mathbf{g}_k)(\mathbf{f}_i \odot \mathbf{g}_k)^H \\ &\mathbf{C}_k = \sigma_r^2 \; \mathrm{diag}(|g_{k1}|^2, ..., |g_{kN}|^2) \\ &\mathbf{D} = \mathrm{diag}(D_{11}, ..., D_{NN}) \text{ with } D_{ii} = \sum_{j=1}^{N} P_{S_j} |f_{ji}|^2 + \sigma_r^2 \end{aligned} \tag{5.9}$$

5.3.2 Knowledge of the second-order statistics of the channel coefficients

In wireless relay networks, acquiring instantaneous CSI may be a difficult task. Specially, in fast fading scenarios where the real-time estimation and transmission of the channel coefficients to a central processing node may require a prohibitive signalling overhead. Nevertheless, the second-order statistics of the channels normally evolve at a significantly lower rate.

This approach has been originally proposed in [120] and allows the consideration of some uncertainty in the channel models through introducing the covariance matrices of the channel gains. In practice, only the knowledge of the means and the variances of the channels is required [120, 61]. Let $\bar{f}_{ij}$ and $\bar{g}_{ij}$ denote the means of the backward channels (source-to-relays) and forward channels (relays-to-destinations), respectively, i. e., $\bar{f}_{ij} = E\{f_{ij}\}$ and $\bar{g}_{ij} = E\{g_{ij}\}$, $\forall i \in \mathcal{L} \triangleq \{1, ..., M\}$ and $\forall j \in \mathcal{F} \triangleq \{1, ..., N\}$. In

the same way, let us denote the variances of the forward and the backward channels as $\rho_{ij} = E\{\left|f_{ij} - \bar{f}_{ij}\right|^2\}$ and $\varphi_{ij} = E\{|g_{ij} - \bar{g}_{ij}|^2\}$ $\forall i \in \mathcal{L}$ and $\forall j \in \mathcal{F}$. Assuming that source-to-relays channels and the channels from the relays to the destinations are jointly independent, the (i,j)th entry of the aforementioned matrices $\mathbf{A}_k$, $\mathbf{B}_k$ can be expressed as

$$\begin{aligned}
[\mathbf{A}_k]_{ij} &= P_{S_k}(\bar{f}_{ki}\bar{f}_{kj}^* + \rho_{ki}\delta(i\text{-}j))\cdot(\bar{g}_{ki}\bar{g}_{kj}^* + \varphi_{ki}\delta(i\text{-}j)) \\
[\mathbf{B}_k]_{ij} &= \sum_{l\neq k}^{M} P_{S_l}(\bar{f}_{li}\bar{f}_{lj}^* + \rho_{li}\delta(i\text{-}j))\cdot(\bar{g}_{ki}\bar{g}_{kj}^* + \varphi_{ki}\delta(i\text{-}j)),
\end{aligned} \tag{5.10}$$

where $\delta(\cdot)$ denotes the delta function. The (i,i)th entry of the diagonal matrices $\mathbf{C}_k$ and $\mathbf{D}$ is given by

$$[\mathbf{C}_k]_{ii} = \sigma_r^2(|\bar{g}_{ki}|^2 + \varphi_{ki}) \tag{5.11}$$

$$D_{ii} = \sum_{j=1}^{M} P_{S_j}(\left|\bar{f}_{ji}\right|^2 + \rho_{ji}) + \sigma_r^2, \tag{5.12}$$

5.4 Selection of the minimum number of relay nodes

5.4.1 Problem formulation

In order to reduce the hardware costs as well as the processing and the communications overhead in the multi-user wireless network presented in Fig. 5.1, the number of selected relays will be minimized. In particular, this section deals with the selection of the smallest subset of relays, under per-relay power constraints, which guarantees that the Quality of Service (QoS) at destination nodes is above a certain predefined threshold. Throughout this chapter, the SINR will be used as a measure of the QoS. Formally, the minimum cardinality problem is given by the following optimization problem

$$\min_{\mathbf{w}} \quad \|\mathbf{w}\|_0 \tag{5.13a}$$

$$\text{s.t.} \quad \text{SINR}_k \geq \gamma_k \quad \forall k = 1, ..., M \tag{5.13b}$$

$$p_i \leq P_i^{\max} \quad \forall i = 1, ..., N, \tag{5.13c}$$

where $\|\mathbf{w}\|_0$ denotes the l_0-norm of the beamforming vector $\mathbf{w}$, i.e., the number of its non-zero entries, γ_k is the target SINR at the kth destination and $P_i^{\max}$ denotes the maximum allowable transmit power at the relay i. Taking into account the expressions in (5.8a) and

(5.7), the aforementioned problem can be mathematically expressed as

$$\min_{\mathbf{w}} \quad \|\mathbf{w}\|_0 \tag{5.14a}$$

$$\text{s.t.} \quad \frac{\mathbf{w}^H \mathbf{A}_k \mathbf{w}}{\mathbf{w}^H (\mathbf{B}_k + \mathbf{C}_k)\mathbf{w} + \sigma_d^2} \geq \gamma_k \quad \forall k = 1, ..., M \tag{5.14b}$$

$$D_{ii} \, |w_i|^2 \leq P_i^{\max} \qquad \forall i = 1, ..., N. \tag{5.14c}$$

Since $\mathbf{w}^H(\mathbf{B}_k + \mathbf{C}_k)\mathbf{w} + \sigma_d^2 \geq 0$, the problem in (5.14) can be rewritten as follows

$$\min_{\mathbf{w}} \quad \|\mathbf{w}\|_0 \tag{5.15a}$$

$$\text{s.t.} \quad \mathbf{w}^H \mathbf{T}_k \mathbf{w} \geq \gamma_k \sigma_d^2 \quad \forall k = 1, ..., M \tag{5.15b}$$

$$D_{ii} \, |w_i|^2 \leq P_i^{\max} \quad \forall i = 1, ..., N. \tag{5.15c}$$

where $\mathbf{T}_k = \mathbf{A}_k - \gamma_k(\mathbf{B}_k + \mathbf{C}_k)$. The difficulty of the problem presented in (5.15) lies on its non-convex and discontinuous objective function and on the constraint set defined by (5.15b), which is non-convex in general [120]. Actually, the set of constraints defined by (5.15b) will be convex if and only if the quadratic functions $\mathbf{w}^H \mathbf{T}_k \mathbf{w}$ are concave for all k. In other words, negative semidefiniteness of the matrices $\mathbf{T}_k$, $\forall k = 1, ..., M$, is required for the constraints in (5.15b) in order to define a convex set. Nonetheless, in this case, the resulting feasible set will be empty because this fact implies that $\mathbf{w}^H \mathbf{T}_k \mathbf{w} \leq 0$ for all k and the minimum SINR at the kth destination has to be strictly larger than zero ($\gamma_k > 0$) for all k. Otherwise, when $\gamma_k = 0$, the kth source-destination will not be scheduled to be served. As a result, we can conclude that all the matrices $\{\mathbf{T}_k\}_{k=1}^M$ have to be indefinite matrices (with positive and negative eigenvalues).

5.4.2 DC program reformulation

Since the problem in (5.15) is non-convex, finding a global optimum is computationally expensive (or even intractable). In the following, the minimum cardinality problem exposed in (5.15) will be transformed into a more tractable DC program. The aim of this reformulation is to develop a low-complexity algorithm to find a high quality sub-optimal solution of this problem.

As it has been introduced above, the intractability of the problem presented in (5.14) is not only due to the non-convexity, but also due to the discontinuity of the l_0-norm in the objective function. The natural approach to deal with this discontinuity is to approximate

the l_0-norm by a continuous surrogate. In particular, the log-sum surrogate [23, 11] is considered here. It is defined as $h(\mathbf{w}) = \sum_{i=1}^{i=N} \log(|w_i| + \varepsilon)$ with $\varepsilon > 0$ (where ε is a small constant that prevents the cost function from tending to $-\infty$). By replacing the l_0-norm by the log-sum surrogate in the minimum cardinality problem presented in (5.15), we arrive to the following optimization problem

$$\min_{\mathbf{w}} \quad \sum_{i=1}^{i=N} \log(|w_i| + \varepsilon) \quad \text{s.t.} \quad (5.15b),\ (5.15c), \tag{5.16}$$

which is equivalent to

$$\min_{\mathbf{w},\mathbf{v}} \sum_{i=1}^{N} \log(v_i{+}\varepsilon) \qquad \text{s.t.} \qquad |w_i| \leq v_i,\ (5.15b),\ (5.15c), \tag{5.17}$$

where $\mathbf{v}{=}[v_1, ..., v_N]^T \in \mathbb{R}^N$. Both problems are equivalent in the sense that if $\mathbf{w}^*$ is the solution to (5.16), then $(\mathbf{w}^*,|\mathbf{w}^*|)$ is the solution to the problem in (5.17). The function in the objective of (5.17) is concave and differentiable. Thus, in order to rewrite the problem exposed in (5.17) as a DC program of type (5.1), we need to rewrite the SINR constraints in (5.15*b*) as the difference of two convex functions. With this aim in mind, let us define $\tilde{\mathbf{T}}_k{=}{-}\mathbf{T}_k{=}\gamma_k(\mathbf{B}_k + \mathbf{C}_k) - \mathbf{A}_k$, $\forall k = 1, ..., M$. The SINR constraints in (5.15b) can be expressed in terms of $\tilde{\mathbf{T}}_k$ as follows

$$\mathbf{w}^H \tilde{\mathbf{T}}_k \mathbf{w} + \gamma_k \sigma_d^2 \leq 0 \quad \forall k = 1, ..., M. \tag{5.18}$$

By considering the following decomposition $\tilde{\mathbf{T}}_k{=}\tilde{\mathbf{T}}_k^{(+)}{-}\tilde{\mathbf{T}}_k^{(-)}$, with $\tilde{\mathbf{T}}_k^{(+)}{=}\ \gamma_k(\mathbf{B}_k + \mathbf{C}_k)$ and $\tilde{\mathbf{T}}_k^{(-)}{=}\mathbf{A}_k$, the set of inequalities in (5.18) can be rewritten as

$$\mathbf{w}^H \tilde{\mathbf{T}}_k^{(+)} \mathbf{w} + \gamma_k \sigma_d^2 - \mathbf{w}^H \tilde{\mathbf{T}}_k^{(-)} \mathbf{w} \leq 0 \quad \forall k = 1, ..., M. \tag{5.19}$$

Note that the matrices $\tilde{\mathbf{T}}_k^{(+)}$ and $\tilde{\mathbf{T}}_k^{(-)}$ are positive semidefinite. By replacing in the problem (5.17) the constraints in (5.15*b*) by (5.19), the problem presented in (5.17) can be reformulated as

$$\min_{\mathbf{w},\mathbf{v}} \quad \sum_{i=1}^{M} \log(v_i{+}\varepsilon) \tag{5.20a}$$

$$\text{s.t.} \quad \mathbf{w}^H \tilde{\mathbf{T}}_k^{(+)} \mathbf{w} + \gamma_k \sigma_d^2 - \mathbf{w}^H \tilde{\mathbf{T}}_k^{(-)} \mathbf{w} {\leq} 0 \quad \forall k{=}1,...,M \tag{5.20b}$$

$$D_{ii}\,|w_i|^2 \leq P_i^{\max} \qquad \forall i{=}1,...,N \tag{5.20c}$$

$$|w_i| \leq v_i \qquad \forall i{=}1,...,N, \tag{5.20d}$$

which is a DC program of the type (5.1).

5.4.3 Fitting the minimum cardinality problem into the CCP framework

The cost function in (5.20a) is concave and the constraints defined by (5.20b) are inequality constraints of DC type. Therefore, the convex-concave procedure can be applied to solve this problem. As it has been introduced in Section 5.2, the CCP is an iterative method that iteratively approximates DC programs by linearizing the non-convex parts of the cost function and the constraints around the solution obtained at each iteration of the method. With this aim in mind, let us denote the log-sum function in (5.20a) by $q_0(\mathbf{v})$. The first-order Taylor approximation $\hat{q}_0(\mathbf{v}, \mathbf{v}^{(l)})$ around the solution of the convex-concave procedure at the lth iteration $(\mathbf{w}^{(l)}, \mathbf{v}^{(l)})$ is given by

$$\hat{q}_0(\mathbf{v}, \mathbf{v}^{(l)}) = \sum_{i=1}^{N} \log(v_i^{(l)} + \varepsilon) + \sum_{i=1}^{N} \frac{v_i - v_i^{(l)}}{v_i^{(l)} + \varepsilon}, \tag{5.21}$$

where $v_i^{(l)}$ denotes the ith entry of the vector $\mathbf{v}^{(l)}$.

The non-convexity of the set of constraints defined by (5.20b) stems from the fact that the function $q_k(\mathbf{w}) = \mathbf{w}^H \tilde{\mathbf{T}}_k^{(-)} \mathbf{w}$ is convex but not concave. The first-order Taylor expansion $\hat{q}_k(\mathbf{w}, \mathbf{w}^{(l)})$ around the solution of the CCP at the lth iteration $(\mathbf{w}^{(l)}, \mathbf{v}^{(l)})$ is results in

$$\hat{q}_k(\mathbf{w}, \mathbf{w}^{(l)}) = 2\Re\{(\mathbf{w}^{(l)})^H \tilde{\mathbf{T}}_k^{(-)} \mathbf{w}\} - (\mathbf{w}^{(l)})^H \tilde{\mathbf{T}}_k^{(-)} \mathbf{w}^{(l)} \ \forall k. \tag{5.22}$$

By considering $\hat{q}_k(\mathbf{w}, \mathbf{w}^{(l)})$, the constraints in (5.20b) can be convexified as

$$\mathbf{w}^H \tilde{\mathbf{T}}_k^{(+)} \mathbf{w} + \gamma_k \sigma_d^2 - \hat{q}_k(\mathbf{w}, \mathbf{w}^{(l)}) \leq 0 \quad \forall k = 1, \ldots, M, \tag{5.23}$$

which is equivalent to

$$\mathbf{w}^H \tilde{\mathbf{T}}_k^{(+)} \mathbf{w} - 2\Re\{(\mathbf{w}^{(l)})^H \tilde{\mathbf{T}}_k^{(-)} \mathbf{w}\} + \gamma_k \sigma_d^2 + (\mathbf{w}^{(l)})^H \tilde{\mathbf{T}}_k^{(-)} \mathbf{w}^{(l)} \leq 0. \tag{5.24}$$

Once the cost function and the SINR constraints have been convexified, we can apply the convex-concave procedure by considering (5.21) and (5.24). Starting with an initial feasible point $(\mathbf{w}^{(0)}, \mathbf{v}^{(0)})$, the optimization problem presented in (5.20) can be iteratively driven to a KKT point using the concave-convex procedure. The *(l+1)*th iteration of the CCP method is given by

$$\begin{aligned} (\mathbf{w}^{(l+1)}, \mathbf{v}^{(l+1)}) = \arg \min_{\mathbf{w} \in \mathbb{C}^N, \mathbf{v} \in \mathbb{R}^N} & \sum_{i=1}^{N} \frac{v_i}{v_i^{(l)} + \varepsilon} \\ \text{s.t.} \quad & (5.24), (5.20c), \ |w_i| \leq v_i \ \forall i = 1, \ldots, N, \end{aligned} \tag{5.25}$$

which is equivalent to

$$\mathbf{w}^{(l+1)} = \arg\min_{\mathbf{w}} \sum_{i=1}^{N} \frac{|w_i|}{\left|w_i^{(l)}\right| + \varepsilon} \tag{5.26a}$$

$$\text{s.t.} \quad (5.24),(5.20c). \tag{5.26b}$$

Note that each iteration in (5.26) solves a weighted l_1-norm minimization problem. The weighting updates encourage the small entries of $\mathbf{w}$ to tend to zero and avoid the inadequate suppression of large entries of the beamformer $\mathbf{w}$. The aim of the parameter ε is twofold. First, it provides stability. Second, it allows that a zero entry of $\mathbf{w}^{(l)}$ could become a non-zero estimate at the next iteration. This problem can be easily reformulated as a second order cone programming (SOCP) [114, 126] and usually takes few iterations to converge. The iterative method presented in (5.26) should be stopped once convergence is achieved or the maximum number of iterations $N_{it}^{\max}$ is reached.

5.4.4 Initialization of the reweighted algorithm

The aim of this section is to describe several strategies for initializing the reweighted algorithm presented in (5.26). The performance of these initializations will be analyzed later on, in Section 5.6.

Perfect channel state information

When perfect CSI is available, the matrix $\mathbf{A}_k$ is given by $\mathbf{A}_k{=}P_{S_k}(\mathbf{f}_k \odot \mathbf{g}_k)(\mathbf{f}_k \odot \mathbf{g}_k)^H$. This rank-one property can be exploited to approximate the QoS constraints in (5.14b) by Second Order Cone (SOC) constraints. Inequalities in (5.14b) can be rewritten as

$$\frac{P_{S_k}\mathbf{w}^H(\mathbf{f}_k \odot \mathbf{g}_k)(\mathbf{f}_k \odot \mathbf{g}_k)^H\mathbf{w}}{\mathbf{w}^H(\mathbf{B}_k{+}\mathbf{C}_k)\mathbf{w} + \sigma_d^2} \geq \gamma_k \quad \forall k = 1,...,M, \tag{5.27}$$

which are equivalent to

$$\left|\mathbf{w}^H\mathbf{h}_k\right| \geq \sqrt{\frac{\gamma_k}{P_{S_k}}} \left\| \begin{bmatrix} (\mathbf{B}_k + \mathbf{C}_k)^{1/2}\mathbf{w} \\ \sigma_d \end{bmatrix} \right\|_2 \quad \forall k = 1,...,M, \tag{5.28}$$

where $\|\cdot\|_2$ denotes the Euclidean norm. Recall that $\mathbf{h}_k = \mathbf{f}_k \odot \mathbf{g}_k$. Since $\left|\mathbf{w}^H\mathbf{h}_k\right| \geq \Re\left\{\mathbf{w}^H\mathbf{h}_k\right\}$, where $\Re\{\cdot\}$ denotes the real part operator, the non-convex constraints in

(5.28) can be strengthened using the following (convex) second-order cone constraints

$$\Re\left\{\mathbf{w}^H\mathbf{h}_k\right\} \geq \sqrt{\frac{\gamma_k}{P_{S_k}}}\left\| \begin{bmatrix} (\mathbf{B}_k+\mathbf{C}_k)^{1/2}\mathbf{w} \\ \sigma_d \end{bmatrix} \right\|_2 \quad \forall k{=}1,...,M. \tag{5.29}$$

This conservative approximation of the QoS constraints has been considered in references [127] and [128]. Note that the inequality $\left|\mathbf{w}^H\mathbf{h}_k\right| \geq \Re\left\{\mathbf{w}^H\mathbf{h}_k\right\}$ is fulfilled with equality if and only if $\mathbf{w}^H\mathbf{h}_k$ is real and positive. The approximation is optimal only for the single source-destination case ($M = 1$). In the multi-user scenario, its performance depends on how the set of non-convex QoS constraints is approximated by (5.29) and may be rather poor when the number of source-destination pairs increases [128]. This issue will be analyzed in detail later in Section 5.6 by means of numerical simulations.

Next, let us focus on the relaxation of the non-convex objective function (5.14a). The most common way to circumvent the computational bottleneck of combinatorial optimization problems is to replace the l_0-norm by its best convex surrogate, the l_1-norm [26], which is defined as $\|\mathbf{w}\|_1 = \sum_{i=1}^{i=N} |w_i|$. By considering the $\|\mathbf{w}\|_1$ and the approximation of the SINR constraints exposed in (5.29), the cardinality minimization problem in (5.14) can be relaxed as

$$\min_{\mathbf{w}} \quad \|\mathbf{w}\|_1 \quad \text{s.t.} \quad (5.20c),\ (5.29). \tag{5.30}$$

It is worth noting that the strengthening of the SINR constraints presented in (5.29) leads to a restricted convex feasible set that is a subset of the original feasible set of the minimum cardinality problem (5.15). Hence, if the solution of (5.30) exists, it is feasible for the original problem presented in (5.15). As will be shown below in Section 5.6, this relaxation exhibits a poor performance. Nevertheless, whenever this problem is feasible, it can provide a starting point for the reweighted algorithm presented in (5.26).

Non-perfect channel CSI

In the situations where no perfect CSI is available, $\mathbf{A}_k$ is no longer a rank-one matrix and, therefore, the relaxation of the SINR requirements exposed in the previous section cannot be directly applied. Nevertheless, we can approximate the matrix $\mathbf{A}_k$ by its principal component to make the aforementioned initialization applicable to the higher rank case. The SINR requirements in (5.14b) can be expressed as

$$\sqrt{\mathbf{w}^H\mathbf{A}_k\mathbf{w}} \geq \sqrt{\gamma_k\left(\mathbf{w}^H(\mathbf{B}_k{+}\mathbf{C}_k)\mathbf{w} + \sigma_d^2\right)} \quad \forall k = 1, ..., M. \tag{5.31}$$

To obtain a second-order cone approximation, the left-hand side of the inequality needs to be linearized. With this aim in mind, let us consider the eigendecomposition of the matrix $\mathbf{A}_k$: $\mathbf{A}_k = \sum_{i=1}^{i=N} \lambda_{k,i} \vartheta_{k,i} \vartheta_{k,i}^H$. The left-hand side of inequality (5.31) can be strenghtened as

$$\sqrt{\mathbf{w}^H \mathbf{A}_k \mathbf{w}} = \sqrt{\sum_{i=1}^{i=N} \lambda_{k,i} \left| w^H \vartheta_{k,i} \right|^2} \geq \sqrt{\lambda_k^{\max}} \left| w_k^H \vartheta_k^{\max} \right| \quad \forall k = 1, ..., M, \tag{5.32}$$

where $\lambda_k^{\max}$ and $\vartheta_k^{\max}$ denote the maximum eigenvalue and eigenvector of the matrix $\mathbf{A}_k$, respectively. Since $\left| w^H \vartheta_k^{\max} \right| \geq \Re \left\{ w^H \vartheta_k^{\max} \right\}$, then $\sqrt{\mathbf{w}^H \mathbf{A}_k \mathbf{w}} \geq \sqrt{\lambda_k^{\max}} \Re \left\{ w^H \vartheta_k^{\max} \right\}$. Using this last inequality, the SINR requirements in (5.31) can be strengthened with the following conservative approximation

$$\sqrt{\lambda_k^{\max}} \Re \left\{ w^H \vartheta_k^{\max} \right\} \geq \sqrt{\gamma_k \left(\mathbf{w}^H (\mathbf{B}_k + \mathbf{C}_k) \mathbf{w} + \sigma_d^2 \right)} \quad \forall k = 1, ..., M, \tag{5.33}$$

which can be easily rewritten as a second-order cone:

$$\Re \left\{ w^H \vartheta_k^{\max} \right\} \geq \sqrt{\frac{\gamma_k}{\lambda_k^{\max}}} \left\| \begin{bmatrix} (\mathbf{B}_k + \mathbf{C}_k)^{1/2} \mathbf{w} \\ \sigma_d \end{bmatrix} \right\|_2 \quad \forall k = 1, ..., M. \tag{5.34}$$

This approximation of the QoS requirements was used in [129] to initialize the iterative method proposed therein for the computation of the transmit beamforming in a multigroup multicasting scenario based on the knowledge of the second-order channel state information of the wireless relay network.

The reweighted procedure in (5.26) can be initialized in a way similar to (5.30), using this approximation of the SINR requirements, i.e., replacing (5.29) by (5.34). Hence, in a scenario with statistical CSI, the iterative algorithm in (5.26) can be initialized with the solution of the next problem:

$$\min_{\mathbf{w}} \quad \|\mathbf{w}\|_1 \quad \text{s.t.} \quad (5.20c), (5.34). \tag{5.35}$$

The convex-concave procedure applied to the minimum cardinality problem presented in (5.15) is summarized in Algorithm 5.

Random initial point

The aforementioned initialization procedures rely on the assumption that problems (5.30) and (5.35) are feasible. However, this assumption may not hold true. One of the main drawbacks of strenghtening the QoS constraints with (5.29) and (5.34) for the perfect CSI

Algorithm 5 Reweighted procedure initialized with QoS relaxation + l_1-norm

Initialize the algorithm to a *feasible* initial point $\mathbf{w}^{(0)}$ obtained with (5.30) in case of perfect CSI or (5.35) for the statistical CSI case and set $l = 0$.
while convergence is not achieved or the maximum number of iterations is not reached ($l \leq N_{it}^{max}$) **do**
1) Set the value of $\mathbf{w}^{(l+1)}$ to the solution of (5.26).
2) *Update iteration:* $l \leftarrow l + 1$
end while

and non-perfect CSI scenario, respectively, is that these approximations are very conservative [128]. Even if the original problem (5.15) is feasible, whenever the feasible set described by the restricted constraints shrinks to an empty set, the aforementioned approximations of the SINR requirements can turn an original feasible problem into an infeasible one.

When the initialization problems presented in (5.30) and (5.35) are infeasible, the most straightforward strategy for solving (5.26) is to apply the penalty convex-concave procedure described in Section 5.2, initialized with a random point. With this aim in mind, Algorithm 6 is proposed. We have considered slack variables only in the non-convex SINR constraints. Furthermore, the value of the parameter τ, which balances the tradeoff between the objective function and the penalty on the constraint violations, is kept fixed over the iterations. A large value of τ (i.e., $\tau \gg 1$) must be considered in order push the vector of slack variables $\mathbf{s}$ towards zero or, i.e., to push the iterates towards the feasible region of the problem (5.14). High values of τ ensure that when a feasible point is found, the subsequent iterates will remain in the feasible region of (5.14). Once the feasibility slacks become zero, the constraints are satisfied and, consequently, slacks can be removed from algorithm 6. In other words, once a feasible point is found, we can remove the slack variables and switch to the traditional CCP, guaranteeing that the constraints will be satisfied in the future iterates.

It should be remarked that if no feasible point is found with Algorithm 6, some admission control procedures should be considered to reduce the number of source-destination pairs. Nevertheless, this approach is out of the scope of this work.

Algorithm 6 Reweighted procedure initialized with a random point

Initialization: Set $l = 0$ and generate a random initial point $\mathbf{w}^{(0)}$

while convergence is not achieved or the maximum number of iterations is not reached ($l \leq N_{it}^{max}$) **do**

1) ***Compute the diagonal weighting matrix*** $\mathbf{\Omega}^{(l)}$

$$\Omega_{ii}^{(l)} = \frac{1}{\left|w_i^{(l)}\right| + \varepsilon}$$

2) ***Solve the convexified problem with the slack variables***: Set the value of $\mathbf{w}^{(l+1)}$ to the solution of

$$\begin{aligned}
&\min_{\mathbf{w},\mathbf{s}} \quad \left\|\mathbf{\Omega}^{(l)}\mathbf{w}\right\|_1 + \tau \sum_{i=1}^{M} s_i \\
&\text{s.t.} \quad \mathbf{w}^H \tilde{\mathbf{T}}_k^{(+)} \mathbf{w} - 2\Re\{(\mathbf{w}^{(l)})^H \tilde{\mathbf{T}}_k^{(-)} \mathbf{w}\} \leq s_k - \gamma_k \sigma_d^2 - (\mathbf{w}^{(l)})^H \tilde{\mathbf{T}}_k^{(-)} \mathbf{w}^{(l)} \qquad \forall k{=}1_{,\ldots,}M \\
&D_{ii}\,|w_i|^2 \leq P_i^{\max} \qquad \forall i{=}1_{,\ldots,}N \\
&s_k \geq 0 \qquad \forall k{=}1_{,\ldots,}M
\end{aligned}$$

3) ***Update the iteration number:*** $l \leftarrow l + 1$

end while

5.5 Selection of the subset of relays that minimizes the total relay transmit power

In Section 5.4, we have addressed the problem of selecting the minimum number of relays that guarantees a given performance at the destination nodes in a multiuser peer-to-peer wireless relay network. However, if a higher complexity is allowed in the network, the selection of a higher number of cooperative nodes could be of interest in order to reduce the total power consumption of the wireless relay network.

This section deals with the selection of the subset of K cooperative nodes that minimizes the total relay transmit power. This problem is addressed considering per-relay power constraints and guaranteeing that the QoS requirements at the destinations are above a certain predefined threshold. In particular, we aim to solve the following optimization problem:

$$\min_{\mathbf{w}} \; P_T \tag{5.36a}$$

$$\text{s.t.} \quad SINR_k \geq \gamma_k \quad \forall k \in \mathcal{L} \tag{5.36b}$$

$$p_i \leq P_i^{\max} \quad \forall i \in \mathcal{F} \tag{5.36c}$$

$$\text{card}(\mathbf{w}) = K. \tag{5.36d}$$

where $\mathcal{L} \triangleq \{1, ..., M\}$ and $\mathcal{F} \triangleq \{1, ..., N\}$. Throughout this section, we assume that the desired cardinality, which is denoted by K, is larger than the minimum cardinality that guarantees the fulfillment of the constraints. In other words, it is assumed that problem (5.36) is feasible. Formally, the aforementioned cardinality-constrained problem can be formulated as

$$\min_{\mathbf{w}} \; \mathbf{wDw} \tag{5.37a}$$

$$\text{s.t.} \quad \mathbf{w}^H \mathbf{T}_k \mathbf{w} \geq \gamma_k \sigma_d^2 \quad \forall k \in \mathcal{L} \tag{5.37b}$$

$$D_{ii} \left| w_i \right|^2 \leq P_i^{\max} \quad \forall i \in \mathcal{F} \tag{5.37c}$$

$$\text{card}(\mathbf{w}) = K. \tag{5.37d}$$

Let us introduce a set of binary variables $b_i \in \{0, 1\}$ for $i = 1, ..., N$ to indicate the cooperation group membership. If $b_i = 1$, the ith relay is assigned to the set of cooperative relays and, otherwise, when $b_i = 0$, the relay is not selected for the cooperation. Problem

(5.37) can be rewritten as

$$\min_{\mathbf{w},\mathbf{b}} \ \mathbf{w}^H\mathbf{D}\mathbf{w} \tag{5.38a}$$

$$\text{s.t.} \ \mathbf{w}^H\mathbf{T}_k\mathbf{w} \geq \gamma_k\sigma_d^2 \qquad \forall k \in \mathcal{L} \tag{5.38b}$$

$$D_{ii}\left|w_i\right|^2 \leq b_i P_i^{\max} \quad \forall i \in \mathcal{F} \tag{5.38c}$$

$$\mathbf{1}_N^T\mathbf{b} = K \tag{5.38d}$$

$$b_i \in \{0,1\} \qquad \forall i \in \mathcal{F}, \tag{5.38e}$$

where $\mathbf{b} = [b_1, ..., b_N]$ is a vector of binary variables, i.e., $\mathbf{b} \in \{0,1\}^N$, and $\mathbf{1}_N$ denotes an all-ones column-vector of length N. Note that b_i is a binary indicator variable that controls the continuous variable $\mathbf{w}$, i.e., $b_i = 0$ implies that $\left|w_i\right|^2 = 0$ and therefore, when $b_i = 0$ the ith relay does not transmit.

This problem combines a complex-valued unknown vector $\mathbf{w}$ with a vector of binary variables $\mathbf{b}$ and falls within the class of {0,1}-non-convex mixed integer nonlinear programs [55] due to the non-convex SINR constraints in (5.38b). This kind of problems are well-known to be NP-hard [55] and even the task of finding a sub-optimal solution to this type of problems is challenging. The main reason is that the continuous relaxation of the binary constraints does not lead to a tractable formulation due to non-convexity of the constraints. In the case under analysis, due to the SINR requirements. A detailed description of non-convex mixed integer nonlinear programs is out of the scope of this chapter and we refer interested readers to reference [55], which constitutes a comprehensive survey about this topic.

5.5.1 Perspective reformulation

In Mixed Integer Nonlinear Programs (MINLP), having a tight formulation of the problem is of paramount importance to obtain a tight continuous relaxation [130]. The main problem of the formulation presented in (5.38) is that the upper bounds on the relay transmit powers defined by (5.38c) are loose and this results in weak continuous relaxations. Thus, the formulation presented in (5.38) needs to be strengthened.

In order to develop a tight continuous relaxation of the cardinality-constrained optimization problem in the next sections, here we adopt the so-called perspective reformulation approach, which has been recently proposed in [131, 36, 130]. This technique consists in tightening the constraints involving binary indicator variables. Having this goal in mind, let us introduce a set of auxiliary optimization variables $\{t_i \geq 0, \forall i \in \mathcal{F}\}$ to model the

power needed by each relay in the cooperation process and use t_i to replace the loose upper bound $P_i^{\max}$ in (5.38c). Then, the on-off constraint in (5.38c) can be expressed as

$$D_{ii}\left|w_i\right|^2 \leq b_i t_i \qquad \forall i \in \mathcal{F}, \tag{5.39}$$

which can be easily transformed into a second-order cone constraint [126]

$$\left\| \left[\begin{array}{cc} 2\sqrt{D_{ii}}w_i, & b_i - t_i \end{array} \right] \right\|_2 \leq b_i + t_i \qquad \forall i \in \mathcal{F}. \tag{5.40}$$

Using this new on-off constraint and the auxiliary variables t_i the problem exposed in (5.38) can reformulated as

$$\begin{aligned}
\min_{\mathbf{w}\in\mathbb{C}^N, \mathbf{b}, \mathbf{t}\in\mathbb{R}^N} \quad & \sum_{i=1}^{N} t_i && && \text{(5.41a)}\\
\text{s.t.} \quad & \mathbf{w}^H \mathbf{T}_k \mathbf{w} \geq \gamma_k \sigma_d^2 && \forall k \in \mathcal{L} && \text{(5.41b)}\\
& \left\| [2\sqrt{D_{ii}}w_i,\, b_i - t_i] \right\|_2 \leq b_i + t_i && \forall i \in \mathcal{F} && \text{(5.41c)}\\
& t_i \leq b_i P_i^{\max} && \forall i \in \mathcal{F} && \text{(5.41d)}\\
& \mathbf{1}_N^T \mathbf{b} = K && && \text{(5.41e)}\\
& b_i \in \{0, 1\} && \forall i \in \mathcal{F}, && \text{(5.41f)}
\end{aligned}$$

where $\mathbf{t} = [t_1, \ldots, t_N]^T$. The constraints in (5.41d) are problem-specific cuts added to obtain tighter continuous relaxations. Cuts are convex constraints, normally linear, added to a MINLP to reduce the size of the feasible set associated to the continuous relaxation of the problem [132], as illustrated in Fig. 5.2. This type of constraints are redundant in the sense that they do no affect the feasible set of the original cardinality-constrained problem, but they reduce the size of the feasible set associated to the continuous relaxation. Both formulations, (5.41) and (5.38), are equivalent, nonetheless, (5.41) is preferred because it leads to a tighter relaxation.

5.5.2 DC program reformulation

The difficulty of the optimization problem exposed in (5.41) lies on the set of non-convex SINR constraints and on the binary variables. In this section, the problem will be transformed into a more tractable DC program. The aim of this reformulation is to develop a sub-optimal method based on the penalty convex-concave procedure.

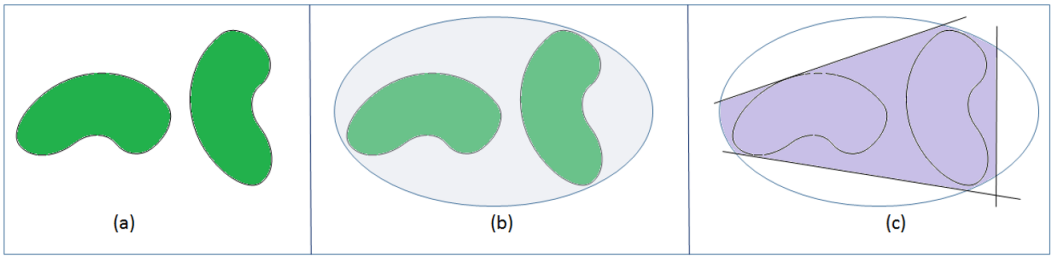

Figure 5.2: (a) Original (disconnected) feasible set of the non-convex MINLP problem. (b) Feasible set associated to the continuous relaxation of the MINLP. (c) Feasible set of the continuous relaxation with the cuts.

The first step in this process is to formulate (5.41) as a continuous quadratic problem. With this objective in mind, let us consider the next concave function [53, 133, 45]

$$\bar{q}(\mathbf{b}) = \sum_{i=1}^{i=N} b_i(1-b_i) = \mathbf{1}_N^T\mathbf{b} - \mathbf{b}^T\mathbf{b}. \tag{5.42}$$

Note that $\mathbf{b} \in \{0,1\}^N \iff \bar{q}(\mathbf{b}) = 0$. Since $\bar{q}$ is a finite nonnegative concave function in $\mathbf{b} \in [0,1]^N$, the binary constraints exposed in (5.41f) can be straightforwardly rewritten as $\bar{q}(\mathbf{b}) \leq 0$ with $\mathbf{b} \in [0,1]^N$. Taking into account this equivalence, problem (5.41) can be expressed as the following continuous formulation:

$$\min_{\mathbf{w},\mathbf{b},\mathbf{t}} \quad \sum_{i=1}^{N} t_i \tag{5.43a}$$

$$\text{s.t.} \quad \mathbf{w}^H\mathbf{T}_k\mathbf{w} \geq \gamma_k\sigma_d^2 \qquad \forall k \in \mathcal{L} \tag{5.43b}$$

$$\left\| [2\sqrt{D_{ii}}w_i,\ b_i - t_i] \right\|_2 \leq b_i + t_i \quad \forall i \in \mathcal{F} \tag{5.43c}$$

$$t_i \leq b_i P_i^{\max} \qquad \forall i \in \mathcal{F} \tag{5.43d}$$

$$\mathbf{1}_N^T\mathbf{b} = K \tag{5.43e}$$

$$\mathbf{1}_N^T\mathbf{b} - \mathbf{b}^T\mathbf{b} \leq 0 \tag{5.43f}$$

$$b_i \leq 1 \qquad \forall i \in \mathcal{F}. \tag{5.43g}$$

Note that the inequalities $b_i \geq 0$, $\forall i \in \mathcal{F}$, which correspond to the lower bound of the closed interval $[0,1]^N$, are implicit in the per-relay power constraints (5.43*c*) and therefore can be omitted.

As already exposed above, the SINR constraints can be rewritten as the set DC constraints presented in (5.19). By replacing (5.43*b*) by (5.19), the optimization problem (5.43)

yields the next continuous DC program

$$\min_{\mathbf{w},\mathbf{b},\mathbf{t}} \sum_{i=1}^{N} t_i \tag{5.44a}$$

$$\text{s.t. } (5.19), (5.43c) - (5.43g). \tag{5.44b}$$

5.5.3 Fitting the DC reformulation into the penalty CCP framework

In order to apply the convex-concave procedure, we need to linearize the concave constraint in (5.43f). The first-order Taylor approximation of this constraint around the solution of the convex-concave solution in the lth iteration $(\mathbf{w}^{(l)}, \mathbf{b}^{(l)})$ is given by

$$(\mathbf{1}_N^T - 2(\mathbf{b}^{(l)})^T)\mathbf{b} + (\mathbf{b}^{(l)})^T\mathbf{b}^{(l)} \leq 0. \tag{5.45}$$

Using this linearization and considering the convexification of the QoS constraints exposed in (5.24), we can apply the penalty CCP heuristic to the DC problem (5.44). Starting from a random initial point $(\mathbf{w}^{(0)}, \mathbf{b}^{(0)})$, the $(l+1)$th iteration of the penalty CCP method applied to (5.44) is given by

$$(\mathbf{w}^{(l+1)}, \mathbf{b}^{(l+1)}) = \arg \min_{\mathbf{w},\mathbf{b},\mathbf{t},s_{\text{bin}},\{s_k^{\text{sinr}}\}_{k=1}^M} \sum_{i=1}^{N} t_i + \tau_{\text{sinr}} \sum_{k=1}^{M} s_k^{\text{sinr}} + \tau_{\text{bin}}^{(l)} s_{\text{bin}} \tag{5.46a}$$

$$\text{s.t.}$$

$$(\mathbf{1}_N^T - 2(\mathbf{b}^{(l)})^T)\mathbf{b} + (\mathbf{b}^{(l)})^T\mathbf{b}^{(l)} \leq s_{\text{bin}} \tag{5.46b}$$

$$\mathbf{w}^H\tilde{\mathbf{T}}_k^{(+)}\mathbf{w} - 2\Re\{(\mathbf{w}^{(l)})^H\tilde{\mathbf{T}}_k^{(-)}\mathbf{w}\} + \gamma_k\sigma_d^2 + (\mathbf{w}^{(l)})^H\tilde{\mathbf{T}}_k^{(-)}\mathbf{w}^{(l)} \leq s_k^{\text{sinr}} \quad \forall k \in \mathcal{L} \tag{5.46c}$$

$$s_{\text{bin}} \geq 0, s_k^{\text{sinr}} \geq 0 \qquad \forall k \in \mathcal{L}, \tag{5.46d}$$

$$(5.43c) - (5.43e), (5.43g), \tag{5.46e}$$

where s_{bin} and $\{s_k^{\text{sinr}}\}_{k=1}^M$ are slack variables that measure the violation of the binary constraint in (5.46b) and the SINR requirements (5.46c), respectively. Note that different penalty values are considered for the violation of the QoS requirements and the binary constraints, i.e., $\tau_{\text{sinr}} \neq \tau_{\text{bin}}^{(l)}$. Moreover, $\tau_{\text{bin}}^{(l)}$ depends on the iteration number l. The way the slack variables are handled is exposed in the next section. This problem is convex and can be easily rewritten as a SOCP [114, 126]. The whole method is summarized in Algorithm 7.

Algorithm 7 Penalty CCP for the cardinality-constrained problem with random point initializ.

Initialization: Set $l = 0$ and define $\tau_{\text{bin}}^{(0)} > 0$,$\tau_{\text{sinr}} > 0$, $\mu > 1$ and τ_{bin}^{max} and generate a random initial point $(\mathbf{w}^{(0)}, \mathbf{b}^{(0)})$, with $0 \leq b_i^{(0)} \leq 1$.

repeat

1) Set the value of $(\mathbf{w}^{(l+1)}, \mathbf{b}^{(l+1)})$ to the solution of

$$\begin{aligned} \min_{\mathbf{w},\mathbf{b},\mathbf{t},s_{\text{bin}},\{s_k^{\text{sinr}}\}_{k=1}^M} \quad & \sum_{i=1}^N t_i \quad + \tau_{\text{sinr}} \sum_{k=1}^M s_k^{\text{sinr}} + \tau_{\text{bin}}^{(l)} s_{\text{bin}} \\ \text{s.t.} \quad & (5.46b) - (5.46e) \end{aligned}$$

2) Update the penalty factor τ_{bin} and the iteration number: $\tau_{\text{bin}}^{(l+1)} \leftarrow \min(\mu\tau_{\text{bin}}^{(l)}, \tau_{\text{bin}}^{max})$, $l \leftarrow l + 1$.

until convergence or the maximum number of iterations is reached ($l \leq N_{it}^{max}$)

5.5.4 Enforcing the constraints

In contrast to the approach presented in Section 5.4 for the minimum cardinality problem, Algorithm 7 considers different penalties on the violation of the SINR requirements in (5.46c) and the binary-promoting constraint in (5.46b). The values of the penalty factors, which are denoted by τ_{sinr} and τ_{bin}, are chosen per constraint basis, prioritizing the satisfaction of certain constraints over the others. In particular, in Algorithm 7, we propose to use a large and fixed value of τ_{sinr}, i.e., $\tau_{\text{sinr}} \gg 1$, to push the iterates towards the fulfillment of the QoS requirements. On the contrary, for the binary constraint, rather than considering a fixed τ_{bin}, the value of this parameter is modified in the algorithm. Initially, a low penalty on the violation of the binary constraint is considered and then it is increased at each iteration of the method, using the following updating rule: $\tau_{\text{bin}}^{(l+1)} \leftarrow \mu\tau_{\text{bin}}^{(l)}$ with $\mu > 1$.

The rationale behind this approach is that the feasible sets for the cardinality-constrained problem presented in (5.37) are disconnected, as illustrated in Fig. 5.2 (a). Putting a large penalty factor τ_{bin} on the violation of the binary constraint, in this case, would promote the selection of a subset of cooperative nodes during the first iterates of the penalty CCP, penalizing the change of subset in the subsequent iterations. In order to let the algorithm change the selected cooperative nodes along the iterations, rather than considering a fixed value for τ_{bin}, a temporal violation of the binary constraint is allowed during the first iterations of the method. Inspired by the procedure presented in [59], the value of τ_{bin} is initialized to a low value and it is increased at each iteration of the algorithm. By considering this approach, we allow the procedure to find a more favorable subset of cooperative

relays along the iterations, instead of constraining the algorithm to a certain subset of nodes during the first steps. Numerical simulations in Section 5.6 show that the proposed procedure clearly outperforms the 'fixed penalty' approach.

5.5.5 The two-step procedure

A variation of Algorithm 7 consists in decoupling the convexification of the QoS requirements and the fulfillment of the binary constraint. The method presented in Algorithm 8 considers two separated phases: i) an initial step to reach a more favorable region of SINR constraints, and ii) a second step to promote a binary feasible solution initialized with the solution obtained in the first phase. Note that during the first phase the violation of the binary constraint is allowed. As shown below, this approach outperforms Algorithm 7.

5.5.6 Algorithm variations: initialization of Algorithms 7 and 8

Algorithms 7 and 8 are based on the penalty convex-concave procedure and have been initialized to a random point. However, similar to the minimum cardinality problem, alternative initializations can be envisaged depending on the available channel state information. The performance of each of these initializations will be evaluated in the next section by means of numerical simulations.

Recall the non-convex MINLP in (5.41). As already explained for the minimum cardinality problem, the QoS constraints in (5.41*b*) can be relaxed using (5.29) in the perfect CSI case and (5.34) in the statistical CSI scenario

$$\text{QoS relaxation} \begin{cases} (5.29) & \text{if perfect CSI} \\ (5.34) & \text{if statistical CSI.} \end{cases} \tag{5.47}$$

Furthermore, the binary constraints in (5.41f) can be relaxed with the so-called continuous relaxation of the variables (a.k.a. box contraints) $0 \leq b_i \leq 1$, $\forall i \in \mathcal{F}$ [43]. Using (5.47) and the box contraints, Algorithms 7 and 8 can be initialized with the solution of the next

Algorithm 8 Two-step method for the cardinality-constrained problem with random initialization

Initialize: Set $l = 0$, define $\tau_{\text{bin}}^{(0)} > 0$,$\tau_{\text{sinr}} > 0$, $\mu > 1$ and τ_{bin}^{max} and generate a random initial point $(\mathbf{w}^{(0)}, \mathbf{b}^{(0)})$, with $0 \leq b_i^{(0)} \leq 1$.

PHASE 1: Find a better region of convexified SINR constraints

repeat

1) Set the value of $(\mathbf{w}^{(l+1)}, \mathbf{b}^{(l+1)})$ to the solution of

$$\begin{aligned} \min_{\mathbf{w},\mathbf{b},\mathbf{t},\{s_k^{\text{sinr}}\}_{k=1}^M} \quad & \sum_{i=1}^N t_i + \tau_{\text{sinr}} \sum_{k=1}^M s_k^{\text{sinr}} \\ \text{s.t.} \quad & (5.46c), (5.46e), \ s_k^{\text{sinr}} \geq 0 \ \ \forall k \in \mathcal{L} \end{aligned}$$

2) Update iteration number: $l \leftarrow l + 1$.

until convergence to a feasible solution ($\sum_{k=1}^M s_k^{\text{sinr}} \approx 0$) or the maximum number of iterations is reached ($l \leq N_1^{max}$)

PHASE 2: Find feasible solution that fulfills the binary-promoting constraint, i.e., with only K active entries in $\mathbf{w}$

if $\mathbf{b}^{(l)}$ is not binary **then**

Initialize $b^{(0)}$ with the result of phase 1 (i.e., $b^{(0)} = b^{(l)}$). Set $l = 0$, define $\tau_{\text{bin}}^{(0)} > 0$, $\mu > 1$ and τ_{bin}^{max}

repeat

Set the value of $(\mathbf{w}^{(l+1)}, \mathbf{b}^{(l+1)})$ to the solution of

$$\begin{aligned} \min_{\mathbf{w},\mathbf{b},\mathbf{t},s_{\text{bin}}} \quad & \sum_{i=1}^N t_i + \tau_{\text{bin}}^{(l)} s_{\text{bin}} \\ \text{s.t.} \quad & \mathbf{w}^H \tilde{\mathbf{T}}_k^{(+)} \mathbf{w} - 2\Re\{(\mathbf{w}^{(l)})^H \tilde{\mathbf{T}}_k^{(-)} \mathbf{w}\} + \gamma_k \sigma_d^2 + (\mathbf{w}^{(l)})^H \tilde{\mathbf{T}}_k^{(-)} \mathbf{w}^{(l)} \leq 0 \ \ \forall k \in \mathcal{L} \\ & (5.46b), (5.46e), \ s_{\text{bin}} \geq 0 \end{aligned}$$

Update the penalty factor and the iteration number: $\tau_{\text{bin}}^{(l+1)} \leftarrow \min(\mu \tau_{\text{bin}}^{(l)}, \tau_{\text{bin}}^{max})$, $l \leftarrow l + 1$.

until convergence to a feasible point ($s_{\text{bin}} \approx 0$) or the maximum number of iterations is reached ($l \leq N_2^{max}$)

end if

convex optimization problem:

$$\min_{\mathbf{w}\in\mathbb{C}^N,\mathbf{b},\mathbf{t}\in\mathbb{R}^N} \quad \sum_{i=1}^{N} t_i \tag{5.48a}$$

$$\text{s.t.} \quad \left\| [2\sqrt{D_{ii}}w_i,\ b_i - t_i] \right\|_2 \leq b_i + t_i \quad \forall i \in \mathcal{F} \tag{5.48b}$$

$$t_i \leq b_i P_i^{\max} \qquad \forall i \in \mathcal{F} \tag{5.48c}$$

$$\mathbf{1}_N^T \mathbf{b} = K \tag{5.48d}$$

$$b_i \leq 1 \quad \forall i \in \mathcal{F}, \text{ (5.47)}. \tag{5.48e}$$

Note that $0 \leq b_i\ \forall i \in \mathcal{F}$ is implicit in the set of on-off constraints in (5.48b) and therefore can be omitted. This relaxed relay selection problem is not equivalent to the original MINLP in (5.41). In particular, the entries of $\mathbf{b}$ are not binary in general, they are fractional, and there are not theoretical guarantees that choosing the indices of $\mathbf{w}$ corresponding to the K largest entries of $\mathbf{b}$ lead to a feasible solution of the original subset selection problem in (5.37). Nevertheless, when the aforementioned problem is feasible, it can provide a proper initialization for Algorithms 7 and 8. As already explained for the minimum cardinality problem, the relaxation of the QoS constraints in (5.47) is an inner convex approximation of the original feasible set of SINR constraints in (5.41*b*). Hence, if the aforementioned problem is feasible, the slack variables that measure the feasibility of the QoS constraints s_k^{sinr} are not needed in Algorithms 7 and 8. In the simulations below, this initialization will be referred as perspective initialization.

5.6 Numerical results

The aim of this section is to evaluate the performance of the proposed algorithms. Throughout the simulations the same transmit power P is considered for all the sources. In the same way, per-relay power constraints are set to P. In particular, we assume $P_{S_k} = P_i^{\max} = P = 27$ dBm $\forall k \in \mathcal{L}, \forall i \in \mathcal{F}$ and we require all the destinations to be above the same SINR threshold, i.e., $\gamma_k = \gamma$, for $k = 1, ..., M$. Furthermore, without loss of generality, the noise powers at the relays and at the destinations are assumed equal to σ^2, i.e., $\sigma_r^2 = \sigma_d^2 = \sigma^2$.

5.6.1 Minimum cardinality problem

In the first scenario under analysis channel coefficients are exactly known at the processing center where the beamforming weights are computed. In particular, these channel coefficients are considered flat and are generated in each simulation run as i.i.d. complex Gaussian random variables with zero mean and unit variance.

Figures 5.3 and 5.4 plot the mean number of selected nodes in a dense wireless cooperative network composed of $N = 40$ potential relays as a function of SINR requirement γ, for $M = 5$ and $M = 3$ source-destination pairs, respectively. In this case, the noise power is set 4 dB below the source powers, i.e., $\sigma^2 = 23$ dBm. The curves were obtained by averaging the results of 500 independent Montecarlo runs. These figures compare the performance in terms of mean number of selected nodes of the reweighted procedure initialized with the l_1-norm plus the QoS relaxation exposed in Algorithm 5 and with the random initialization described in Algorithm 6. For the latter, the considered penalty factor is $\tau = 10^3$. The value of the parameter ε in the reweighted method is set 10^{-5} and the maximum number of iterations is chosen as: $N_{it}^{\max} = 15$. The performance of both initializations is compared against the solution of (5.30), which is denoted as l_1-norm + QoS relax., and the CCP applied to the problem

$$\begin{aligned} \min_{\mathbf{w}} \quad & \|\mathbf{w}\|_1 \\ \text{s.t.} \quad & \mathbf{w}^H \mathbf{T}_k \mathbf{w} \geq \gamma_k \sigma_d^2 \quad \forall k \in \mathcal{L} \\ & D_{ii} \left|w_i\right|^2 \leq P_i^{\max} \quad \forall i \in \mathcal{F}, \end{aligned} \tag{5.49}$$

initialized with (5.30). Note that we have just replaced the l_0-norm in the objective of problem (5.15) by the l_1-norm. Following an analysis similar to the one carried out in Section 5.4, it is straightforward to prove that the lth iteration of the convex-concave procedure applied to this problem is given by:

$$\mathbf{w}^{(l+1)} = \arg\min_{\mathbf{w}} \ \|\mathbf{w}\|_1 \quad \text{s.t.} \quad (5.24), (5.20c). \tag{5.50}$$

As can be seen from Figures 5.3 and 5.4, the initializations of the reweighted algorithm exhibit a similar performance. Furthermore, both clearly outperform the solution of the initialization problem in (5.30) and the aforementioned CCP applied to (5.49). Interestingly enough, the reweighted method is able to deliver high-quality solutions with a reduced number of cooperative nodes and, moreover, the mean number of selected relays is not sensitive to the initial point.

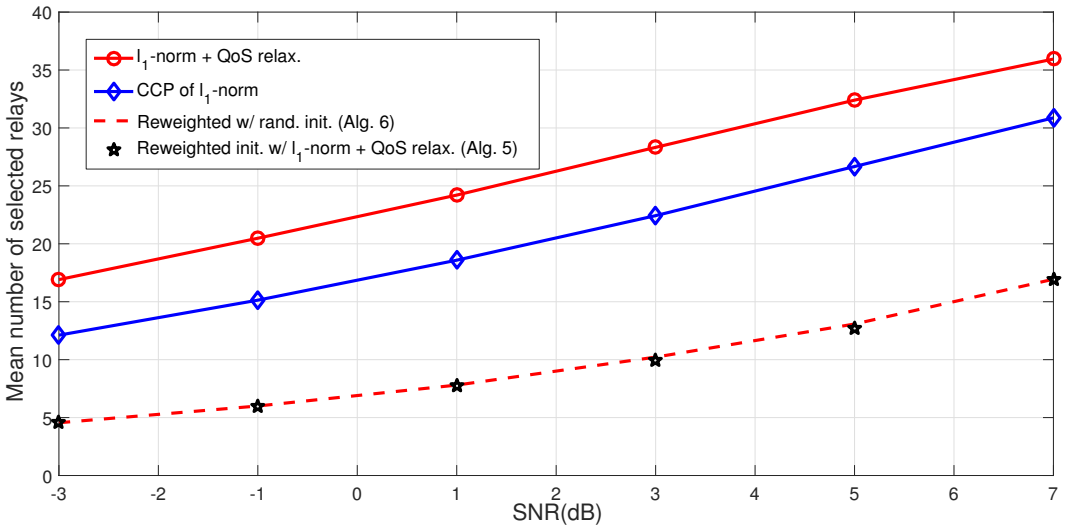

Figure 5.3: Mean number of selected relays as a function of the SINR threshold γ. Perfect CSI, $N = 40$ relays, $M = 5$ source-destination pairs, $P = 27$ dBm, $\sigma^2 = 23$ dBm, $\epsilon = 10^{-5}$, $\tau = 10^3$. Results are averaged over 500 simulation runs. The upper red curve denotes the solution of (5.30), which is the point used to initialize Algorithm 5.

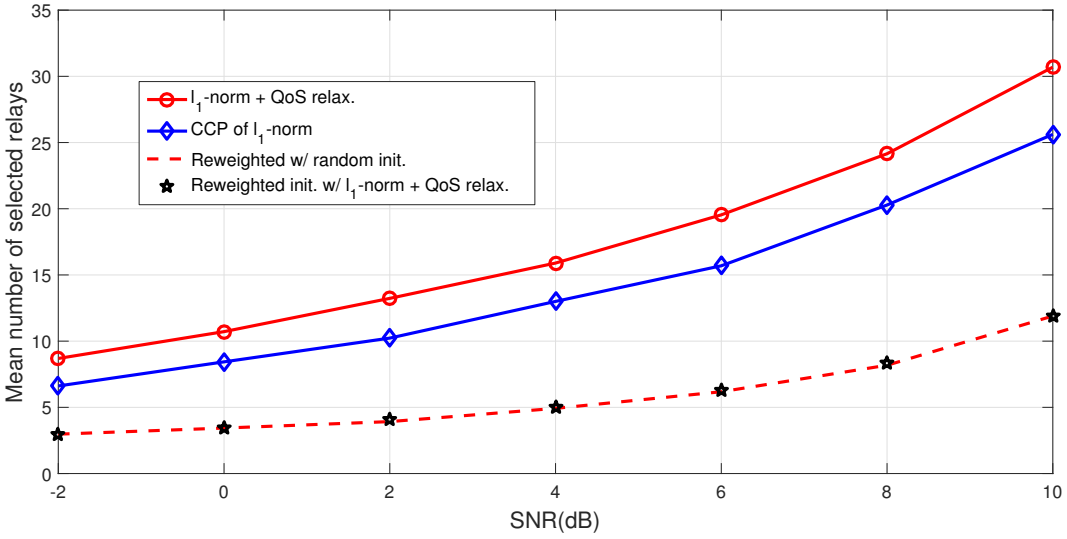

Figure 5.4: Mean number of selected relays as a function of the SINR threshold γ. Perfect CSI, $N = 40$, $M = 3$, $P = 27$ dBm, $\sigma^2 = 23$ dBm . The upper curve denotes the solution of (5.30).

In Figure 5.5 we present the mean number of iterations required by the reweighted algorithm as a function of SINR requirement for $M = 2$ and 5 source-destination pairs. Convergence is declared if $\left\|\mathbf{\Omega}^{(l)}\mathbf{w}^{(l)}\right\|_1 - \left\|\mathbf{\Omega}^{(l)}\mathbf{w}^{(l-1)}\right\|_1 \leq 10^{-2}$, where $\mathbf{\Omega}^{(l)}$ denotes the diagonal weighting matrix at iteration l. The ith entry of the diagonal of this matrix is given by $\Omega_{ii}^{(l)} = 1/(|w_i^{(l)}| + \varepsilon)$. As in our previous simulations, the initialization strategies presented in Section 5.4 are analyzed. Note that the reweighted technique initialized with (5.30) exhibits a good performance in terms of the average number of iterations for low values of the SINR threshold when the number of source-destination pairs is small. However, the performance of this initialization gets worse when the SINR requirement and/or the number of pairs increases. As already introduced in Section 5.4, the QoS approximation in (5.30) is only optimal for the single source-destination scenario (M=1) and the quality of the relaxation is degraded when the parameter M is incremented.

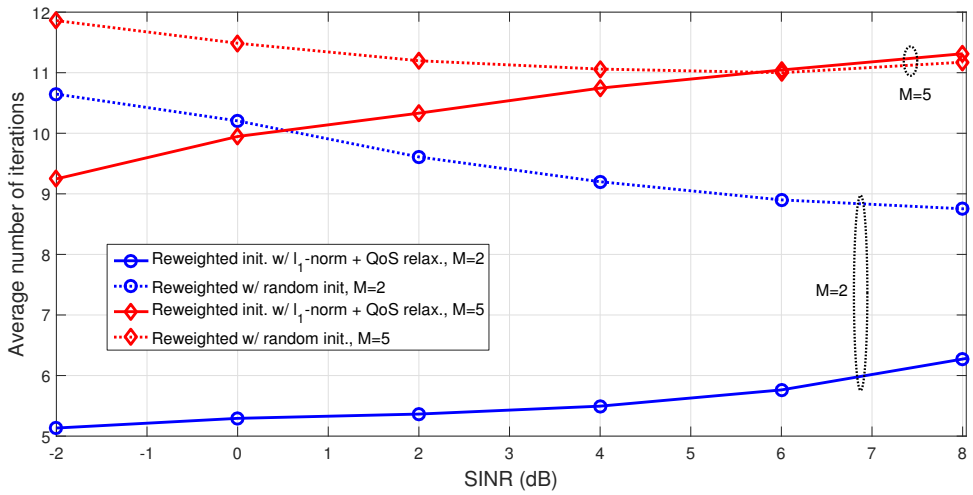

Figure 5.5: Average number of iterations as a function of the SINR threshold for $M = 2$ and $M = 5$ source-destinations pairs. Perfect CSI, $N = 40$ relays, $\epsilon = 10^{-5}$.

In order to evaluate the performance of the algorithm when the ratio P/σ^2 is modified, in Figure 5.6, we show the average number of selected relays as a function of the ratio P/σ^2 for the reweighted method with a random initialization. In particular, P was set to 27 dBm and the value of σ^2 is varied accordingly. Note that the mean number of selected nodes decreases when the ratio increases. Furthermore, it should be also noticed that for a given ratio, the number of cooperative nodes increases when the number of source-destination pairs grows or the SINR requirement is increased.

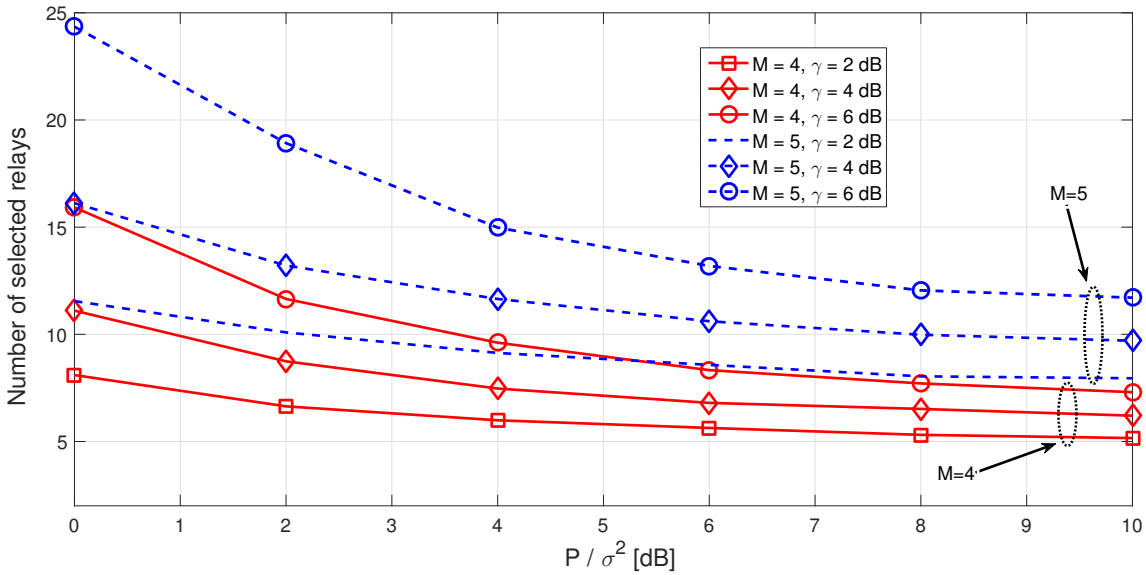

Figure 5.6: Average number of selected cooperative nodes as a function of the ratio P/σ^2 for $M = 4$ and $M = 5$. Perfect CSI, $N = 40$ relays, $\varepsilon = 10^{-5}$, $\tau = 10^3$.

Figure 5.7 shows the percentage of feasible simulation runs of the reweighted method as a function of the SINR requirement γ for M=4 and 5. As in the previous figures, the random initialization (Algorithm 6) and the initialization with the l_1-norm plus the QoS relaxation (Algorithm 5) are compared. In this case, the total number of relays has been set to N=20 and the values of P and σ^2 are set to 27 dBm and 19 dBm, respectively, i.e., the noise powers are set 8 dB below the source powers. The curves are the result of the average of 400 Montecarlo runs. Note that the random initialization clearly outperforms Algorithm 5. The rationale behind this behavior is that when the initialization problem (5.30) is not feasible, Algorithm 5 cannot be initialized. As introduced above, the approximation of the SINR constraints in (5.29) is only optimal for the single source-destination pair and may be rather poor when M is increased [128].

To gain further insights into the problem of infeasibility, Figure 5.8 plots the percentage of feasible simulation runs as a function M for $\gamma = 0$ dB and $\gamma = 6$ dB. As in the previous figure, the percentage of successful cases obtained with the random initialization is much higher than with the Algorithm 5 (l_1-norm + QoS relaxation) due to the poor behavior of the SINR approximation in (5.29) that provokes the infeasibility of the initialization problem (5.30) and, consequently, the poor performance of Algorithm 5.

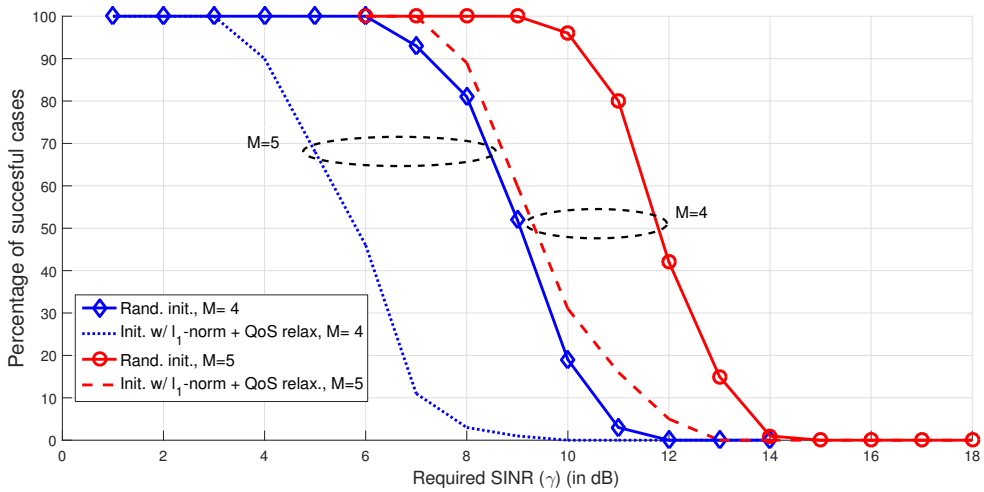

Figure 5.7: Percentage of successful cases as a function of the SINR threshold γ for $M = 4$ and 5 source-destination pairs. $N = 20$ relays, $P = 27$ dBm, $\sigma^2 = 19$ dBm. The channel amplitudes are generated as complex Gaussian random variables with zero mean and unit variance.

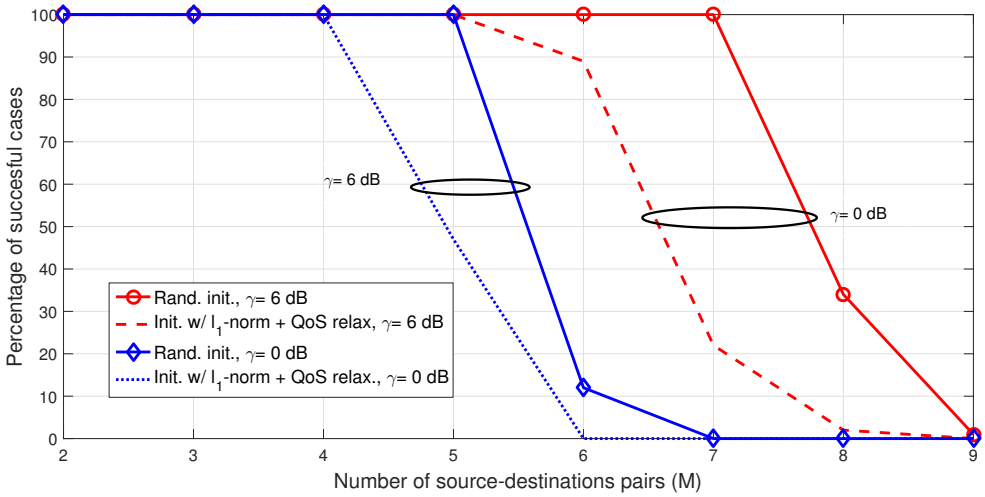

Figure 5.8: Percentage of successful cases as a function of the source-destination pairs M for a fixed γ. $N = 20$ relays, $P = 27$ dBm, $\sigma^2 = 19$ dBm.

Next, we evaluate the performance of the proposed method in a non-perfect CSI scenario. In this case, it is assumed that the second-order statistics of the channel coefficients is known at the central processing node. In particular, for the simulations presented below, we have considered channel model presented in [120].

Assume that the source-to-relays and the relays-to-destination channels, which are denoted by f_{ij} and g_{mk}, respectively, can be modeled as

$$f_{ij} = \bar{f}_{ij} + \tilde{f}_{ij} \quad \forall i \in \mathcal{L}, \forall j \in \mathcal{F}$$
$$g_{mk} = \bar{g}_{mk} + \tilde{g}_{mk} \quad \forall m \in \mathcal{F}, \forall k \in \mathcal{L},$$

where $\bar{f}_{ij}$ and $\bar{g}_{mk}$ are known channel means and $\tilde{f}_{ij}$ and $\tilde{g}_{ij}$ are zero-mean random variables. We assume that the channel coefficients are mutually independent. According to [120], the channel means $\bar{f}_{ij}$ and $\bar{g}_{mk}$ are generated as

$$\bar{f}_{ij} = e^{j\theta_{ij}}/\sqrt{1+\alpha_f} \; \forall i \in \mathcal{L}, \forall j \in \mathcal{F}$$
$$\bar{g}_{mk} = e^{j\phi_{mk}}/\sqrt{1+\alpha_g} \; \forall m \in \mathcal{F}, \forall k \in \mathcal{L},$$

where θ_{ij} and ϕ_{mk} are random variables uniformly distributed on the interval $[0, 2\pi]$. The parameters α_f and α_g are positive constants that determine the uncertainty of the channel coefficients. The variances of the random variables $\tilde{f}_{ij}$ and $\tilde{g}_{mk}$ are given by

$$\text{var}\{\tilde{f}_{ij}\} = \alpha_f/(1+\alpha_f) \; \forall i \in \mathcal{L}, \forall j \in \mathcal{F}$$
$$\text{var}\,\{\tilde{g}_{mk}\} = \alpha_g/(1+\alpha_g) \; \forall m \in \mathcal{F}, \forall k \in \mathcal{L}.$$

The justification for this channel model is explained in reference [120]. It should be noticed that $E\{|f_{ij}|^2\} = 1$. Therefore, when the parameter α_f is increased, the mean value of the channel f_{ij} is decreased accordingly. The same concept applies to the parameter α_g that controls the uncertainty of the channels between the relays and the destinations. Based on the channel model described above, in each trial of the Montecarlo simulation, the matrices $\mathbf{A}_k$, $\mathbf{B}_k$, $\mathbf{C}_k$ and $\mathbf{D}$ are generated according to these values.

Figure 5.9 shows the mean number of selected relays as a function of the SINR threshold in a dense network of N=40 potential relays when second-order CSI is considered. The source transmit powers and the per-relay constraints are set to 27 dBm. In this scenario, the considered noise power is 10 dB below the source transmit power (σ^2=17 dBm). For this simulation, and similar to [120], the considered values for α_f and α_g are α_f=α_g=−10 dB. As in the perfect channel state information case, the performance of the reweighted algorithm initialized with an arbitrary random point (Algorithm 6) and with the QoS

relaxation (Algorithm 5) is compared against the solution of problem (5.35), which is denoted as l_1-norm + QoS relaxation, and the convex-concave procedure applied to the problem (5.49). Similar to the perfect CSI scenario, from Figure 5.9 we can conclude that the reweighted technique clearly outperforms the rest of methods and is quite insensitive to the initialization point, because Algorithm 5 and Algorithm 6 have a similar performance in terms of the average number of selected nodes.

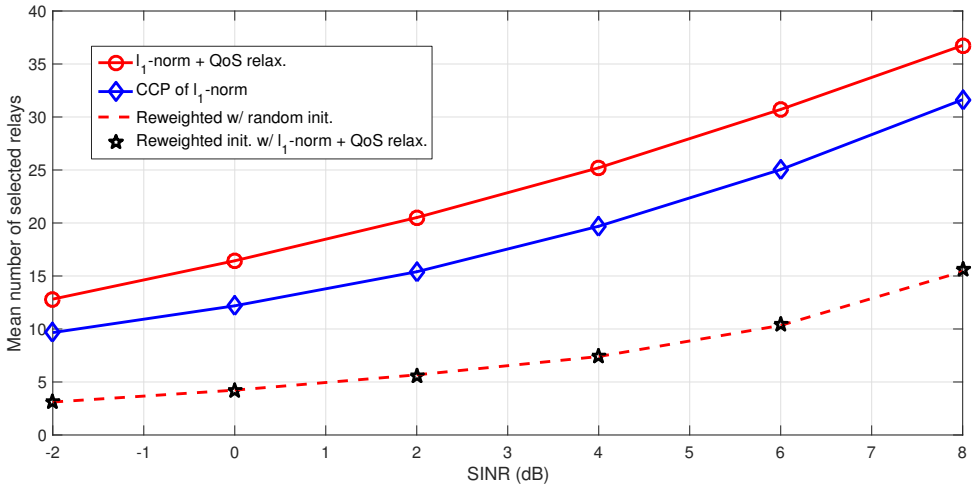

Figure 5.9: Mean number of selected relays as a function of the SINR. $N = 40$ relays, $P_{S_k} = 27$ dBm, $\sigma^2 = 17$ dBm and statistical CSI with $\alpha_f = \alpha_g = -10$ dB

In order to assess the performance of the reweighted method as a function of the level of uncertainty of the channels, Figure 5.10 plots the mean number of selected nodes as a function of the uncertainty level for the reweighted algorithm with a random initialization. The same value α is used for the uncertainty parameter of the source-to-relays channels and the relays-to-destinations channels, i.e., $\alpha_f = \alpha_g = \alpha$. The considered setup consists in $N = 40$ relays and the values of the parameters P and sigma are set to $P = 27$ dBm and $\sigma^2 = 21$ dBm, respectively. Thus, in this case, the ratio P/σ^2 is equal to 6 dB. Note that when the value of α increases, the quality of all the channels is degraded in the same way. The average number of selected relays in Figure 5.10 grows when the value of the parameter α is increased. The rationale behind this behavior is that if α increases, the variance of the channels is increased as a consequence. Hence, a higher number of cooperative nodes is needed to satisfy the SINR thresholds at the destinations.

In Figures 5.9 and 5.10 , we have considered the same uncertainty level α for all the relay links. Nevertheless, in real scenarios, some channels are better than others. Therefore, in

order to emulate a scenario with heterogeneous relay links, we have considered an ad-hoc wireless relay network composed of N= 40 potential relays with $P = 27$ dBm and $\sigma^2 = 21$ dBm. Note that the noise powers are set 6 dB below the source transmit powers. In this case, values of the uncertainty levels of each of the links of the wireless network are generated randomly from -16 dB to -5 dB using a uniform distribution. Figure 5.11 shows the mean number of selected nodes with the reweighted procedure initialized to a random point for $M = 3$ and 4 source-destination pairs.

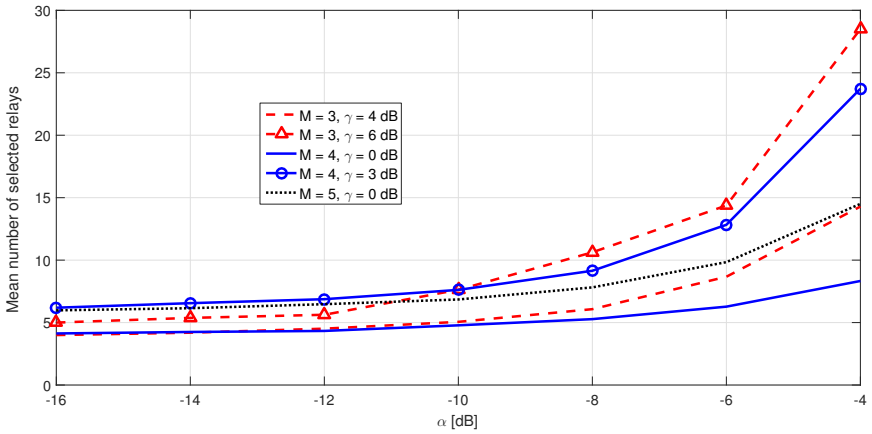

Figure 5.10: Mean number of selected relays as a function of the uncertainty level α. $N = 40$ relays, $P_{S_k} = 27$ dBm, $\sigma^2 = 21$ dBm and statistical CSI.

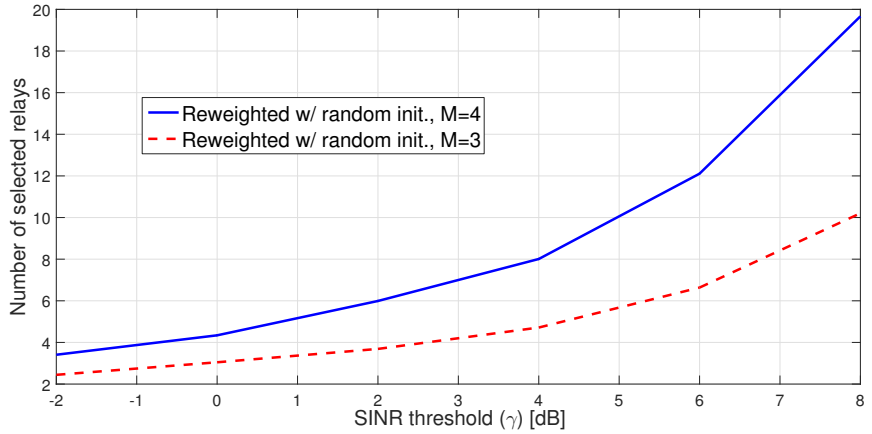

Figure 5.11: Mean number of relays versus the SINR threshold with a random uncertainty level per link.

5.6.2 Minimum transmit power with cardinality constraints

First, we analyze the performance in a scenario with perfect CSI. We have considered a multi-user cooperative network composed of $N = 19$ potential relays, $M = 3$ source-destination pairs. As in the simulations of the minimum cardinality problem with perfect CSI, in each simulation run, the channel coefficients have been generated as i.i.d. complex Gaussian random variables with zero mean and unit variance. The source powers and the maximum allowable power per relay are set to 27 dBm and the considered noise power is set 10 dB below the source transmit power, i.e., σ^2=17 dBm.

Hereinafter, the following methods are compared:

- The penalty CCP initialized to a random point (Algorithm 7) and with the perspective problem presented in (5.48). In both cases, we have considered τ_{sinr}=1000, $\tau_{\text{bin}}^{(0)}$=2^{-10}, $N_{it}^{\max}$=18, μ=2.1.
- The penalty CCP in Algorithm 7 with a *fixed penalty factor*. Namely, the next values are considered: τ_{sinr}=τ_{bin}=1000. Note that in this case the penalty factors are fixed and equal.
- The *two-step procedure* described in Algorithm 8 initialized with a random point and with the perspective problem (5.48). The parameters used in both cases are τ_{sinr}=1000, $\tau_{\text{bin}}^{(0)}$=2^{-5}, $N_1^{\max}$=8, $N_2^{\max}$=10, μ=2.1.

For the aforementioned methods, the convergence of the algorithms is declared if the improvement in the objective of the convexified problem is less than 10^{-4}.

In order to analyze the quality of the techniques proposed for the selection of the subset of cooperative nodes that minimizes the total relay transmit power, Figure 5.12 plots the averaged approximation ratio of the algorithms as a function of the number of selected relays K for γ=4.7 dB. The curves are averaged over 200 Montecarlo runs. Here, the approximation ratio is defined as the quotient between the total relay transmit power obtained with the subset of relays selected by the proposed methods and the minimum power. The latter has been obtained by computing by brute force for all the possible subsets of K cooperative nodes, the semidefinite relaxation of the minimum transmit power problem under per-relay power constraints and QoS requirements (i.e., problem (13) in reference [58]). It is worth noting that the approximation ratio is always greater or equal to one.

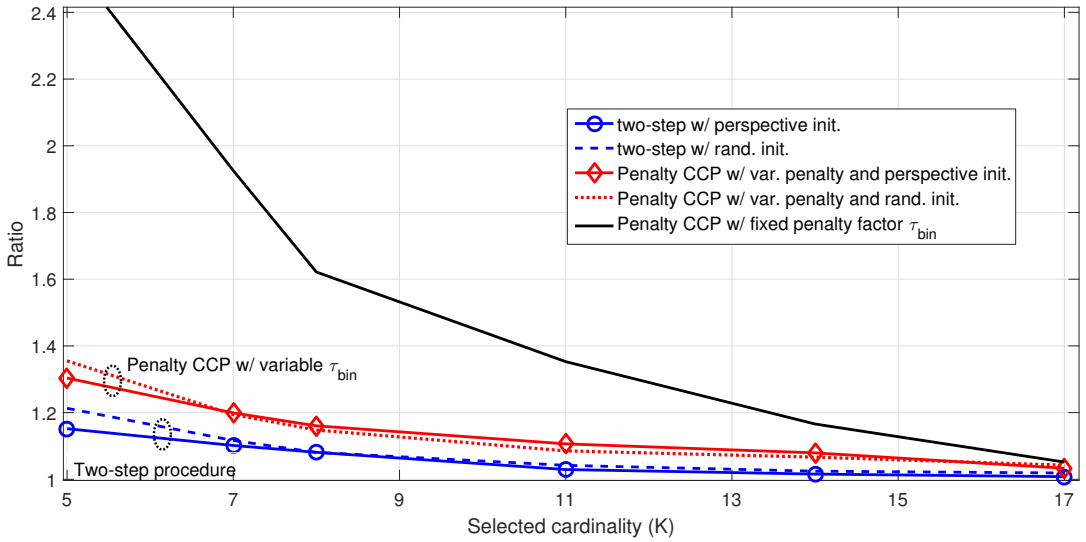

Figure 5.12: Approximation ratio as function of the selected cardinality. Scenario parameters: $N = 19$ potential relays, perfect CSI, $P_{s_k} = P_i^{\max} = 27$ dBm, $\gamma = 4.7$ dB.

As can be seen from Figure 5.12, the penalty CCP with a fixed factor τ_{bin} provides very poor results. The rationale behind this behavior is that a high penalty factor τ_{bin} encourages the selection of the subset of relays during first iterations of Algorithm 7 and penalizes the change of subset in the subsequent iterations. On the contrary, the penalty CCP and the two-step procedure with a variable τ_{bin} are able to provide high-quality solutions with an approximation ratio close to one. It should be noticed that the performance of both methods is quite insensitive to the initial point. It should be remarked as well that the two-step procedure exhibits a better performance than the penalty CCP presented in Algorithm 7. The improvement is around the 10% for all the possible cooperative sizes K. The mean number of iterations required by the two-step procedure and the penalty CCP is presented in Figure 5.13. Note that the initialization of these iterative algorithms with the perspective initialization reduces the total number of iterations. The proposed techniques are able to provide high-quality solutions with a reduced number of iterations. Specially, the two-step procedure initialized with the perspective problem exposed in (5.48).

Next, we evaluate the performance of the aforementioned algorithms in an scenario with second-order CSI. The channel coefficients for the non-perfect CSI scenario are generated as in the previous section and the values of α_f and α_g are set to α_f=α_g=-10 dB. We have considered the aforementioned setup with the exception of the value of SINR requirement. For this case, we have chosen $\gamma = 4$ dB.

Figure 5.14 presents the approximation ratio versus cooperative size K in the non-perfect CSI scenario. From this figure we can conclude that the penalty CCP method with variable penalty factor clearly outperforms the 'fixed penalty' approach that presents a poor performance. It can be also seen that the two-step procedure and the penalty CCP with a variable factor are able to deliver high-quality sub-optimal solutions. As in the perfect CSI scenario, the two-step procedure outperforms the penalty CCP approach described in Algorithm 7.

In order to illustrate the high performance of the proposed methods, Figure 5.15 shows the empirical Cumulative Distribution Function (CDF) as a function of the approximation ratio in the aforementioned second-order CSI environment for a cooperative size K=11. Note that the two-step procedure is able to obtain the optimal subset with a very high probability (more than the 50%). Furthermore, percentile 90th of the approximation ratio is below 1.2. It should be noticed as well that the two-step method delivers a high quality approximate solution, in terms of averaged approximation ratio and worst-case performance.

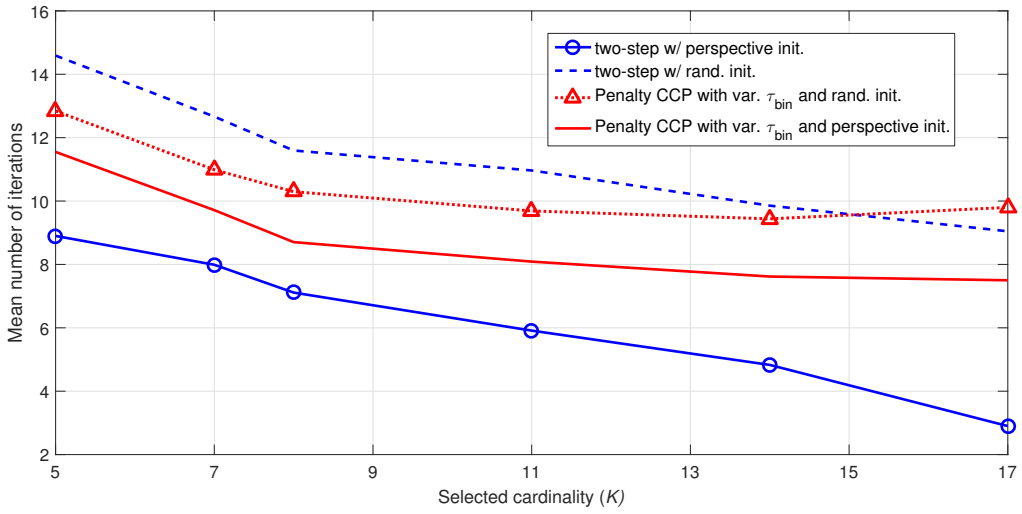

Figure 5.13: Mean number of iterations as function of the selected cardinality. $N = 19$ potential relays, perfect CSI, $P_{s_k} = P_i^{\max} = 27$ dBm, $\gamma = 4.7$ dB

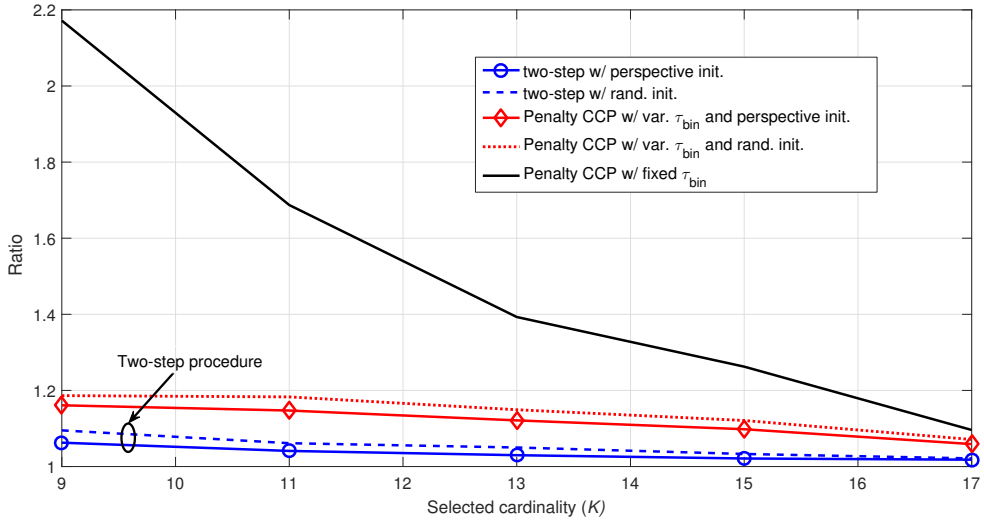

Figure 5.14: Approximation ratio versus the number of selected relays K. Second-order CSI, $N = 19$ potential relays, $P_{s_k} = P_i^{\max} = 27$ dBm, $\gamma = 4$ dB, $\alpha_f = \alpha_g = -10$ dB.

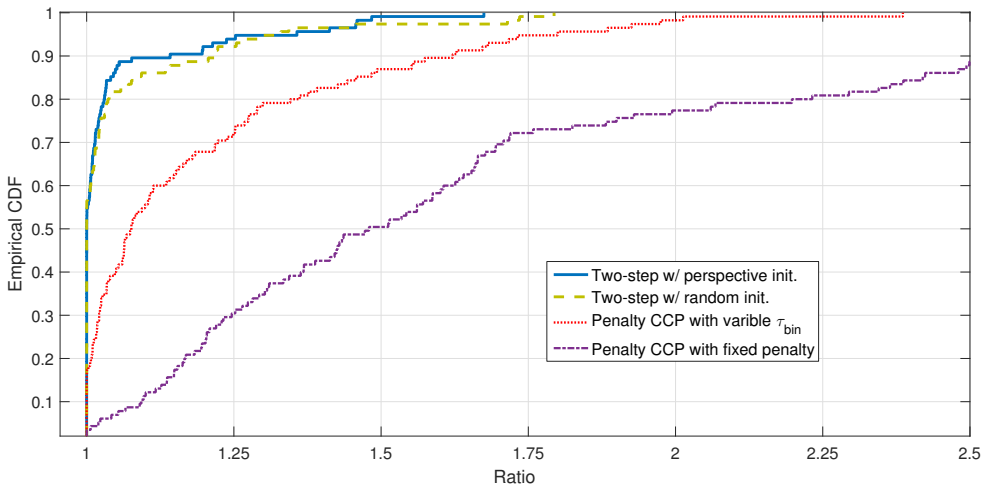

Figure 5.15: CDF of the approximation ratio for $K = 11$ relays. $N = 19$, $\gamma = 4$ dB. Second-order CSI, $\alpha_f = \alpha_g = -10$dB.

5.7 Conclusions

In this chapter, the relay subset selection problem in multi-user wireless relay networks has been addressed. In particular, two different problems have been considered: i) the selection of the minimum number of cooperative nodes that guarantees a given performance at the destination terminals, and ii) the selection of the subset of K relays that minimizes the total transmit power and guarantees the QoS requirements at the destinations. Both problems have been addressed taking into account individual power constraints at the relays. The combinatorial nature of these problems make them computationally demanding. With the aim of reducing the computational cost, different sub-optimal algorithms based on the convex-concave procedure have been presented. Our numerical results show that the proposed techniques are able to achieve a high performance with an affordable computational complexity.

Chapter 6

Conclusions and future research lines

This dissertation has dealt with subset selection problems in wireless communications. The goal of this final chapter is to summarize the main contributions of the thesis and to point out some possible directions for future research.

6.1 Thesis conclusions

In chapter 3, a simple, fast and accurate algorithm was proposed for finding the angles of arrival of multiple sources that impinge on an array of antennas. In contrast to other methods in the literature, the considered technique is not based on ad-hoc regularization parameters and does not require the previous knowledge of the number of incoming sources or a previous initialization. It considers a structured covariance matrix model based on over-complete basis representation and tries to fit the unknown signal powers to the sample covariance. Sparsity was promoted by means of an l_1-norm penalty imposed on the powers. The final problem was transformed into a positive LASSO and solved using the LARS/homotopy algorithm. The proposed method consists in an iterative procedure that solves a reduced-size system of equations at each iteration until a stopping condition is fulfilled. This stopping condition is based on the residual spectrum arising in a natural manner when the LARS/homotopy algorithm is applied to the objective function considered in the problem.

In chapters 4 and 5, the subset selection problem in dense relay-assisted wireless networks has been addressed. In this kind of scenarios, the activation of all the relay links is impractical due to the communications and processing overhead required to maintain the

synchronization amongst all the distributed nodes in the wireless network, which makes the overall network complexity unaffordable. In this context, the selection of the most suitable subset of spatially distributed relays is a key issue, since it has a dramatic effect in the overall system performance.

The multiple relay selection in an ad-hoc wireless network with one source-destination pair was considered in Chapter 4. In particular, we have dealt with the problem of finding the best subset of cooperative nodes, and their beamforming weights, so that the SNR is maximized at destination terminal. This problem was addressed considering the second-order channel state information of the relay channels and individual power constraints at the cooperative nodes. A sub-optimal method with a near-optimal performance was proposed to solve this problem. It is based on the use of the l_1-norm squared and the Charnes-Cooper transformation and naturally leads to a semidefinite programming relaxation with an affordable computational cost.

Chapter 5 has dealt with the joint relay assignment and beamforming optimization in multi-user wireless relay networks. Two different problems have been addressed in this chapter:

1. The selection of the minimum number of relay nodes that guarantees some predefined SINR requirements at the destination nodes in a multi-user peer-to-peer network. This problem has been addressed taking into account per-relay power constraints. The mathematical formulation of the aforementioned problem involves a non-convex objective with non-convex constraints and it has been reformulated as a DC program. To solve it an iterative method, based on the convex-concave procedure, was proposed.

2. The joint design of the distributed beamforming and the selection of the best subset of K nodes that minimizes the total relay transmit power. This problem was addressed considering QoS requirements at the destinations and per-relay power constraints. Its mathematical formulation involves non-convex constraints due to the QoS requirements and binary constraints and constitutes a challenging non-convex mixed-integer nonlinear program (MINLP). It was solved using several variations of the penalty convex-concave procedure. The proposed sub-optimal techniques are able to achieve a high performance with a feasible computational complexity.

6.2 Future work

6.2.1 Distributed algorithm computation using alternating direction method of multipliers

For the relay assignment problems addressed in chapter 5 we have considered the traditional centralized approach. This strategy has been widely used in the literature of wireless relay networks, e.g. [121,53,58,120]. It relies on the existence of a central controller that collects information from all the users and relays, compute the optimal weights of the beamformer and then sends the results back to the cooperative nodes. Nonetheless, in ultra-dense networks [31] a distributed algorithm can be more attractive. In such a case, the joint relay assignment and beamforming optimization can be distributed between the different relays and completed independently. In this context, the Alternating Direction Method of Multipliers (ADMM) [134] is a powerful mathematical tool. The subset selection problems exposed in chapter 5 can be easily put within this framework.

Following an approach similar to the recent results on the ADMM for non-convex quadratically constrained quadratic programs [135], the optimization problems presented in chapter 5 can be implemented in a distributed fashion with a small communication overhead. With the adoption of this strategy and after some necessary exchange of data between the terminals, based on its local channel and the interference information, each cooperative node can take the decision on whether to join the cooperative group of relays and can compute its corresponding weight. As a final remark, let us to point out that the ADMM framework has been already considered by the author in reference [136] in the context of multibeam satellite precoding.

6.2.2 User clustering in non-orthogonal multiple access systems

Non-Orthogonal Multiple Access (NOMA) [137,138,139,140,141] is a very promising technology that has recently been proposed as a key enabler for 5G and beyond 5G cellular networks. By exploiting the channel gain differences, multiple users are multiplexed into the "transmission power domain" and then are non-orthogonally scheduled for transmission on the same frequency band. NOMA provides spectrum efficiency and improves the throughput of cell-edge users with a low transmit latency.

In NOMA systems, multiple users share the same frequency band at the same time by adjusting their transmitted power. At the receiver side, the terminals apply a Successive Interference Cancelation (SIC) process to decode the transmitted messages. To obtain

the desired signal, each receiver first decodes the dominant interference signals and then subtract them from the superposed signal. Since each user equipment receives all the signals multiplexed over the same frequency band, including the desired one and the interference transmissions, it is important to have different power levels of the superimposed incoming signals in order to carry out the SIC process at the receiver.

In the framework of NOMA networks, user clustering has recently deserved a great interest from the wireless research community (see [137, 142, 143] and references therein). In particular, reference [137] addresses the dynamic user clustering and power allocation problem in NOMA systems. This problem is optimized under SIC constraints and considering minimum rate requirements for the user equipments. It yields a mathematical formulation with a combinatorial nature that can be expressed as a MINLP. In this context, techniques based on the penalty convex-concave procedure, similar to the algorithms presented in chapter 5, can be considered to solve the user clustering problem in NOMA systems.

6.2.3 5G and ultra-dense networks

Subset selection problems appear across many of the enabling technologies that are nowadays under consideration for the next generation of cellular networks. In order to cope with the immense amounts of traffic in 5G and beyond 5G cellular systems, ultra-dense networks have been proposed [31]. In future wireless networks, the number of access nodes and/or the number of communication links per unit area will be densified. Consequently, subset selection problems arise naturally to reduce the network complexity in many of the key technology enablers that are under consideration for the next generation of wireless networks, such as for instance: in Cloud-RAN [144,145], device-to-device communications [37], coordinated multipoint (CoMP) [146] and in the aforementioned NOMA systems. In this context, techniques based on the mathematical tools proposed throughout the dissertation can be considered for solving the combinatorial optimization problems that appear in the mentioned technologies.

Amongst the many possible combinatorial problems that can be considered in the 5G framework, let us highlight, for instance, the joint Remote Radio Head (RRH) selection and beamforming computation in Cloud-RAN network architectures, addressed in [144], or the clustering problem for device-to-device assisted Virtual MIMO (VMIMO) systems with limited feedback that has been presented in [37].

References

[1] S. Boyd and L. Vandenberghe, *Convex Optimization*. Cambridge University Press, Mar. 2004.

[2] B. Korte and J. Vygen, *Combinatorial Optimization: Theory and Algorithms*, 4th ed. Springer Publishing Company, 2007.

[3] J. Song, P. Babu, and D. P. Palomar, "Sparse generalized eigenvalue problem via smooth optimization," *IEEE Transactions on Signal Processing*, vol. 63, no. 7, pp. 1627–1642, April 2015.

[4] F. R. Bach, R. Jenatton, J. Mairal, and G. Obozinski, "Optimization with sparsity-inducing penalties," *Foundations and Trends in Machine Learning*, vol. 4, no. 1, pp. 1–106, 2012.

[5] F. Bach, R. Jenatton, J. Mairal, and G. Obozinkski, *Convex optimization with sparsity-inducing norms*. In S. Sra, S. Nowozin, S.J. Wright., editors, Optimization for Machine Learning, MIT Press, 2011.

[6] F. Bach, R. Jenatton, J. Mairal, and G. Obozinski, "Structured sparsity through convex optimization," *Statistical Science*, vol. 27, no. 4, pp. 450–468, 2012.

[7] F. Marvasti, A. Amini, F. Haddadi, M. Soltanolkotabi, B. H. Khalaj, A. Aldroubi, S. Sanei, and J. Chambers, "A unified approach to sparse signal processing," *EURASIP Journal on Advances in Signal Processing*, vol. 2012, no. 1, p. 44, 2012.

[8] M. Elad, *Sparse and Redundant Representations: From Theory to Applications in Signal and Image Processing*, 1st ed. Springer, 2010.

[9] A. Davenport, M. F. Duarte, Y. C. Eldar, and G. Kutyniok, *Introduction to Compressed Sensing, in Compressed Sensing: Theory and Applications, Y. Eldar and G. Kutyniok, eds.* Cambridge University Press, 2011.

[10] S. Foucart and H. Rauhut, *A Mathematical Introduction to Compressive Sensing*, 2013.

[11] J. Mairal, F. Bach, and J. Ponce, "Sparse modeling for image and vision processing," *Foundations and Trends in Computer Graphics and Vision*, vol. 8, no. 2-3, pp. 85–283, Dec. 2014.

[12] A. M. Bruckstein, D. L. Donoho, and M. Elad, "From sparse solutions of systems of equations to sparse modeling of signals and images," *SIAM Rev.*, vol. 51, no. 1, pp. 34–81, Feb. 2009.

[13] Z. Tan, Y. C. Eldar, and A. Nehorai, "Direction of arrival estimation using co-prime arrays: A super resolution viewpoint," *IEEE Transactions on Signal Processing*, vol. 62, no. 21, pp. 5565–5576, Nov 2014.

[14] D. L. Donoho and M. Elad, "Optimally sparse representation in general (nonorthogonal) dictionaries via l_1 minimization," *Proceedings of The National Academy of Sciences*, 2003.

[15] J. Tropp and S. Wright, "Computational methods for sparse solution of linear inverse problems," *Proceedings of the IEEE*, vol. 98, no. 6, pp. 948–958, 2010.

[16] F. Bach, R. Jenatton, and J. Mairal, *Optimization with Sparsity-Inducing Penalties (Foundations and Trends in Machine Learning)*. Now Publishers Inc., 2012.

[17] T. T. Cai and L. Wang, "Orthogonal matching pursuit for sparse signal recovery with noise," *IEEE Transactions on Information Theory*, vol. 57, no. 7, pp. 4680–4688, July 2011.

[18] Y. Jin and B. D. Rao, "Performance limits of matching pursuit algorithms," in *2008 IEEE International Symposium on Information Theory*, July 2008, pp. 2444–2448.

[19] D. L. Donoho, "For most large underdetermined systems of equations, the minimal l_1-norm near-solution approximates the sparsest near-solution," *Communications on pure and applied mathematics*, vol. 59, no. 7, pp. 907–934, 2006.

[20] E. J. Candes and T. Tao, "Near-optimal signal recovery from random projections: universal encoding strategies," *IEEE Trans. Inf. Theory*, vol. 52, no. 12, pp. 5406–5425, 2006.

[21] ——, "Decoding by linear programming," *IEEE Trans. Inf. Theory*, vol. 51, no. 12, pp. 4203–4215, 2005.

[22] J. A. Tropp, "Greed is good: algorithmic results for sparse approximation," *IEEE Transactions on Information Theory*, vol. 50, no. 10, pp. 2231–2242, Oct 2004.

[23] E. J. Candès, M. B. Wakin, and S. P. Boyd, "Enhancing sparsity by reweighted l_1 minimization," *Journal of Fourier Analysis and Applications*, vol. 14, no. 5, pp. 877–905, 2008.

[24] E. Lagunas and M. Nájar, "Compressed spectrum sensing in the presence of interference: Comparison of sparse recovery strategies," in *22nd European Signal Processing Conference (EUSIPCO)*, Sept 2014, pp. 1721–1725.

[25] R. Tibshirani, "Regression shrinkage and selection via the lasso," *Journal of the Royal Statistical Society, Series B*, vol. 58, pp. 267–288, 1996.

[26] T. Hastie, R. Tibshirani, and M. Wainwright, *Statistical Learning with Sparsity. The Lasso and Generalizations*. Chapman and Hall/CRC, 2015.

[27] G. James, D. Witten, T. Hastie, and R. Tibshirani, *An Introduction to Statistical Learning: With Applications in R*. Springer Publishing Company, Incorporated, 2014.

[28] T. Hastie, R. Tibshirani, and J. Friedman, *The Elements of Statistical Learning*. Springer series in statistics, 2009.

[29] S. P. Chepuri and G. Leus, "Sparsity-promoting sensor selection for non-linear measurement models," *IEEE Transactions on Signal Processing*, vol. 63, no. 3, pp. 684–698, Feb 2015.

[30] H. Jamali-Rad, A. Simonetto, and G. Leus, "Sparsity-aware sensor selection: Centralized and distributed algorithms," *IEEE Signal Processing Letters*, vol. 21, no. 2, pp. 217–220, Feb 2014.

[31] M. Kamel, W. Hamouda, and A. Youssef, "Ultra-dense networks: A survey," *IEEE Communications Surveys Tutorials*, vol. 18, no. 4, pp. 2522–2545, 2016.

[32] J. Wu, "Green wireless communications: from concept to reality [industry perspectives]," *IEEE Wireless Communications*, vol. 19, no. 4, pp. 4–5, August 2012.

[33] Y. Shi, J. Zhang, and K. B. Letaief, "Group sparse beamforming for Green Cloud-RAN," *IEEE Transactions on Wireless Communications*, vol. 13, no. 5, pp. 2809–2823, May 2014.

[34] C. Pan, H. Zhu, N. J. Gomes, and J. Wang, "Joint precoding and RRH Selection for Green MIMO C-RAN," in *2016 IEEE Global Communications Conference (GLOBECOM)*, Dec 2016, pp. 1–5.

[35] S. Kuang and N. Liu, "Energy minimization via BS selection and beamforming for Cloud-RAN under finite fronthaul capacity constraints," in *2016 IEEE 83rd Vehicular Technology Conference (VTC Spring)*, May 2016, pp. 1–6.

[36] Y. Cheng, M. Pesavento, and A. Philipp, "Joint network optimization and downlink beamforming for CoMP transmissions using mixed integer conic programming," *IEEE Transactions on Signal Processing*, vol. 61, no. 16, pp. 3972–3987, Aug 2013.

[37] S. H. Seyedmehdi and G. Boudreau, "An efficient clustering algorithm for Device-to-Device assisted Virtual MIMO," *IEEE Transactions on Wireless Communications*, vol. 13, no. 3, pp. 1334–1343, March 2014.

[38] O. Mehanna, N. D. Sidiropoulos, and G. B. Giannakis, "Joint multicast beamforming and antenna selection," *IEEE Transactions on Signal Processing*, vol. 61, no. 10, pp. 2660–2674, May 2013.

[39] O. Mehanna, N. Sidiropoulos, and G. B. Giannakis, "Multicast beamforming with antenna selection," *in Proc. of the 13th SPAWC*, Jun. 2012.

[40] K. Adachi and N. T. Trendafilov, "Sparse principal component analysis subject to prespecified cardinality of loadings," *Computational Statistics*, vol. 31, no. 4, pp. 1403–1427, 2016.

[41] M. Calvo-Fullana, J. Matamoros, and C. Antón-Haro, "Sensor selection and power allocation strategies for energy harvesting wireless sensor networks," *IEEE Journal on Selected Areas in Communications*, vol. 34, no. 12, pp. 3685–3695, Dec 2016.

[42] S. Liu, S. Kar, M. Fardad, and P. K. Varshney, "Sparsity-aware sensor collaboration for linear coherent estimation," *IEEE Transactions on Signal Processing*, vol. 63, no. 10, pp. 2582–2596, May 2015.

[43] S. Joshi and S. Boyd, "Sensor selection via convex optimization," *IEEE Transactions on Signal Processing*, vol. 57, no. 2, pp. 451–462, Feb 2009.

[44] Z.-q. Luo, W.-k. Ma, A. So, Y. Ye, and S. Zhang, "Semidefinite relaxation of quadratic optimization problems," *IEEE Signal Processing Magazine*, vol. 27, no. 3, pp. 20–34, May 2010.

[45] T. Pham Dinh and H. An Le Thi, "Recent advances in DC programming and DCA," *Transactions on Computational Collective Intelligence*, vol. 8432, 2014.

[46] B. Efron, T. Hastie, I. Johnstone, and R. Tibshirani, "Least angle regression," *Annals of Statistics*, vol. 32, pp. 407–499, 2004.

[47] Y. Zhang and R. S. Cheng, "Relay subset selection in cooperative systems with beamforming and limited feedback," *IEEE Transactions on Wireless Communications*, vol. 12, no. 10, pp. 5271–5281, Oct. 2013.

[48] S. Zhang and V. K. N. La, "Multi-relay selection design and analysis for multi-stream cooperative communications," *IEEE Transactions on Wireless Communications*, vol. 10, no. 4, pp. 173–189, Apr. 2011.

[49] H. Nguyen, H. Nguyen, and T. Le-Ngoc, "Diversity analysis of relay selection schemes for two-way wireless relay networks," *Wireless Personal Communications*, vol. 59, no. 2, pp. 173–189, Jul. 2011.

[50] J. Lee and N. Al-Dhahir, "Exploiting sparsity for multiple relay selection with relay gain control in large AF relay networks," *IEEE Wireless Commun. Letters*, vol. 2, no. 3, pp. 347–350, Jun. 2013.

[51] S. Atapattu, Y. Jing, H. Jiang, and C. Tellambura, "Relay selection schemes and performance analysis approximations for two-way networks," *IEEE Transactions on Communications*, vol. 61, no. 3, pp. 987–998, Mar. 2013.

[52] Y. Jing and H. Jafarkhani, "Single and multiple relay selection schemes and their achievable diversity orders," *IEEE Trans. Wireless Communications*, vol. 8, no. 3, pp. 1414–1423, Mar. 2009.

[53] E. Che, H. D. Tuan, and H. H. Nguyen, "Joint optimization of cooperative beamforming and relay assignment in multi-user wireless relay networks," *IEEE Transactions on Wireless Communications*, vol. 13, no. 10, pp. 5481–5495, Oct 2014.

[54] A. L. Yuille and A. Rangarajan, "The concave-convex procedure," *Neural Comput.*, vol. 15, no. 4, Apr. 2003.

[55] S. Burer and A. N. Letchford, "Non-convex mixed-integer nonlinear programming: A survey," *Surveys in Operations Research and Management Science*, vol. 17, no. 2, pp. 97 – 106, 2012.

[56] O. Mehanna, K. Huang, B. Gopalakrishnan, A. Konar, and N. D. Sidiropoulos, "Feasible point pursuit and successive approximation of non-convex QCQPs," *IEEE Signal Processing Letters*, vol. 22, no. 7, October 2014.

[57] J. Park and S. Boyd, "General heuristics for nonconvex quadratically constrained quadratic programming," *arXiv preprint arXiv:1703.07870*, Mar. 2017.

[58] A. H. Phan, H. D. Tuan, H. H. Kha, and H. H. Nguyen, "Beamforming optimization in multi-user amplify-and-forward wireless relay networks," *IEEE Trans. Wireless Communications*, vol. 11, no. 4, pp. 1510–1520, 2012.

[59] T. Lipp and S. Boyd, "Variations and extension of the convex–concave procedure," *Optimization and Engineering*, vol. 17, no. 2, pp. 263–287, Jun. 2016.

[60] X. Shen, S. Diamond, Y. Gu, and S. Boyd, "Disciplined convex-concave programming," *arXiv preprint arXiv:1604.02639*, Apr. 2016.

[61] L. Blanco and M. Nájar, "Sparse multiple relay selection for network beamforming with individual power constraints using semidefinite relaxation," *IEEE Trans. on Wireless Communications*, vol. 15, no. 2, pp. 1206–1217, Feb 2016.

[62] L. Blanco and M. Nájar, "Sparse covariance fitting for direction of arrival estimation," *EURASIP Journal on Advances in Signal Processing*, vol. 2012, no. 1, p. 111, 2012.

[63] ——, "Relay subset selection in cognitive networks with imperfect csi and individual power constraints," in *23rd European Signal Processing Conference (EUSIPCO)*, Aug 2015, pp. 1456–1460.

[64] ——, "Subset relay selection in wireless cooperative networks using sparsity-inducing norms," in *11th International Symposium on Wireless Communications Systems (ISWCS)*, Aug 2014, pp. 501–505.

[65] P. Charbonnier, L. Blanc-féraud, G. Aubert, and M. Barlaud, "Deterministic edge-preserving regularization in computed imaging," *IEEE Trans. Image Processing*, vol. 6, pp. 298–311, 1997.

[66] H. Zou and T. Hastie, "Regularization and variable selection via the elastic net," *Journal Of The Royal Statistical Society Series B*, vol. 67, no. 2, pp. 301–320, 2005.

[67] D. L. Donoho, "Compressed sensing." *IEEE Transactions on Information Theory*, pp. 1289–1306, 2006.

[68] R. Chartrand, "Exact reconstruction of sparse signals via nonconvex minimization." *IEEE Signal Process. Lett.*, vol. 14, no. 10, pp. 707–710, 2007.

[69] T. Park and G. Casella, "The Bayesian Lasso," *Journal of the American Statistical Association*, vol. 103, no. 482, pp. 681–686, 2008.

[70] D. P. Wipf and B. D. Rao, "Sparse bayesian learning for basis selection." *IEEE Transactions on Signal Processing*, vol. 52, no. 8, pp. 2153–2164, 2004.

[71] S. Mallat and Z. Zhang, "Matching pursuit with time-frequency dictionaries," *IEEE Trans. on Signal Processing*, vol. 41, no. 12, pp. 3397–3415, Dec. 1993.

[72] F. R. Bach, R. Jenatton, J. Mairal, and G. Obozinski, "Convex optimization with sparsity-inducing norms," *Optimization for Machine Learning, MIT Press*, pp. 19–53, 2011.

[73] S. S. Chen, D. L. Donoho, Michael, and A. Saunders, "Atomic decomposition by basis pursuit," *SIAM Journal on Scientific Computing*, vol. 20, pp. 33–61, 1998.

[74] R. Tibshirani, "Regression shrinkage and selection via the lasso," *Journal of the Royal Statistical Society, Series B*, vol. 58, pp. 267–288, 1996.

[75] D. L. Donoho and Y. Tsaig, "Fast solution of l1-norm minimization problems when the solution may be sparse," *IEEE Transactions on Information Theory*, vol. 54, pp. 4789–4812, 2008.

[76] M. R. Osborne, B. Presnell, and B. A. Turlach, "A new approach to variable selection in least squares problems," *IMA Journal of Numerical Analysis*, vol. 20, no. 3, pp. 389–403, 2000.

[77] H. L. V. Trees, *Detection, estimation, and modulation theory, part IV: optimum array processing.* John Wiley & Sons, New York, USA, 2002.

[78] J. Capon, "High-resolution frequency-wavenumber spectrum analysis," *Proc. IEEE*, vol. 57, no. 8, pp. 1408–1418, 1969.

[79] M. A. Lagunas and A. Gasull, "An improved maximum likelihood method for power spectral density estimation," *IEEE Transactions on Acoustics Speech Signal Processing*, vol. ASSP-32, no. 1, pp. 170–173, Feb. 1984.

[80] R. Schmidt, "Multiple emitter location and signal parameter estimation," *IEEE Transactions on Antennas and Propagation*, vol. 34, no. 3, pp. 276–280, 1986.

[81] P. Stoica and A. Nehorai, "Performance study of conditional and unconditional direction-of-arrival estimation," *Acoustics, Speech and Signal Processing, IEEE Transactions on*, vol. 38, no. 10, pp. 1783 –1795, oct 1990.

[82] J. A. Högbom, "Aperture synthesis with a non-regular distribution of interferometer baselines," *Astronomy and Astrohpysics, Suppl. 15*, pp. 417–426, 1974.

[83] P. Stoica and R. Moses, *Spectral analysis of signals*. Prentice Hall, NJ, USA, 2005.

[84] T. E. Tuncer and B. Friedlander, *Classical and modern Direction-of-Arrival estimation*. Elsevier academic press, Burlington, USA, 2009.

[85] I. F. Gorodnitsky and B. D. Rao, "Sparse signal reconstruction from limited data using FOCUSS: A re-weighted minimum norm algorithm," *IEEE Trans. Signal Processing*, pp. 600–616, 1997.

[86] J. Fuchs, "Linear programming in spectral estimation: application to array processing," in *In Proc. ICASSP, vol III*, 1996, pp. 3161–3164.

[87] S. F. Cotter, B. D. Rao, K. E., and K. Kreutz-delgado, "Sparse solutions to linear inverse problems with multiple measurement vectors," *IEEE Trans. Signal Processing*, pp. 2477–2488, 2005.

[88] T. Yardibi, J. Li, P. Stoica, M. Xue, and A. B. Baggeroboer, "Source localization and sensing: A nonparametric iterative adaptive approach based on weighted least squares," *IEEE Trans. on Aerospace and Electronic Systems*, vol. 46, no. 1, pp. 425–443, Jan 2010.

[89] D. M. Malioutov, M. Çetin, and A. S. Willsky, "A sparse signal reconstruction perspective for source localization with sensor arrays," *IEEE Transactions on Signal Processing*, vol. 53, pp. 3010–3022, 2005.

[90] Y. C. Eldar and H. Rauhut, "Average case analysis of multichannel sparse recovery using convex relaxation," *IIEEE Trans. Inf. Theory*, vol. 56, no. 1, pp. 505–519, Jan 2010.

[91] T. Yardibi, J. Li, P. Stoica, and L. N. Cattafesta, "Sparsity constrained deconvolution approaches for acoustic source mapping," *Journal of The Acoustical Society of America*, vol. 123, 2008.

[92] J. S. Picard and A. J. Weiss, "Direction finding of multiple emitters by spatial sparsity and linear programming," in *Proceedings of the 9th International Symposium on Communications and Information Technologies (ISCIT)*, 2009, pp. 1258–1262.

[93] P. Stoica, P. Babu, and J. Li, "Spice: A sparse covariance-based estimation method for array processing," *IEEE Transactions on Signal Processing*, vol. 59, no. 2, pp. 629–638, 2011.

[94] Z. Liu, Z. Huang, and Y. Zhou, "Direction-of-arrival estimation of wideband signals via covariance matrix sparse representation," *IEEE Transactions on Signal Processing*, vol. 59, no. 9, pp. 4256–4270, 2011.

[95] P. Stoica, P. Babu, and J. Li, "A sparse covariance-based method for direction of arrival estimation," in *ICASSP*. IEEE, 2011, pp. 2844–2847.

[96] M. Mørup, K. H. Madsen, and L. K. Hansen, "Approximate l_0 constrained non-negative matrix and tensor factorization," in *In proc. International Conference on Circuits and Systems, ISCAS 2008*, 2008.

[97] I. Loris, "L1packv2: A mathematica package for minimizing an l_1-penalized functional," *Computer Physics Communications*, vol. 179, no. 12, pp. 895 – 902, 2008.

[98] B. W. Rust and D. P. O'Leary, "Residual periodograms for choosing regularization parameters for ill-posed problems," *Inverse Problems*, vol. 24, 2008.

[99] P. Hansen, M. Kilmer, and R. Kjeldsen, "Exploiting residual information in the parameter choice for discrete ill-posed problems," *BIT Numerical Mathematics*, vol. 46, no. 1, pp. 41–59, 2006.

[100] M. Bartlett, *An introduction to Stochastic Processes*. Cambridge University Press, 1966.

[101] J. Durbin, "Tests for serial correlation in regression analysis based on the periodogram of least-squares residuals," *Biometrika*, vol. 56, no. 1, pp. 1–15, 1969.

[102] J. Laneman, D. Tse, and G. Wornell, "Cooperative diversity in wireless networks: efficient protocols and outage behavior," *IEEE Trans. Inf. Theory*, vol. 50, no. 12, pp. 3062–3080, Dec. 2004.

[103] M. Janani, A. Hedayat, T. E. Hunter, and A. Nosratinia, "Coded cooperation in wireless communications: space-time transmission and iterative decoding," *IEEE Trans. Signal Processing*, vol. 52, no. 2, pp. 362–371, Feb. 2004.

[104] V. Havary-Nassab, S. Shahbazpanahi, A. Grami, and Z.-Q. Luo, "Distributed beamforming for relay networks based on second-order statistics of the channel state information," *IEEE Trans. Signal Processing*, vol. 56, no. 9, pp. 4306–4316, Sept. 2008.

[105] A. S. Ibrahim, A. K. Sadek, W. Su, and K. J. R. Liu, "Cooperative communications with relay-selection: when to cooperate and whom to cooperate with?" *IEEE Trans. Wireless Communications*, vol. 7, no. 7, pp. 2814–2827, Jul. 2008.

[106] Y. Zhao, R. Adve, and T. J. Lim, "Symbol error rate of selection amplify-and-forward relay systems." *IEEE Communications Letters*, vol. 10, no. 11, pp. 757–759, Nov. 2006.

[107] D. S. Michalopoulos, G. K. Karagiannidis, T. A. Tsiftsis, and R. K. Mallik, "An optimized user selection method for cooperative diversity systems," *in Proc. IEEE GLOBECOM*, Dec. 2006.

[108] J. N. Laneman and G. W. Wornell, "Distributed space-time-coded protocols for exploiting cooperative diversity in wireless networks," *IEEE Trans. Inf. Theory*, vol. 49, no. 10, pp. 2415–2425, Oct. 2003.

[109] J. Xu, H. Zhang, D. Yuan, Q. Jin, and C.-X. Wang, "Novel multiple relay selection schemes in two-hop cognitive relay networks," *in Proc. Int. Conference on Communications and Mobile Computing (CMC)*, pp. 307–310, Apr. 2011.

[110] Y. Jing and H. Jafarkhani, "Network beamforming using relays with perfect channel information," *IEEE Trans. Information Theory*, vol. 55, no. 6, pp. 2499–2517, June 2009.

[111] A. Piltan and S. Salari, "Distributed beamforming in cognitive relay networks with partial channel state information," *IET Communications*, vol. 6, no. 9, pp. 1011–1018, Jun. 2012.

[112] J. Li, A. Petropulu, and H. Poor, "Cooperative transmission for relay networks based on second-order statistics of channel state information," *IEEE Trans. Signal Processing*, vol. 59, no. 3, pp. 1280–1291, Mar. 2011.

[113] A. B. Gershman, N. D. Sidiropoulos, S. Shahbazpanahi, M. Bengtsson, and B. Ottersten, "Convex optimization-based beamforming: from receive to transmit and network designs," *IEEE Signal Proc. Magazine*, vol. 27, no. 3, pp. 62–75, May 2010.

[114] S. Boyd and L. Vandenberghe, *Convex Optimization*. New York, NY, USA: Cambridge University Press, 2004.

[115] A. Charnes and W. W. Cooper, "Programming with linear fractional functionals," *Naval Research Logistics*, vol. 9, no. 3-4, pp. 181–186, 1962.

[116] J. F. Sturm, "Using sedumi 1.02, a MATLAB toolbox for optimization over symmetric cones," *Optimization Methods and Software*, vol. 11–12, pp. 625–653, 1999.

[117] N. Bourbaki, H. Eggleston, and S. Madan, *Topological Vector Spaces*. Springer-Verlag, 1987.

[118] "CVX: Matlab software for Disciplined Convex Programming." [Online]. Available: http://cvxr.com/cvx/

[119] K. B. Petersen and M. S. Pedersen, "The matrix cookbook," Nov. 2012. [Online]. Available: http://www2.imm.dtu.dk/pubdb/p.php?3274

[120] S. Fazeli-Dehkordy, S. Shahbazpanahi, and S. Gazor, "Multiple peer-to-peer communications using a network of relays," *IEEE Transactions on Signal Processing*, vol. 57, no. 8, pp. 3053–3062, Aug 2009.

[121] J. Lin, Q. Li, C. Jiang, and H. Shao, "Joint multi-relay selection, power allocation and beamformer design for multi-user decode-and-forward relay networks," *IEEE Transactions on Vehicular Technology*, July 2015.

[122] S. Zhou, J. Xu, and Z. Niu, "Interference-aware relay selection scheme for two-hop relay networks with multiple source-destination pairs," *IEEE Trans. on Vehicular Technology*, vol. 62, no. 5, pp. 2327–2337, June 2013.

[123] G. R. Lanckriet and B. K. Sriperumbudur, "On the convergence of the concave-convex procedure," 2009.

[124] D. R. Hunter, K. Lange, D. O. Biomathematics, and H. Genetics, "A tutorial on MM algorithms," *The American Statistician*, vol. 58, pp. 30–37, 2004.

[125] H. Li and T. Adali, "Complex valued adaptive signal processing using nonlinear functions," *EURASIP Journal on Advances on Signal Processing*, 2008.

[126] M. S. Lobo, L. Vandenberghe, S. Boyd, and H. Lebret, "Applications of second-order cone programming," *Linear Algebra and its Applications*, vol. 284, pp. 193–228, 1998.

[127] H. Chen, A. B. Gershman, and S. Shahbazpanahi, "Distributed peer-to-peer beamforming for multiuser relay networks," in *2009 IEEE International Conference on Acoustics, Speech and Signal Processing*, April 2009, pp. 2265–2268.

[128] N. Bornhorst, M. Pesavento, and A. B. Gershman, "Distributed beamforming for multi-group multicasting relay networks," *IEEE Transactions on Signal Processing*, vol. 60, no. 1, pp. 221–232, Jan 2012.

[129] N. Bornhorst, "Energy-efficient distributed multicast beamforming using iterative second-order cone programming," Ph.D. dissertation, Technische Universität, Darmstadt, 2015.

[130] O. Günlük and J. Linderoth, *Perspective Reformulation and Applications.* New York, NY: Springer New York, 2012, pp. 61–89.

[131] ——, "Perspective reformulations of mixed integer nonlinear programs with indicator variables," *Mathematical Programming*, vol. 124, no. 1, pp. 183–205, 2010.

[132] J. Lee and S. Leyffer, *Mixed Integer Nonlinear Programming.* IMA Volumes in Math. and its Applications. Springer, Jan. 2012.

[133] M. Thiao, T. P. Dinh, and H. A. L. Thi, "A DC programming approach for sparse eigenvalue problem," *in Proc. 27th International Conference on Machine Learning (ICML)*, Aug. 2010.

[134] S. Boyd, N. Parikh, E. Chu, B. Peleato, and J. Eckstein, "Distributed optimization and statistical learning via the alternating direction method of multipliers," *Found. Trends Mach. Learn.*, vol. 3, no. 1, pp. 1–122, Jan. 2011.

[135] K. Huang and N. D. Sidiropoulos, "Consensus-ADMM for general quadratically constrained quadratic programming," *IEEE Transactions on Signal Processing*, vol. 64, no. 20, pp. 5297–5310, Oct 2016.

[136] M. A. Vázquez, A. Konar, L. Blanco, N. D. Sidiropoulos, and A. I. Pérez-Neira, "Nonconvex consensus ADMM for satellite precoder design," in *In proceedings of IEEE International Conference on Acoustics, Speech and Signal Processing (ICASSP)*, March 2017.

[137] M. S. Ali, H. Tabassum, and E. Hossain, "Dynamic user clustering and power allocation for uplink and downlink non-orthogonal multiple access (NOMA) systems," *IEEE Access. Special section on optimization for emerging wireless networks: IoT, 5G and smart grid communications*, vol. 4, pp. 6325–6343, August 2016.

[138] S. Lee, "Non-orthogonal multiple access schemes with partial relay selection," *IET Communications*, vol. 11, pp. 846–854(8), April 2017.

[139] Z. Ding, H. Dai, and H. V. Poor, "Relay selection for cooperative NOMA," *IEEE Wireless Communications Letters*, vol. 5, no. 4, pp. 416–419, Aug 2016.

[140] Z. Ding, M. Peng, and H. V. Poor, "Cooperative non-orthogonal multiple access in 5G systems," *IEEE Communications Letters*, vol. 19, no. 8, pp. 1462–1465, Aug 2015.

[141] Z. Ding, P. Fan, and H. V. Poor, "Impact of user pairing on 5G nonorthogonal multiple-access downlink transmissions," *IEEE Transactions on Vehicular Technology*, vol. 65, no. 8, pp. 6010–6023, Aug 2016.

[142] Z. Liu, L. Lei, N. Zhang, G. Kang, and S. S. Chatzinotas, "Joint beamforming and power optimization with iterative user clustering for MISO-NOMA systems," *IEEE Access*, vol. PP, no. 99, pp. 1–1, 2017.

[143] S. Ali, E. Hossain, and D. I. Kim, "Non-orthogonal multiple access (NOMA) for downlink multiuser MIMO systems: User clustering, beamforming, and power allocation," *IEEE Access. Special issue on physical layer and medium access control layer advances in 5G wireless networks*, vol. 5, pp. 565–577, 2017.

[144] J. Tang, W. P. Tay, and T. Q. S. Quek, "Cross-layer resource allocation in cloud radio access network," in *2014 IEEE Global Conference on Signal and Information Processing (GlobalSIP)*, Dec 2014, pp. 158–162.

[145] J. Tang, W. P. Tay, T. Q. S. Quek, and B. Liang, "System cost minimization in Cloud RAN with limited fronthaul capacity," *IEEE Transactions on Wireless Communications*, vol. 16, no. 5, pp. 3371–3384, May 2017.

[146] V. N. Ha, L. B. Le, and N. D. Dào, "Coordinated multipoint transmission design for Cloud-RANs with limited fronthaul capacity constraints," *IEEE Transactions on Vehicular Technology*, vol. 65, no. 9, pp. 7432–7447, Sept 2016.